농학박사학위논문

Characterization of Forkhead Transcription Factor Genes in the Rice Blast Fungus and Development of Novel Tools for Functional Genomics in Fungi

벼 도열병균 Forkhead 유전자군 특성 규명 및 새로운 유전체 기능 분석법 개발

2014년 8월

서울대학교 대학원

농생명공학부 식물미생물학전공

박 재 진

Characterization of Forkhead Transcription Factor Genes in the Rice Blast Fungus and Development of Novel Tools for Functional Genomics in Fungi

A dissertation submitted in partial
fulfillment of the requirement for
the degree of

DOCTOR OF PHILOSOPHY

to the Faculty of
Department of Agricultural Biotechnology

at

SEOUL NATIONAL UNIVERSITY

by

Jaejin Park

AUGUST, 2014

농학박사학위논문

벼 도열병균 Forkhead 유전자군 특성 규명 및 새로운 유전체 기능 분석법 개발

지도교수 이 용 환

이 논문을 농학박사학위논문으로 제출함
2014년 5월

서울대학교 대학원
농생명공학부 식물미생물학전공
박 재 진

박 재 진의 박사학위논문을 인준함
2014년 6월

위 원 장 이 인 원

부 위원장 이 용 환

위 원 김 영 호

위 원 강 경 수

위 원 박 숙 영

A THESIS FOR THE DEGREE OF DOCTOR OF PHILOSOPHY

Characterization of Forkhead Transcription Factor Genes in the Rice Blast Fungus and Development of Novel Tools for Functional Genomics in Fungi

UNDER THE DIRECTION OF DR. YONG-HWAN LEE

SUBMITTED TO THE FACULTY OF THE GRADUATE SCHOOL
OF SEOUL NATIONAL UNIVERSITY

BY

JAEJIN PARK

MAJOR IN PLANT MICROBIOLOGY
DEPARTMENT OF AGRICULTURAL BIOTECHNOLOGY

JUNE 2014

APPROVED AS A QUALIFIED THESIS OF JAEJIN PARK FOR
THE DEGREE OF DOCTOR OF PHILOSOPHY
BY THE COMMITTEE MEMBERS

CHAIRMAN Yin-Won Lee

VICE CHAIRMAN Yong-Hwan Lee

MEMBER Kyong Ho Kim

MEMBER Kyoung Su Kim

MEMBER Sook-Young Park

Characterization of Forkhead Transcription Factor Genes in the Rice Blast Fungus and Development of Novel Tools for Functional Genomics in Fungi

Jaejin Park

ABSTRACT

Rapid accumulation of genome data and application of high-throughput mutagenesis technology allowed large-scale gene characterization. However, phenotype screening is a bottleneck as it entails time-consuming and labor-intensive processes. Thus there is a demand for a novel high-throughput phenotyping (HTP) platform. Although several microplate-based assays are currently available, their application on organisms growing in filamentous form has been met with considerable difficulty due to uneven distribution of cells. As a solution, a new phenomics platform in filamentous fungi called 'pHenome' was developed. This platform is based on the pH change in the culturing media, reflecting physiological status of cells. The pH in culturing

media is continuously measured by a microplate reader using an optimized medium amended with pH indicators and cellular responses to various stresses can be characterized within 24 hours. The validity of the system was comprehensively evaluated with strains of *Magnaporthe oryzae*, the causal agent of rice blast. To uncover the roles of genes encoding putative forkhead-box (FOX) transcription factors (TFs) in *M. oryzae*, gene-deleted mutants were generated and characterized via targeted-gene replacement (TGR) and phenotype screenings including the pHenome, respectively. Deletions of two genes (*MoFKH1* and *MoHCM1*) correspond to Ascomycota-specific members of the FOX TF family resulted in reduced mycelial growth and conidial germination and higher sensitivity to the cell cycle inhibitors, suggesting their role in cell cycle control. Loss of *MoFKH1* also exhibited increased septation, abnormal stress responses, and reduced virulence. On the other hand, disruption of two other FOX TF genes (*MoFOX1* and *MoFOX2*) did not show any noticeable changes and was not successful even after repeated attempts, respectively. These results suggested that *MoFKH1* and *MoHCM1* are important in fungal development and that *MoFKH1* is further implicated in pathogenicity and stress response in *M. oryzae*. During the TGR of FOX TF genes, undesirable ectopic transformants were dominantly produced and hindered efficient progress. To compensate for the low efficiency of gene

disruption by TGR, a novel Bidirectional-Genetics (BiG) platform which combines both forward and reverse genetic strategies by recycling ectopic transformants as a source for random insertional mutants was developed. Ectopic transformants with mutations in three genes involved in histidine biosynthesis (*MoHIS5*), vegetative growth (*MoVPS74*), or conidiophore formation (*MoFRQ*) were discovered and characterized in *M. oryzae*. Furthermore, an improved screening method for gene-deleted mutants was proposed for rapid classification of desired mutants and ectopic transformants. This PCR-only method which consisted of 1) direct and priority-based PCR and 2) inverse PCR retains high accuracy and dramatically reduces the time, labor, and expenditure. Taken together, these studies would provide efficient methods for high-throughput functional genomic studies in fungi.

KEY WORDS: *Magnaporthe oryzae*, Forkhead-box transcription factor, Bidirectional genetics platform, Two-step-PCR based mutant screening, pHenome platform, High-throughput phenotyping.

Student number: 2007-21371

CONTENTS

CHAPTER 2. Roles of Forkhead-box Transcription Factors in Controlling Development, Pathogenicity, and Stress Response in *Magnaporthe oryzae*

CHAPTER 3. Bidirectional Genetics Platform: a Dual Purpose Mutagenesis Strategy for Filamentous Fungi

CHAPTER 4. A Quick and Accurate Screening Method for Fungal Gene-deletion Mutants by Direct, Priority-based, and Inverse PCRs

LIST OF TABLES

LIST OF FIGURES

page

CHAPTER 1

CHAPTER 2

CHAPTER 3

CHAPTER 4

CHAPTER 1

pHenome: a Novel Platform for Systematic Phenotype Screening of Filamentous Fungi

ABSTRACT

Rapid accumulation of genome sequence data, in combination with high-throughput mutagenesis techniques, accelerates large-scale gene functional studies. Screening of phenotypes associated with resulting mutants often becomes a main bottleneck in such studies due to time-consuming and labor-intensive natures of most screening schemes, which calls for a novel platform for high-throughput phenotype screening. Although several microplate-based assays exist, their application to filamentous fungi has been difficult due to uneven distribution of cells. Here, we present pHenome - a new phenomics platform for filamentous fungi. This platform is based on pH change of culture media, caused by physiological status of fungal cells, in response to various stimuli. Change in medium pH, indicated by two pH-sensitive dyes (bromocresol purple and phenol red), was continuously monitored using a microplate reader. The platform was validated using *Magnaporthe oryzae* strains, which showed that fungal responses to various stresses could be reliably detected within 24 hours. This phenomics platform offers a novel, high-throughput method for systematically studying gene function in filamentous fungi, facilitating functional genomic analyses.

INTRODUCTION

Massive release of genome information with annotating a lot of hypothetical genes (Choi et al., 2013) and numerous mutant libraries generated via targeted or random mutagenesis have facilitated the functional genomic studies. To understand the each gene function using the mutant libraries, there is a demand for systematic evaluation of mutant phenotype which is called the high-throughput phenotyping (HTP). In fungal research, several HTPs were used to analyze the effect of mutation on phenotypes. In yeast *Saccharomyces cerevisiae*, an almost complete collection of gene-deleted mutants was constructed and phenotypically analyzed with molecular bar codes to show the genes essential for several conditions (Giaever et al., 2002). Jeon et al. reported a massive phenotype screening of mutants generated via *Agrobacterium tumafaciens*-mediated transformation (ATMT) and found 202 novel pathogenicity loci in genome of the rice blast fungus *Magnaporthe oryzae* (Jeon et al., 2007). *Neurospora* mutant strains bearing deletions of 103 genes encoding transcription factors were analyzed and revealed multiple defects (Colot et al., 2006). Son et al. generated null mutants of 657 putative transcription factor genes in *Fusarium graminearum* and systemically screened the phenotypes of them in 17 categories (Son et al., 2011).

Additionally, HTP is also essential for profiling the representative isolates of wild-type lineages and experimentally evolved strains (Jeon et al., 2013), or to observe differences caused by epigenetic changes (Rando and Verstrepen, 2007). Given that the phenotypic profiling is fundamental in almost field of biological research, it promises the versatility of HTP.

The mostly used method for observing the response of wild-type and mutant strains to various environments is based on the inhibition rate of mycelial growth. However, this method is inadequate in a large-scale experiment because it is time-consuming and entails labor-intensive processes. The methodological diversity also causes bottleneck and hinders the comparative phenotypic analysis. Thus there is a demand for more efficient, rapid, and standardized HTP platform. Warringer and Blomberg proposed an automated HTP method for yeast *Saccharomyces cerevisiae* using the micro-cultivation. To quantitatively compare the growth responses of yeast strains to various conditions, they continuously measured the optical density (OD) of liquid culture to estimate cell concentration (Warringer and Blomberg, 2003). The Phenotype Microarray technology is also well-known system which automatically and continuously monitors the cellular responses by the colorimetric measurement of respiration using a tetrazolium dye (Bochner et al., 2001). Additionally, the real-time cell electric sensing method was

proposed for label-free monitoring in cell-based assays via measuring the electrical impedance as an indicator (Solly et al., 2004). Although these automated HTP methods enhanced the efficiency of phenomic study, they are not optimized for analyzing multicellular organisms such as filamentous fungi. Given that current methods are measuring the light absorbance by cells, indicator conversion in cells, or change in electric impedance via cell attachment to estimate growth, they are not suitable for examine the organisms with showing the cells that are unevenly distributed or grow filamentous form without attachment on the bottom of plate. In addition, some of them require high-priced reagents and specialized instruments (Bochner et al., 2001; Solly et al., 2004).

To solve the problem, we proposed a novel HTP system called 'pHenome' for proper analysis of filamentous fungi. Given that many fungi such as *Alternaria alternata* (Eshel et al., 2002), *Aspergillus nidulans* (Freitas et al., 2007), *Botrytis cinerea* (Manteau et al., 2003), *Colletotrichum* sp. (Prusky et al., 2001), *Metarhizium anisopliae* (St Leger et al., 1999), *Penicillium* sp. (Prusky et al., 2004), and *Sclerotinia sclerotiorum* (Rollins, 2003) are reported to continuously change its ambient pH in culture, pHenome measures the culture pH with a chemical indicator and evaluates the physiological status of cells indirectly. To validate the pHenome, we used the rice blast fungus, *M. oryzae*

as a model. This fungus is a causal agent of the most destructive disease on rice and one of actively researched filamentous fungi with its completely sequenced genome (Dean et al., 2005) and several large-scale mutant libraries generated via ATMT (Jeon et al., 2007) and restriction enzyme-mediated integration (REMI) (Sweigard et al., 1998). The background research about pH modifying activity of *M. oryzae* and design of pHenome system with its validation with several *M. oryzae* strains will be presented. Additionally, to confirm the validity of pHenome in other filamentous fungi, we analyzed the pH modifying activity of the head blight fungus, *F. graminearum* and further directions for employing pHenome in various fungal species will be discussed.

MATERIALS AND METHODS

I. Fungal strains and culture conditions

M. oryzae wild-type (KJ201, 70-15, and Guy11) and mutant (Δ*Mocrz1* and Δ*Mohox5*) (Choi et al., 2009; Kim et al., 2009) strains were obtained from the Center for Fungal Genetic Resources at Seoul National University (CFGR, http://genebank.snu.ac.kr) and cultured on V8 juice agar (V8A) (80 ml of V8 juice, 310 μl of 10N NaOH, and 15 g of agar per liter) under 25℃ and constant fluorescent light to promote conidiation. *F. graminearum* wild-type (Z-3639) strain was obtained from the Mycotoxicology Laboratory, Seoul National University, Seoul, Korea and cultured on modified conidiation-promoting agar for *Fusarium* (MCAF) (2.5 g of peptone, 1 g of yeast extract, 30 g of casamino acids, 2 g of $NaNO_3$, 1 g of KH_2PO_4, 0.5 g of $MgSO_4 \cdot 7H_2O$, 0.5 g of KCl, 0.2 ml of trace element solution, 10 ml of vitamin supplement solution, and 15 g of agar per liter) under 25℃ and well-aerated condition to induce conidiation.

II. Preparation of fungal spores

Conidial suspension was used as an inoculum for liquid culture. To inoculate *M. oryzae* in large volume (100 ml) of liquid media, conidia were collected from over 7-day-old V8A culture via gently rubbing surfaces using scraper with 2 ml of sterile water. Concentration of conidial suspension was evaluated using a hemacytometer. To inoculate *M. oryzae* and *F. graminearum* in small volume (100 or 26 μl) of liquid culture in a 96- or 384-well microplate, conidia were collected from 7 to 10-day-old V8A culture and 2-day-old MCAF culture, respectively, via gently rubbing surfaces using scraper with 1 ml of sterile water. After the harvest, conidial suspension was centrifuged (5,000 rpm, 10 min, RT) to remove supernatant (residuals of media). As a washing step, conidia were resuspended by adding 1 ml of sterile water and centrifuged again (5,000 rpm, 10 min, RT) to remove supernatant. Before inoculation, conidia were resuspended using 0.5-1.5 ml of sterile water and filtered with Miracloth (Calbiochem, USA), followed by adjusting their concentrations using a hemacytometer. If there are more than two strains to be inoculated, the concentrations of conidial suspensions were adjusted to be equal.

III. Monitoring of ambient pH change using a pH meter

To measure culture pH over time, 500 μl of conidial suspension of *M. oryzae* KJ201 (approximately 4×10^6 conidia ml^{-1}) was inoculated in 100 ml liquid complete medium (CM; 10 g of glucose, 2 g of peptone, 1 g of yeast extract, 1 g of casamino acids, 6 g of $NaNO_3$, 0.5 g of KCl, 0.5 g of $MgSO_4$, 1.5 g of KH_2PO_4, 1 ml of trace element solution, and 1 ml of vitamin supplement solution per liter) (Talbot et al., 1993), minimal medium (MM; CM without peptone, yeast extract, and casamino acids), and TB3 (10 g of glucose, 200 g of sucrose, 3 g of yeast extract, and 3 g of casamino acids per liter) with three replicates. Initial pH of each medium was adjusted to 6.0-6.5 with 10N NaOH. Cultures were incubated at 25℃ with shaking (150 rpm). Culture filtrates were collected at multiple time points and their pH was measured using a pH meter (SevenEasy pH, Mettler-Toledo, Switzerland).

IV. Monitoring of ambient pH change using two pH indicators

For colorimetric detection of pH change, two chemical indicators, bromocresol purple (BCP) and phenol red (PR), were used. The color of BCP shifts from yellow to purple when pH increases from 5.2 to 6.8, while the color of PR changes from yellow to reddish-pink as pH increases from 6.8 to 8.2. Quantitative analysis of color change via these indicators was performed using

a 96-well microplate and microplate reader (Epoch, BioTek, USA) by measuring the optical density (OD). OD spectra of each pH indicator were determined to identify optimal wavelengths for measurement. After dissolving BCP and PR (final concentration was 0.01%) in 2.5 mM L-aspartic acid solution at various pH (pH 3.5, 4.0, 4.5, 5.0, 5.5, 6.0, 6.5, 7.0, 7.5, 8.0, 8.5, and 9.0), their ODs were measured at 350-700 nm wavelength at 1 nm intervals. Based on the OD spectra, wavelengths of 432, 490, 589, and 700 nm were used for measurements of BCP-dissolved media and 433, 480, 558, and 700 nm were used for PR-dissolved media.

To observe the fungal-driven pH changes in culture filtrates using BCP and PR, conidial suspension of *M. oryzae* KJ201 was inoculated in liquid CM and MM, followed by incubated at 25℃ with shaking (150 rpm). After 15 days of incubation, BCP and PR were added to each culture filtrate at the final concentration of 0.01% to observe the color changes. To detect the possible adverse effects of BCP and PR on mycelial growth of *M. oryzae*, diameters of KJ201 colony grown on solid CM (CM with 1.5% agar) amended with 0.01% BCP or PR were measured at 6 days post-inoculation with three replicates.

V. Characterization of ambient pH change during culturing of *M. oryzae* and *F. graminearum*

To identify an effect of each nutrient on pH by *M. oryzae*, we used a 384-well microplate and inoculated 6.5 μl of conidial suspension of KJ201, Guy11, and 70-15 (approximately 3 to 5 × 10^5 conidia ml^{-1}), followed by adding 6.5 μl of sterile water to help conidia settle down. After pre-incubation for 1 day at 25℃, 13 μl of BCP-dissolved (at final concentration of 0.006%, initial pH 5.0) media which contained individual amino acids (glycine, L-alanine, L-serine, L-threonine, L-cysteine, L-valine, L-leucine, L-isoleucine, L-methionine, L-proline, L-phenylalanine, L-tyrosine, L-tryptophan, L-aspartic acid, L-glutamic acid, L-asparagine, L-glutamine, L-histidine, L-lysine, or L-arginine, initial pH 5.0, at final concentration of 2.5 mM), mixture of 20 amino acids (at final concentration of 0.125 mM each), and sugars (D-arabinose, L-arabinose, D-ribose, D-xylose, D-glucose, D-mannose, D-galactose, D-fructose, L-sorbose, maltose, sucrose, trehalose, lactose, or D-cellobiose, at final concentration of 25 mM) were added and the ODs were measured at predefined wavelengths for 24 hours in 20 minutes interval. To prevent evaporation and ammonia diffusion, optical adhesive film was used to cover top. Data reduction for estimating the culture pH and calculation of pH

modifying activity (ACT_{pH}) were conducted using Gen5 2.0 software (BioTek, USA).

To observe if certain sugars inhibit the ambient alkalinization in *M. oryzae*, conidial suspension of KJ201 (approximately 3 to 5×10^5 conidia ml^{-1}) was inoculated and BCP-dissolved media containing the 2.5 mM L-aspartic acid and 2.5 mM of individual sugars were added after 1 day of pre-incubation, followed by measuring ODs for 24 hours.

To verify if the chemical agents of ambient pH change is volatile, conidial suspension of KJ201 (approximately 3 to 5×10^5 conidia ml^{-1}) was inoculated in 100 μl of 2.5 mM L-aspartic acid (initial pH 5.0) or liquid TB3 (initial pH 7.0) with 0.01% BCP. After 5 days of incubation, color changes of each culture and adjacent wells were observed. Detection of ammonium in culture filtrate was conducted by using Tetratest ammonia test kit (Tetra, Germany).

To monitor the effect of each nutrient on pH by *F. graminearum*, conidial suspension of Z-3639 (approximately 3 to 5×10^5 conidia ml^{-1}) was inoculated and analyzed through the same method used for *M. oryzae*.

VI. Conditions used for phenotype screening

Chemicals that cause stress and their concentrations used for large-scale phenotype screening are shown in Table 1. After dissolving each chemical in

water or EtOH, it was sterilized using a membrane filter with 0.22 μm pore size (Milipore, USA) and added into liquid cultures.

To compare the stress responses of different strains of *M. oryzae*, we inoculated 6.5 μl of conidial suspensions (approximately 3 to 5×10^5 conidia ml^{-1}) in each well of a 384-well microplate, followed by adding 6.5 μl of sterile water to help conidia settle down and then put 6.5 μl of condition determinant solutions (3X concentration of stress-inducible solutions). After 1 day of pre-incubation at 25℃, 6.5 μl of alkalinization-inducing medium (4X concentration; 10 mM L-aspartic acid and 0.024% BCP for *M. oryzae*) was added to each cultures to initiate the alkalinization. Color change of BCP from yellow to purple was continuously recorded using microplate reader for 24 hours in 20 minutes interval. After the measurement, data was corrected and used to calculate response index (RI) to compare different strains as described in result section.

Table 1.Stress inducing compounds used for pHenome screening and the nature of stress caused by them

Name	Description	Final concentration
Water	Control	-
EtOH	Control[a]	0.5%
NaCl	Ionic stress	200 mM
KCl	Ionic stress	200 mM
$MgCl_2$	Ionic stress	200 mM
LiCl	Ionic stress, affecting calcium signaling	100 mM
$CaCl_2$	Ionic stress, affecting calcium signaling	200 mM
FK506	Calcineurin inhibitor	3.3 µg/ml
$LaCl_3$	Blocking calcium channels	0.01 mM
$CuSO_4$	Heavy metal stress	0.01 mM
$ZnSO_4$	Heavy metal stress	0.1 mM
$MnCl_2$	Heavy metal stress	0.1 mM
$CoCl_2$	Heavy metal stress, mimic agent of hypoxic condition	0.01 mM
EDTA	Chelation of metal ions	0.5 mM
2,2-Bipyridyl	Chelation of intracellular Fe^{2+}	0.1 mM

Caffeine	Affecting cAMP signaling	5 mM
Cycloheximide	Protein synthesis inhibitor	0.5 μM
3-Amino-1,2,4-triazole	Amino acid synthesis inhibitor, competitively inhibit HIS3	2 mM
Calcofluor white	Cell wall stress	133 ppm
SDS	Cell wall stress	0.005%
Guanidine thiocyanate	General protein denaturant	10 mM
DTT	ER stress, inhibit disulfide bond formation	0.1 mM
Methyl viologen	Oxidative stress (generate ROS in the cytoplasm)	100 ppm
H_2O_2	Oxidative stress	0.8 mM
p-Coumaric acid	Inhibit fungal growth, plant phenolic compound	70 ppm
$KClO_3$	Toxic analog of KNO3	20 mM
Hydroxyurea	DNA synthesis inhibitor	30 mM
Benomyl	Spindle depolymerization, inhibit chromosome segregation	5 μg/ml

[a] Control for FK506, $CoCl_2$, BIP, and benomyl

RESULTS

I. Patterns of ambient pH change in fungal culture media over time

To follow pH change during vegetative growth of *M. oryzae* in culture, we inoculated KJ201 conidia in liquid complete medium (CM), minimal medium (MM), and TB3. During incubation for up to 15 days, culture pH continually changed, ranging from pH 4 to pH 8 (Fig. 1A). Gradual alkalinization of medium was detected when KJ201 was grown in MM. *M. oryzae* weakly acidified CM during initial few days and then began strongly alkalinizing the medium. After strong acidification in TB3, which contained more sugars (sucrose and glucose) than the other media, during the first week, pH slowly increased. Only the alkalinization was observed after 9 days of incubation in all of three media.

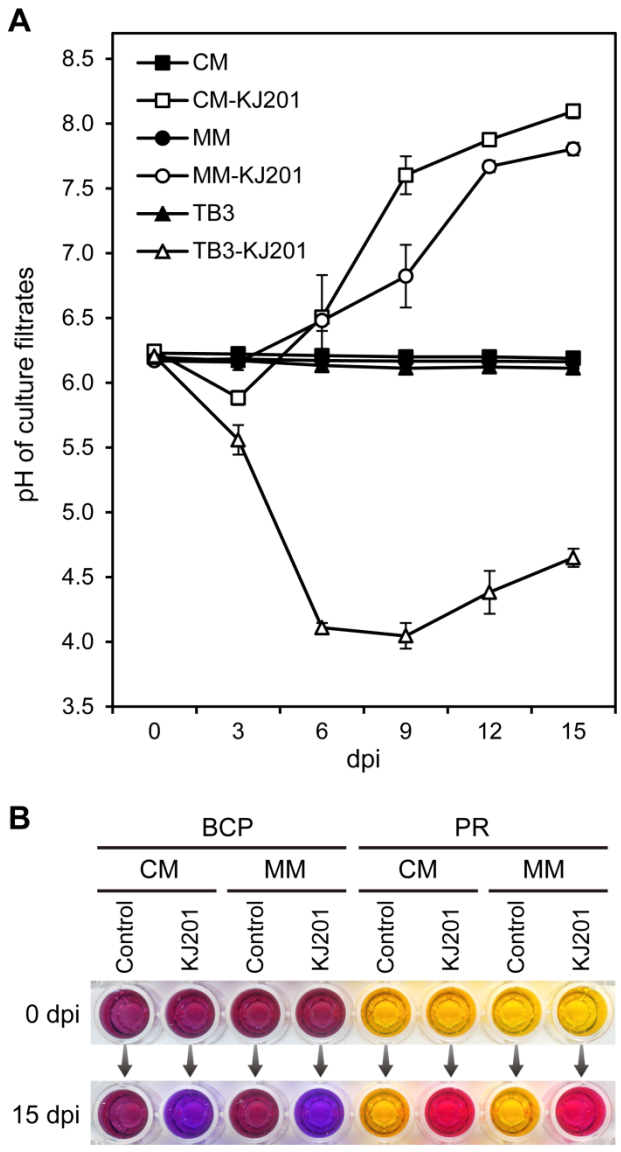

Fig. 1. Changes of pH in *M. oryzae* culture media.

(A) Patterns of pH change in liquid cultures of KJ201 in CM, MM, and TB3 are shown. (B) Two pH indicators, BCP and PR, used for colorimetric detection of culture pH are shown.

II. Quantification of pH change in cultures by measuring optical density (OD)

For rapid analysis of pH change, we used two chemical indicators, bromocresol purple (BCP), and phenol red (PR), based on their transition pH ranges that were corresponded the range of pH change by *M. oryzae*. Alkalinization in CM and MM by KJ201 was easily detected via color change with adding these indicators (Fig. 1B). We analyzed OD spectra of BCP and PR and found that ODs at 589 and 558 nm wavelengths (OD589 and OD558) were increased while ODs at 432 and 433 nm (OD432 and OD433) were decreased during alkalinization and the 490 and 480 nm wavelengths were isosbestic point in BCP- and PR-dissolved media, respectively. The least amount of light was absorbed at 650-700 nm in both two indicators (Fig. 2A and 2B). Because there exist background OD due to light absorbance by a microplate, media without a pH indicator, grown mycelia, optical adhesive film which is used to cover top, and dews formed on cover, ODs at 700 nm (OD700) were measured to estimate the background. To quantitatively evaluate pH change, OD589, OD432, and OD700 of liquid containing BCP and OD558, OD433, and OD700 of liquid containing PR were measured by microplate reader. OD at 490 nm (OD490) and 480 nm (OD480) were optionally checked to detect possible degradation or inactivation of BCP or PR,

respectively. After the measurement, OD700 was subtracted from other ODs to eliminate background. These corrected ODs (cODs) were used to estimate and monitor the pH change with calculations adopted from a previous study (Xu et al., 2006). Since BCP and PR exhibited reversible acid-base behavior, the acid dissociation constant of acid form (IndH) and base form (Ind) is:

$K = [Ind] \times [H^+] / [IndH]$, (where "Ind" means pH indicator)

And relation between the pH and concentration of each form of pH indicator is:

$pH = -\log_{10}[H^+]$,

$pK = -\log_{10}K$,

$pH = pK + \log_{10}([Ind] / [IndH])$ (1)

By the definition of OD and Lambert-Beer's law,

$cOD589 \text{ or } cOD558 = -\log_{10}(I_{Ind} / I_0) = \varepsilon_{Ind} \times [Ind] \times d$ (2),

$cOD432 \text{ or } cOD433 = -\log_{10}(I_{IndH} / I_0) = \varepsilon_{IndH} \times [IndH] \times d$ (3)

(where "I" is transmitted light intensity with each form of pH indicator, "I_0" means incident light intensity, "ε" is the extinction coefficient of each form of pH indicator, and "d" is the distance the light pass through the material)

From the equations (1), (2), and (3),

$pH = pK + \log_{10}(\varepsilon_{IndH} / \varepsilon_{Ind}) + \log_{10}(cOD589 / cOD432)$ for BCP,

$pH = pK + \log_{10}(\varepsilon_{IndH} / \varepsilon_{Ind}) + \log_{10}(cOD558 / cOD433)$ for PR

Based on these formula, we calculated $\Delta\log_{10}(cOD589 / cOD432)$ and $\Delta\log_{10}(cOD558 / cOD433)$ that reflects pH change for further analysis. The $\log_{10}(cOD589 / cOD432)$ and $\log_{10}(cOD558 / cOD433)$ was also showed linear correlations with pH in certain ranges (Fig. 2C and 2D). To assess if BCP and PR has an adverse effect to *M. oryzae* growth, colonial growths of KJ201 on solid CM amended with 0.01% BCP or PR were observed. As a result, BCP was selected to be a major indicator because it didn't inhibit the growth of *M. oryzae* while PR led to slight retardation (Fig. 2E). To estimate the pH modifying activity from OD data, the area under the curve (AUC) of $\Delta\log_{10}(cOD589 / cOD432)$ versus time graph was calculated (Fig. 3). As an abbreviation, $\log_{10}(cOD589 / cOD432)$, $\Delta\log_{10}(cOD589 / cOD432)$, and pH modifying activity was called 'OD_{pH}', 'ΔOD_{pH}', and 'ACT_{pH}', respectively.

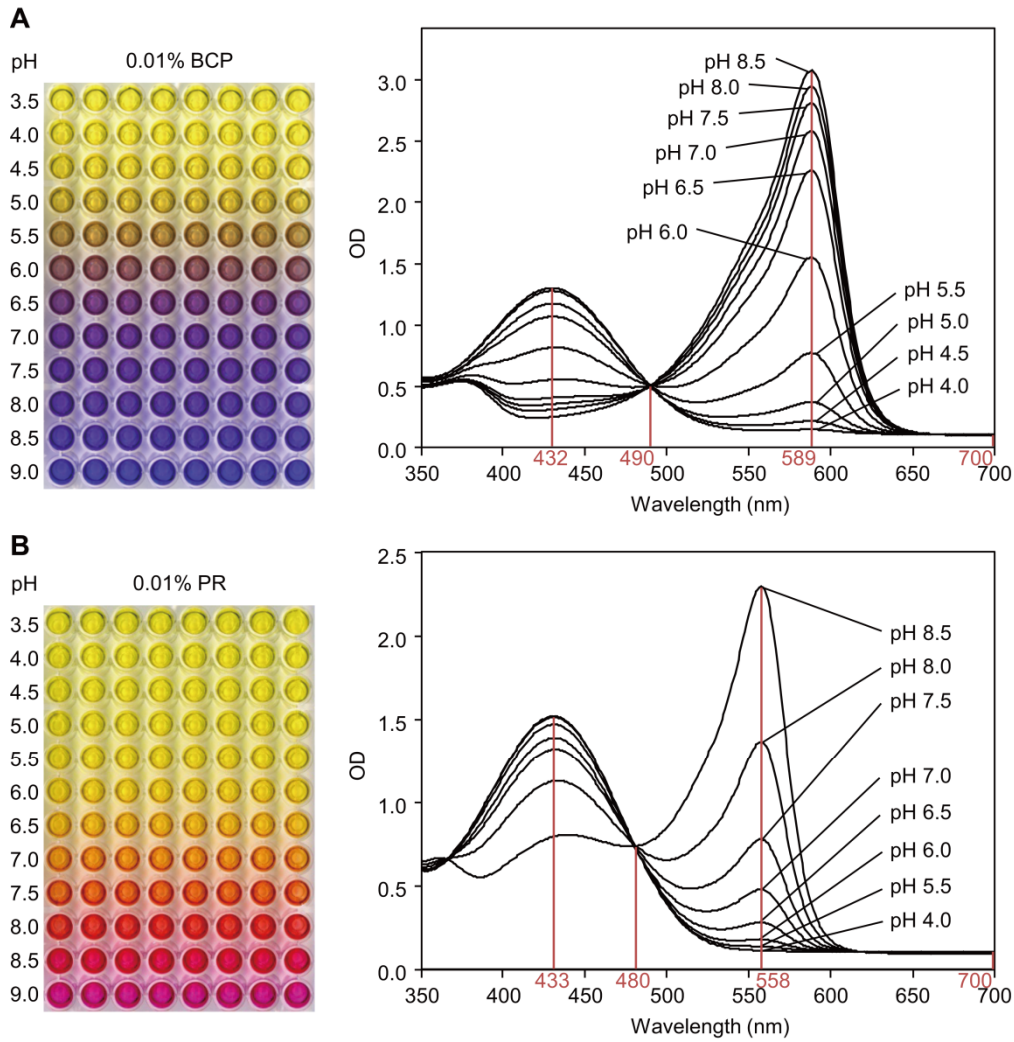
A
pH
0.01% BCP
3.5
4.0
4.5
5.0
5.5
6.0
6.5
7.0
7.5
8.0
8.5
9.0
pH 8.5
pH 8.0
pH 7.5
pH 7.0
pH 6.5
pH 6.0
pH 5.5
pH 5.0
pH 4.5
pH 4.0
OD
Wavelength (nm)
432
490
589
700
B
pH
0.01% PR
pH 8.5
pH 8.0
pH 7.5
pH 7.0
pH 6.5
pH 6.0
pH 5.5
pH 4.0
OD
Wavelength (nm)
433
480
558
700
C
y = 0.827x - 4.7499
R² = 0.9955
BCP
pH
D
y = 0.702x - 5.4611
R² = 0.9975
PR
pH
E
Mycelial growth (mm)
TCM
TCM + 0.01% BCP
TCM + 0.01% PR
*

Fig. 2. Estimation of pH by measuring ODs in BCP- and PR-dissolved media and adverse effect of PR in fungal growth.

Color changes and OD spectra of (A) BCP and (B) PR in various pH are shown. Linear correlations between OD_{pH} and pH in (C) BCP- or (D) PR-dissolved media are shown. (E) Mycelial growth of *M. oryzae* on solid CM amended with 0.01% BCP or PR is shown.

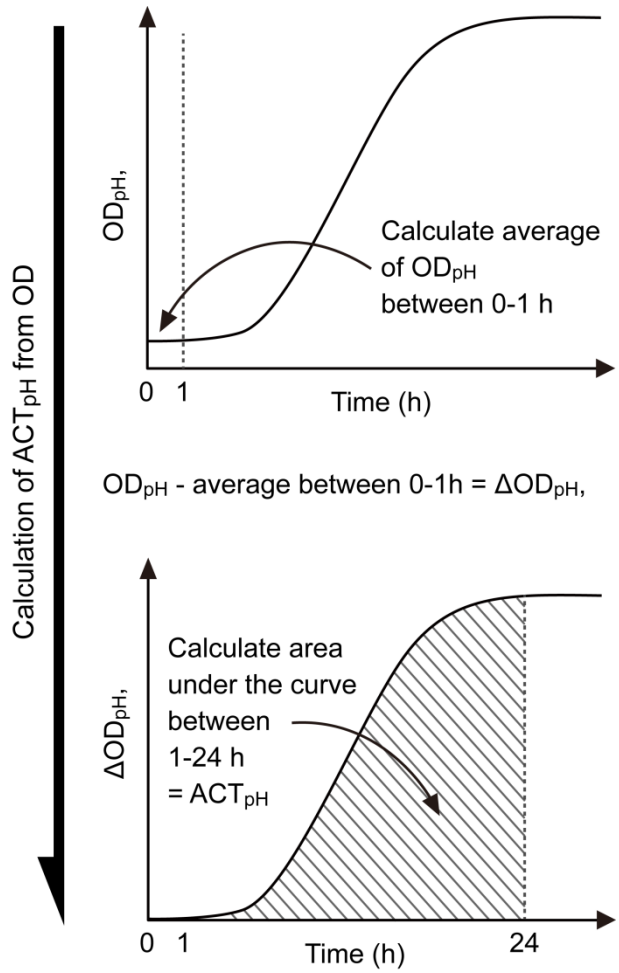

Fig. 3. Calculation of ACT_{pH} via OD measurement.

From the mean of initial OD_{pH}s between 0-1 hours after measurement, ΔOH_{pH} is calculated. The area under the curve of ΔOD_{pH} versus time graph was regarded as ACT_{pH}.

III. Alkalinization was driven by ammonium secretion and strongly induced by certain amino acids

Amino acids can be used as a nutrient through the deamination process and it causes production and secretion of excess amount of ammonium, followed by alkalinizing ambient. To observe the amino acid-induced alkalinization in *M. oryzae*, we inoculated conidia of wild-type strains (KJ201, Guy11, and 70-15) in microplate with individual or mixed amino acids. Nine out of 20 amino acids, glycine, L-alanine, L-serine, L-proline, L-aspartic acid, L-glutamic acid, L-asparagine, L-glutamine, and L-arginine led to significant alkalinization within 24 hours and among them, L-aspartic acid induced the most significant change in all of three wild-type strains (Fig. 4A). As a result, L-aspartic acid was used for inducing rapid alkalinization by *M. oryzae* in further study. The alkalinizing agent was volatile and diffused to adjacent wells in a microplate (Fig. 4B) and 1-day-old KJ201 cultures in 2.5 mM L-aspartic acid accumulated ammonium while sucrose reduced the ammonium production (Fig. 4C).

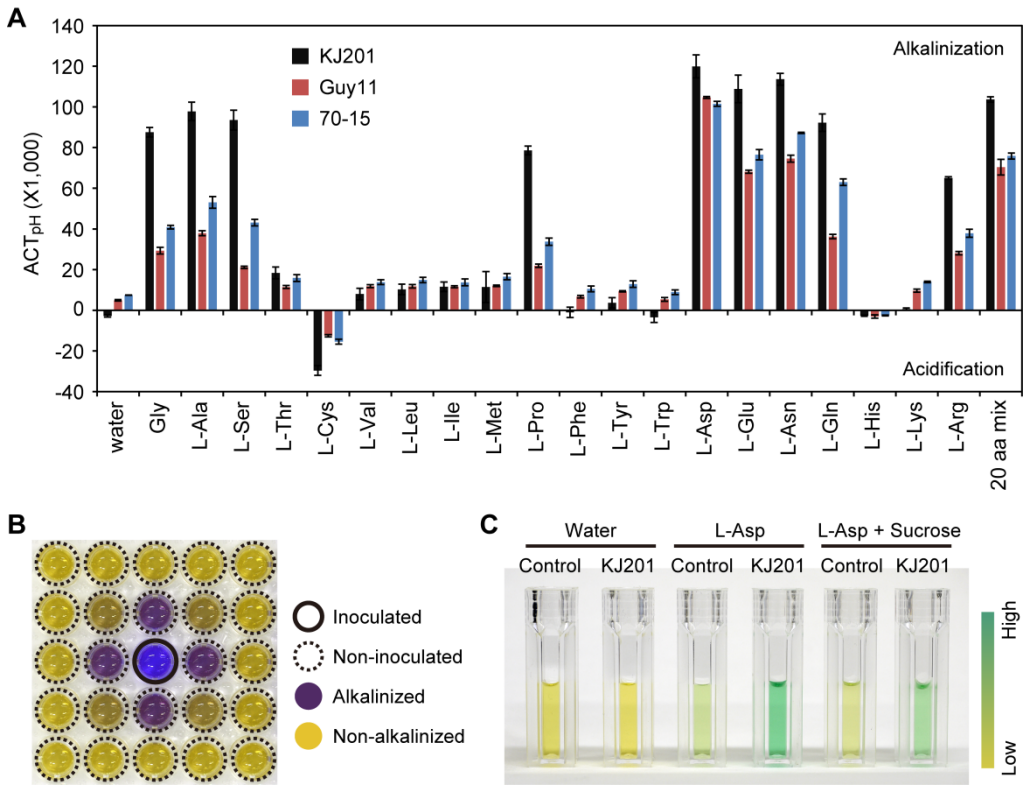

Fig. 4. Ammonium accumulation and ambient alkalinization in *M. oryzae* cultures by certain amino acids.

(A) The ACT_{pH}s of *M. oryzae* wild-type strains (KJ201, Guy11, and 70-15) driven by individual or mixed amino acids are shown. (B) *M. oryzae* produced volatile compound that was responsible for alkalinization. (C) Accumulations of ammonium in liquid cultures of KJ201 are shown.

IV. Sugars induce acidification

Since high concentration of sugar (sucrose and glucose) in TB3 is possibly responsible to dramatic acidification by *M. oryzae*, we observed cultures of KJ201, 70-15, and Guy11 with individual sugars. Seven out of 14 sugars, D-glucose, D-mannose, D-fructose, maltose, sucrose, trehalose, and D-cellobiose led significant acidification within 24 hours in all of three wild-type strains (Fig. 5A) and when individual sugars and L-aspartic acid were mixed in culture, alkalinization was significantly delayed (Fig. 5B). The acidifying agent was non-volatile and did not diffuse to adjacent wells (Fig. 5C). Although D-xylose, D-galactose, and L-sorbose didn't induce acidification, they inhibited alkalinization which indicated that this inhibition is not due to production of acidifying agents.

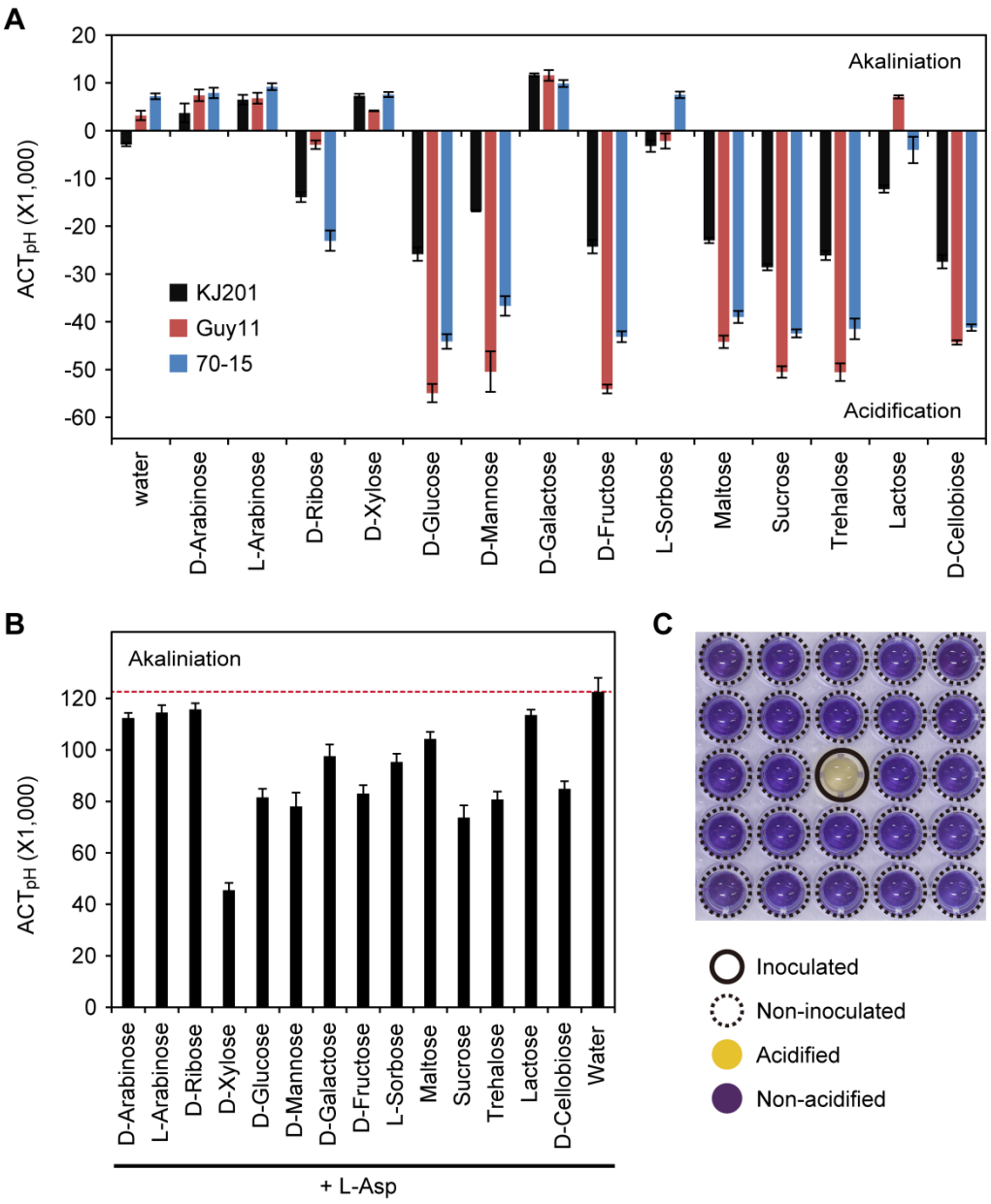

Fig. 5. Ambient acidification and reduced alkalinization in *M. oryzae* cultures by certain sugars.

Fig. 5. (continued)

The ACT_{pHS} of *M. oryzae* wild-type strains (KJ201, Guy11, and 70-15) driven by (A) individual sugars and (B) mixture of sugar and L-aspartic acid are shown. (C) Compound responsible for ambient acidification was non-volatile.

V. Design of a HTP platform based on alkalinizing activity

A new HTP platform optimized for filamentous fungi was designed based on patterns of the ambient pH change in fungal culture as indirect indicators of cellular response to individual conditions or stimuli. Although *M. oryzae* has a dual ability to alkalinize or acidify the ambient, the former was selected as an indicator because it showed most rapid and reproducible results with L-aspartic acid. Additionally, acidification was effectively repressed via nutritional control during measurement of alkalinization whereas alkalinization was difficult to repress completely even by adding sugars. Protocol of this HTP system called 'pHenome' is presented in Fig. 6. Conidia of individual *M. oryzae* strains were inoculated in microplate with or without treatment of chemicals causing stresses. After the pre-incubation for 24 hours, the ‘alkalinization-inducing medium’ containing L-aspartic acid and BCP was added to induce alkalinization and we continuously measured ODs to examine the changes in ACT_{pH} by specific stresses. To validate pHenome, liquid cultures of KJ201 were analyzed after treatment of hydroxyurea, cycloheximide, and H_2O_2. We confirmed delayed alkalinization and reduced ACT_{pH} in response to increasing concentration of each stress-inducing chemical (Fig. 7). Finally, response index (RI) of each sample strain (analysis target strain, i.e. mutant) in individual conditions were calculated for easier

comparison with reference strain (standard strain, i.e. wild-type) (Fig. 8). If stress responses of sample and reference strains are same, RI = 1. RI < 1 or RI > 1 means that sample strain is more sensitive or tolerant to stress than reference strain, respectively. RI couldn't be calculated when ACT_{pH} of reference strain was severely decreased (ACT_{pH} in stress / ACT_{pH} in NT < 0.2) because it meant almost conidia lost its activity and it frequently led errors in results.

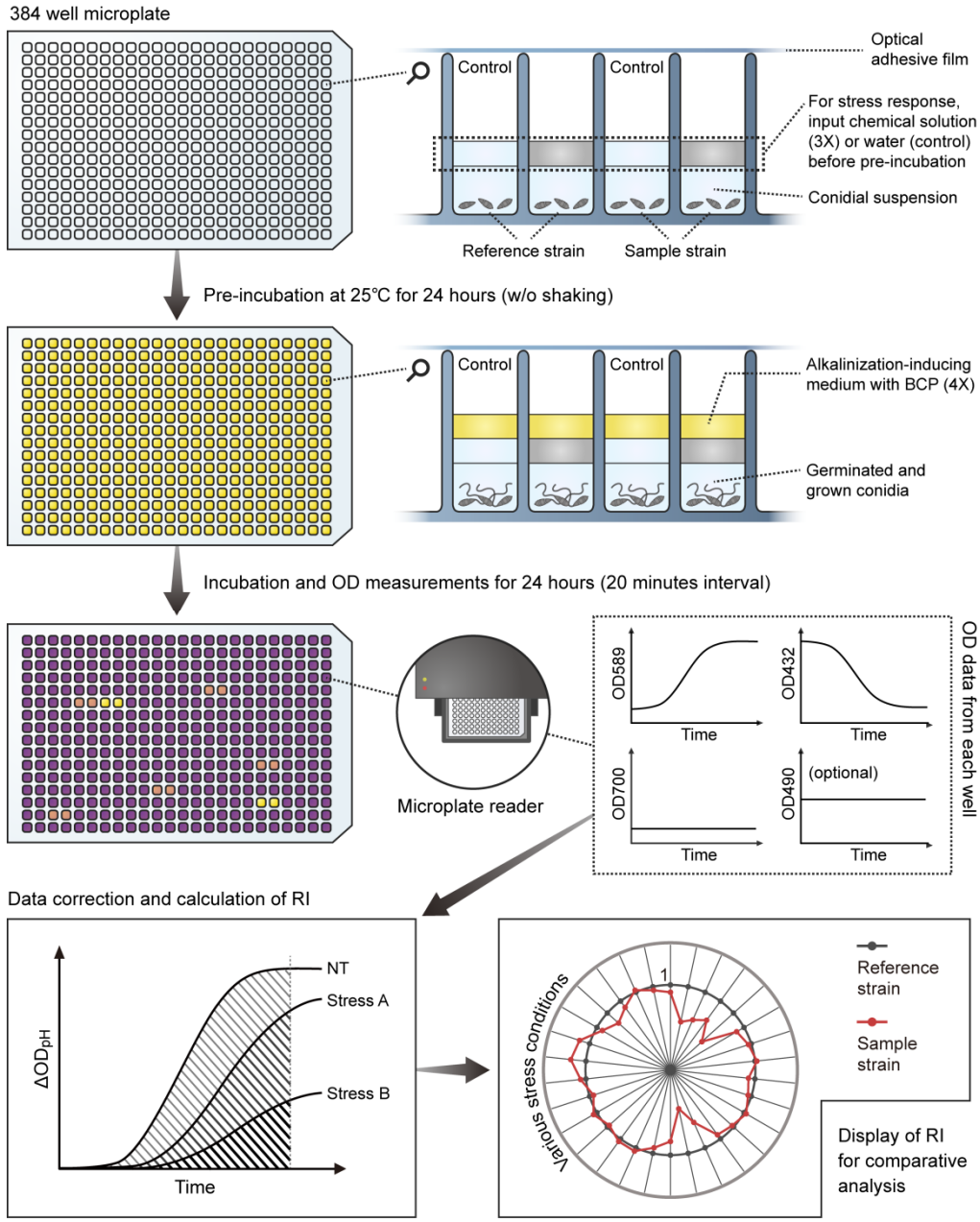

Fig. 6. Schematic diagram of a pHenome protocol.

Fig. 6. (continued)

Stress responses of individual fungal strains are evaluated and compared via monitoring the culture pH under various growth conditions.

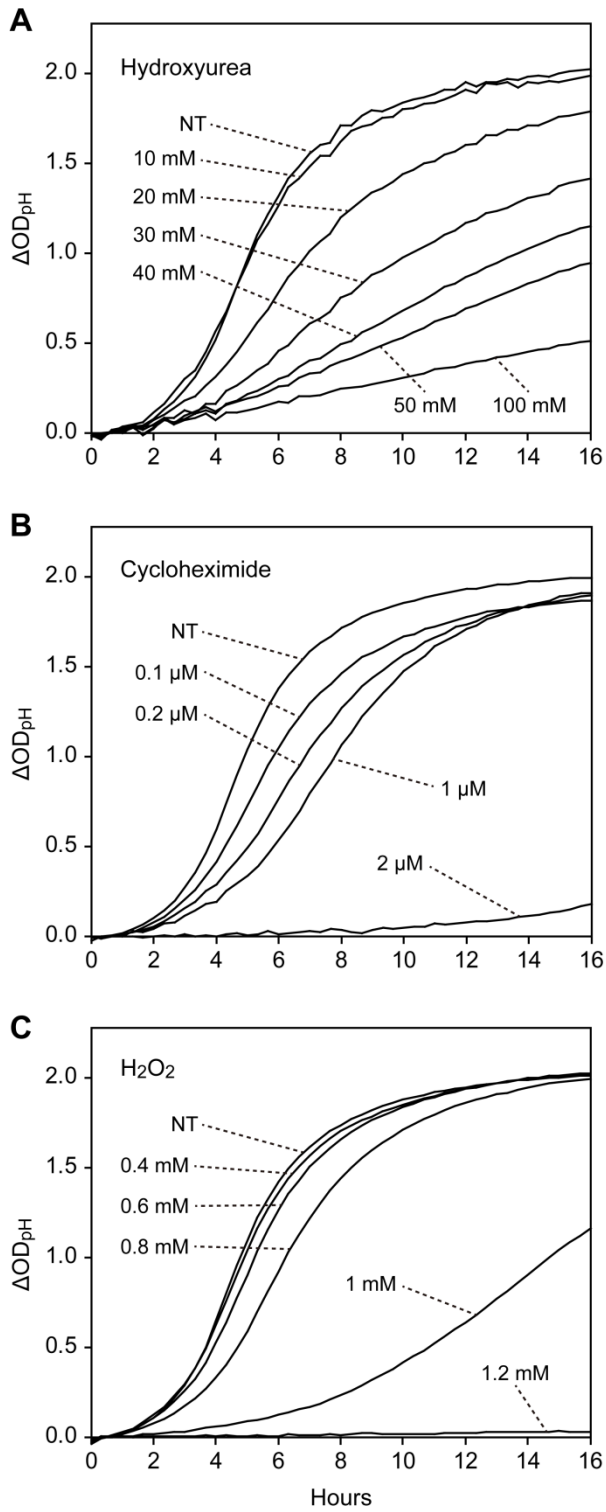
A
Hydroxyurea
NT
10 mM
20 mM
30 mM
40 mM
50 mM
100 mM
ΔODpH
B
Cycloheximide
NT
0.1 μM
0.2 μM
1 μM
2 μM
ΔODpH
C
H2O2
NT
0.4 mM
0.6 mM
0.8 mM
1 mM
1.2 mM
ΔODpH
Hours

Fig. 7. Reduced ΔOD_{pH} under various stressful conditions.

The ΔOD_{pH} versus time graphs resulted from analyzing *M. oryzae* cultures with various concentrations of hydroxyurea, cycloheximide, and H_2O_2 are shown.

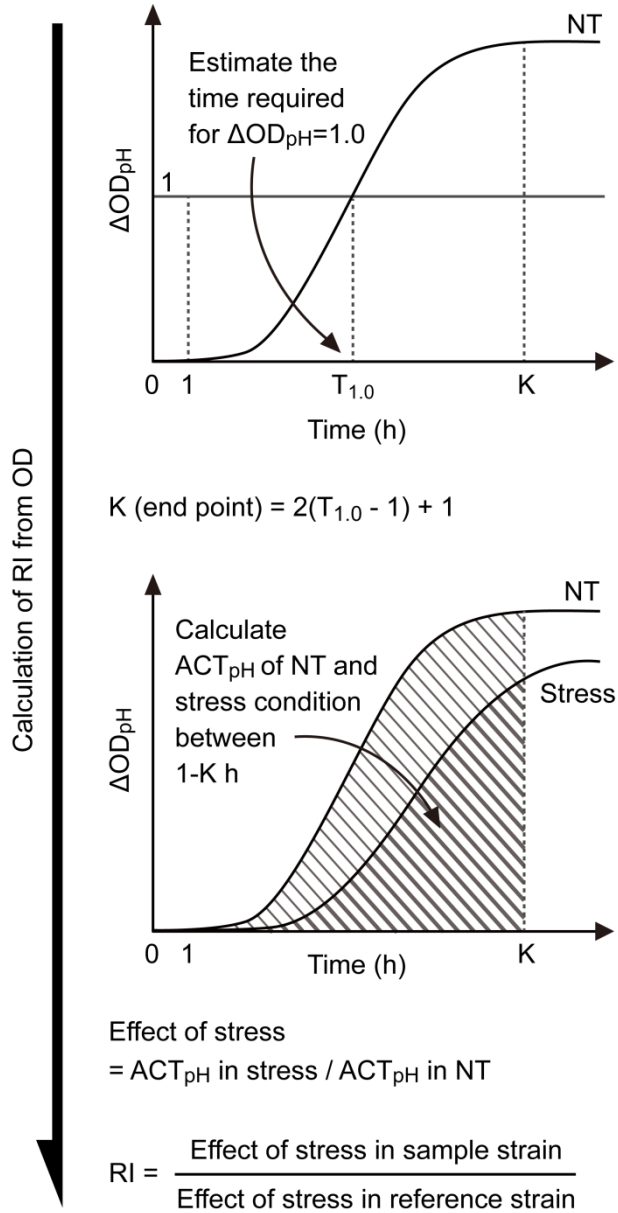

Fig. 8. Calculation of RI to compare sample and reference strains.

Fig. 8. (continued)

Specific end point of incubation time (K) is determined via estimate the time required for $\Delta OD_{pH} = 1$ and then K is used to measure area under the curves (ACT_{pH}). Effect of stress and RI is defined as described.

VI. Stress responses in several *M. oryzae* wild-type and mutant strains

Using pHenome, stress responses of a previously characterized *M. oryzae* mutant, Δ*Mocrz1* (Choi et al., 2009), were evaluated under multiple conditions (Table 1). While most responses of Δ*Mocrz1* were indistinguishable from KJ201, the wild-type strain from which Δ*Mocrz1* was generated, noticeable RI was found with treatment of $CaCl_2$ (Fig. 9A). The Δ*Mohox5* (Kim et al., 2009), a deletion mutant of homeobox transcription factor gene, showed dramatic change in RI with calcium related stress ($CaCl_2$ and $LaCl_3$), heavy metal stress ($ZnSO_4$, $MnCl_2$, and $CoCl_2$), oxidative stress (methyl viologen), and treatment of plant phenolic compound (p-Coumaric acid) (Fig. 9B). When we compared three different wild-type strains of *M. oryzae*, different responses to various stressful conditions were observed. (Fig. 9C).

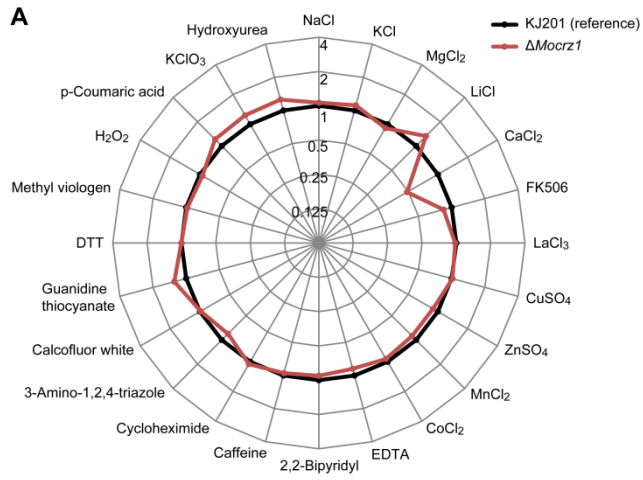
A
KJ201 (reference)
ΔMocrz1
NaCl
KCl
MgCl2
LiCl
CaCl2
FK506
LaCl3
CuSO4
ZnSO4
MnCl2
CoCl2
EDTA
2,2-Bipyridyl
Caffeine
Cycloheximide
3-Amino-1,2,4-triazole
Calcofluor white
Guanidine thiocyanate
DTT
Methyl viologen
H2O2
p-Coumaric acid
KClO3
Hydroxyurea
4
2
1
0.5
0.25
0.125

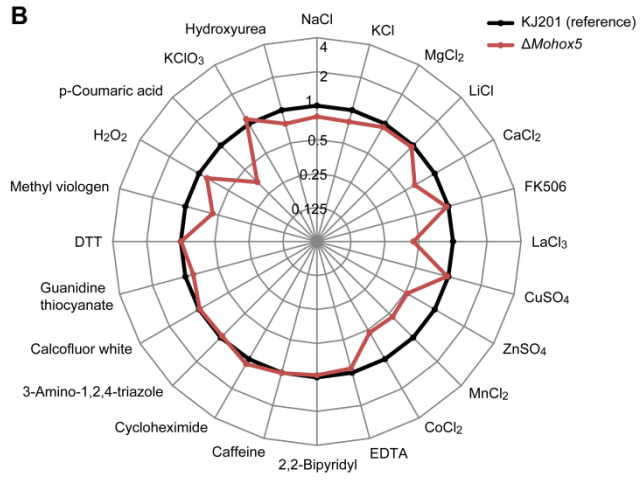
B
KJ201 (reference)
ΔMohox5
NaCl
KCl
MgCl2
LiCl
CaCl2
FK506
LaCl3
CuSO4
ZnSO4
MnCl2
CoCl2
EDTA
2,2-Bipyridyl
Caffeine
Cycloheximide
3-Amino-1,2,4-triazole
Calcofluor white
Guanidine thiocyanate
DTT
Methyl viologen
H2O2
p-Coumaric acid
KClO3
Hydroxyurea
4
2
1
0.5
0.25
0.125

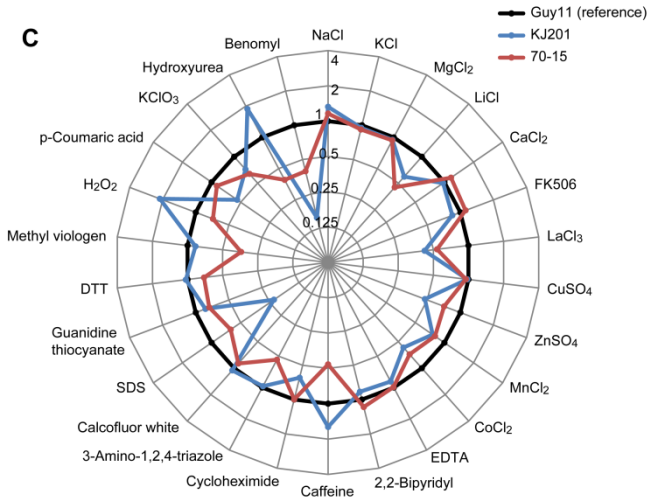
C
Guy11 (reference)
KJ201
70-15
NaCl
KCl
MgCl2
LiCl
CaCl2
FK506
LaCl3
CuSO4
ZnSO4
MnCl2
CoCl2
EDTA
2,2-Bipyridyl
Caffeine
Cycloheximide
3-Amino-1,2,4-triazole
Calcofluor white
SDS
Guanidine thiocyanate
DTT
Methyl viologen
H2O2
p-Coumaric acid
KClO3
Hydroxyurea
Benomyl
4
2
1
0.5
0.25
0.125

Fig. 9. Application of pHenome for comparative analysis of stress responses among different *M. oryzae* strains.

(A) RIs of KJ201 (wild-type) and Δ*Mocrz1* (mutant) in 24 stressful conditions are shown. (B) RIs of KJ201 (wild-type) and Δ*Mohox5* (mutant) in 24 stressful conditions. (C) RIs of three wild-type strains of *M. oryzae* (KJ201, 70-15, and Guy11) in 26 stressful conditions.

VII. Ambient pH change in *F. graminearum* cultures by certain nutrients

To prove the applicability of pHenome in filamentous fungi other than *M. oryzae*, we used *F. graminearum* and analyzed its activity of ambient pH change. When Z-3639 was incubated with individual or mixed amino acids, rapid alkalinization was observed within 24 hours. Among 14 out of 20 amino acids (glycine, L-alanine, L-serine, L-threonine, L-valine, L-isoleucine, L-proline, L-phenylalanine, L-tryptophan, L-aspartic acid, L-glutamic acid, L-asparagine, L-glutamine, and L-arginine) which induced significant pH increase, L-asparagine led the most immediate ambient alkalinization. On the other hand, all of treated sugars except lactose and D-cellobiose induced significant acidification compared to non-treated (water). *M. oryzae* and *F. graminearum* responded similarly to amino acids and sugars but in some nutrients such as L-threonine, L-valine, L-isoleucine, L-phenylalanine, L-tryptophan, D-arabinose, L-arabinose, D-xylose, D-galactose, and L-sorbose, distinct patterns of pH change were detected.

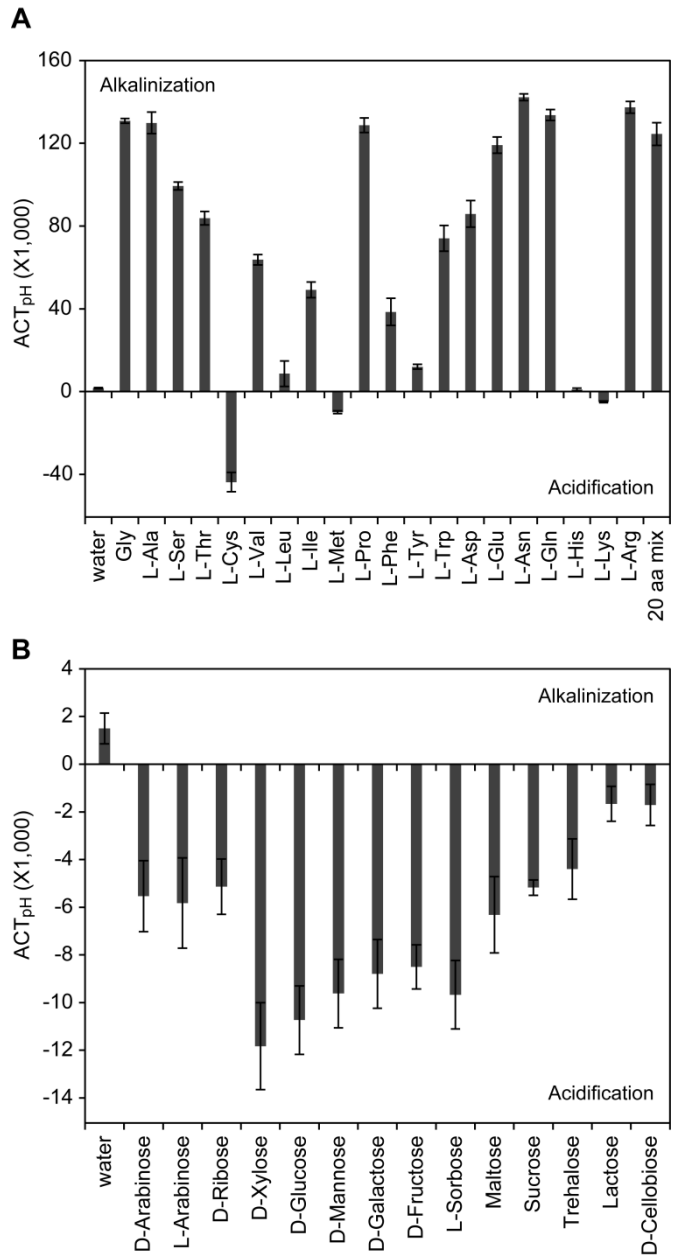

Fig. 10. Ambient alkalinization and acidification by *F. graminearum* by certain amino acids and sugars, respectively.

Fig. 10. (continued)

(A) The ACT_{pH}s of *F. graminearum* z-3639 driven by individual or mixed amino acids in liquid cultures are shown. (B) The ACT_{pH}s of *F. graminearum* z-3639 driven by individual sugars in lquid cultures are shown.

DISCUSSION

Growing needs for HTP in functional genomics demand a novel tool which is easy to employ and standardize and also enables rapid research. This study proposed and validated a new tool, pHenome, for phenomics study in filamentous fungi. Based on the techniques of tracking changes in culture pH via colorimetic measurements and inducing cells to alkalinize the culture rapidly, we used the alkalinizing activity of cells as an indirect indicator and estimated the physiological status of fungal strains under various conditions.

The quad wavelength reads with BCP or PR, including the optional measurement at isosbestic point, showed high accuracy in pH estimation (Fig. 2). Subtraction of OD700 from other ODs countervailed noises caused by background OD and calculating the ratio of cOD589 and cOD432 or cOD558 and cOD433 effectively removed the errors from unequable input of the indicator (probably due to pipetting errors). BCP was mainly used as a pH indicator in pHenome and clearly displayed the culture alkalinization between pH 3.5-7 without affecting the *M. oryzae* growth. Although PR slightly inhibits the mycelial growth, its long-lasting property in culture compared to BCP and alkalescent range of detectable color change (between pH 5-9) still make it usable for assays with longer incubation or higher initial pH.

The ability of changing the ambient pH (alkalinization or acidification) is commonly found in many filamentous fungi (Eshel et al., 2002; Freitas et al., 2007; Manteau et al., 2003; Prusky et al., 2001; Prusky et al., 2004; Rollins, 2003; St Leger et al., 1999) and that supports the broad applicable range of pHenome platform. Our result also indicated the dual ability of *M. oryzae* to changing the culture pH in nutrient-dependent manner. However, the pH change in routinely used media (CM, MM, and TB3) was very slow and takes more than a week to achieve the significant alkalinization. Using L-aspartic acid as a sole nutrient immediately induced the cells to alkalinize and it successfully solved the problem. According to the previous reports showing that the ambient alkalinization is driven by the excretion of ammonium outside the cell (Prusky and Yakoby, 2003), rapid pH change with L-aspartic acid may due to the ammonium production through the deamination of this amino acid. As evidences, we observed that, 1) the alkalinizing agent was volatile, 2) the ammonium was highly accumulated in alkalinized culture filtrate, and 3) the ammonium was less accumulated with reduced alkalinization when certain sugars were added for more preferable carbon sources than L-aspartic acid. Although retarded alkalinization by sugars is partially caused by production of organic acids, some sugars such as D-xylose, D-galactose, and L-sorbose showed little activity of acidification but led to significant inhibition of

alkalinization and this result supported our supposition.

Chemical agents causing stresses affected the culture alkalinization possibly due to 1) changing efficiency of amino acid uptake, 2) altering the catabolism that leads the deamination of amino acids, 3) altering the anabolism that assimilating ammonium to synthesize biomass, and 4) changing the activity of ammonium secretion. The amount of delayed pH change under stressful conditions reflected the influenced cell metabolisms indirectly and based on that, relative response to individual stress was examined and compared among fungal strains. Since the ambient alkalinization can be occurred independent of fungal growth, it may leads to different results in some cases between the pHenome and the mycelial growth-mediated evaluations of stress responses. Although we could not fully understand the mechanisms responsible for stress-induced alkalinization changes because of intricate metabolic transitions, it easily detects significant changes in stress response and provided massive primary information for further characterizations.

The Δ*Mocrz1,* a less-pathogenic and hypersensitive mutant to calcium ion stress (Choi et al., 2009), showed significant phenotypic change under CaCl2 treatment in pHenome analysis and that indicates the validity of this phenotype screening platform. The Δ*Mohox5* was indistinguishable from wild-type in previous report (Kim et al., 2009) but through the pHenome analysis, we could

detect several new phenotypic changes of this mutant. The pHenome was also used to characterize the roles of forkhead-box transcription factors in regulating stress responses in *M. oryzae* (Park et al., 2014). Variations on stress response among geologically and evolutionally distanced *M. oryzae* strains were confirmed via pHenome. Phenotypes of three wild-type strains (KJ201, 70-15 and Guy11) were quite different each other and it will allow us to estimate the relative distance of each strains in phenotypic aspect.

Given that *M. oryzae* showed different patterns of pH change under various nutritional conditions (Fig. 1A) and ACT_{pH} was differed by individual treatment of 20 amino acids and 14 sugars, these correlations would provide a method for comparing the nutrient usability of fungal strains in pHenome. The amino acids inducing rapid alkalinization by *M. oryzae* were included in small (Glycine, L-alanine, and L-serine), polar with uncharged R (L-serine, L-proline, L-asparagine, and L-glutamine), or charged R (L-aspartic acid, L-glutamic acid, and L-arginine) groups. All of amino acids in aromatic R group didn't show rapid alkalinization and differently from others, L-cysteine led to significant acidification within 24 hours. It probably caused by different efficiency and mode of action of amino acid utilization in *M. oryzae*. Similarly, more significant acidification was induced by hexoses than pentoses. Since pHenome observes the color change of pH indicator dissolved in media and

doesn't be affected by the cell distribution, it provides a differentiated tool compared to other microplate-based methods and is especially optimized for multicellular organisms. As additional advantages of this cell distribution-independent measurement, pHenome does not require the shaking incubation and area scanning of each well in microplate and is able to minimize the well-size to use 384- and even 1,536-well plates. Because the pHenome uses indicators that respond to ammonium secretion, followed by the pH increase outside the cell, it does not need to concern the uptake efficiency of indicator into the cell.

Despite the validity of pHenome, there are a few limitations in practical use. Firstly, the stress-inducing chemicals which have their own color (i. e. Congo red) could not be employed in pHenome. Secondly, it is difficult to examine the cellular response to pH-related stresses (extremely high or low pH). Thirdly, results from pHenome might be varied due to using aged conidia as an inoculum and we recommend using conidia approximately the same age in every experiment.

The applicability of pHenome in other fungal species was proved via analyzing the pH modifying activity of *F. graminearum*. Although some nutrients induced different pattern of pH change between *F. graminearum* and *M. oryzae*, overall trend was same that specific amino acids triggered rapid

alkalinization and specific sugars led acidification. From these results we confirmed possibility that we could employ pHenome for various fungal species although we should modify the alkalinization-inducing medium if necessary for optimized assay.

In conclusion, we validated the concept of pHenome and it can be adopted in many other species with the common ability of ambient pH change. It will contribute to elucidating the novel gene functions with large-scale assays and facilitate standardized and comparative analyses in filamentous fungi.

LITERATURE CITED

Bochner, B. R., Gadzinski, P. and Panomitros, E. 2001. Phenotype MicroArrays for high-throughput phenotypic testing and assay of gene function. *Genome Res.* 11:1246-1255.

Choi, J., Cheong, K., Jung, K., Jeon, J., Lee, G.-W., Kang, S., Kim, S., Lee, Y.-W. and Lee, Y.-H. 2013. CFGP 2.0: a versatile web-based platform for supporting comparative and evolutionary genomics of fungi and Oomycetes. *Nucleic Acids Res.* 41:D714-D719.

Choi, J., Kim, Y., Kim, S., Park, J. and Lee, Y.-H. 2009. *MoCRZ1*, a gene encoding a calcineurin-responsive transcription factor, regulates fungal growth and pathogenicity of *Magnaporthe oryzae*. *Fungal Genet. Biol.* 46:243-254.

Colot, H. V., Park, G., Turner, G. E., Ringelberg, C., Crew, C. M., Litvinkova, L., Weiss, R. L., Borkovich, K. A. and Dunlap, J. C. 2006. A high-throughput gene knockout procedure for *Neurospora* reveals functions for multiple transcription factors. *Proc. Natl. Acad. Sci. U. S. A.* 103:10352-10357.

Dean, R. A., Talbot, N. J., Ebbole, D. J., Farman, M. L., Mitchell, T. K., Orbach, M. J., Thon, M., Kulkarni, R., Xu, J.-R., Pan, H., Read, N. D.,

Lee, Y.-H., Carbone, I., Brown, D., Oh, Y. Y., Donofrio, N., Jeong, J. S., Soanes, D. M., Djonovic, S., Kolomiets, E., Rehmeyer, C., Li, W., Harding, M., Kim, S., Lebrun, M.-H., Bohnert, H., Coughlan, S., Butler, J., Calvo, S., Ma, L. J., Nicol, R., Purcell, S., Nusbaum, C., Galagan, J. E. and Birren, B. W. 2005. The genome sequence of the rice blast fungus *Magnaporthe grisea*. *Nature* 434:980-986.

Eshel, D., Miyara, I., Ailing, T., Dinoor, A. and Prusky, D. 2002. pH regulates endoglucanase expression and virulence of *Alternaria alternata* in persimmon fruit. *Mol. Plant Microbe Interact.* 15:774-779.

Freitas, J. S., Silva, E. M. and Rossi, A. 2007. Identification of nutrient-dependent changes in extracellular pH and acid phosphatase secretion in *Aspergillus nidulans*. *Genet. Mol. Res.* 6:721-729.

Giaever, G., Chu, A. M., Ni, L., Connelly, C., Riles, L., Véronneau, S., Dow, S., Lucau-Danila, A., Anderson, K., André, B., Arkin, A. P., Astromoff, A., El Bakkoury, M., Bangham, R., Benito, R., Brachat, S., Campanaro, S., Curtiss, M., Davis, K., Deutschbauer, A., Entian, K.-D., Flaherty, P., Foury, F., Garfinkel, D. J., Gerstein, M., Gotte, D., Güldener, U., Hegemann, J. H., Hempel, S., Herman, Z., Jaramillo, D. F., Kelly, D. E., Kelly, S. L., Kötter, P., LaBonte, D., Lamb, D. C., Lan, N., Liang, H., Liao, H., Liu, L., Luo, C., Lussier, M., Mao, R., Menard, P., Ooi, S.

L., Revuelta, J. L., Roberts, C. J., Rose, M., Ross-Macdonald, P., Scherens, B., Schimmack, G., Shafer, B., Shoemaker, D. D., Sookhai-Mahadeo, S., Storms, R. K., Strathern, J. N., Valle, G., Voet, M., Volckaert, G., Wang, C.-y., Ward, T. R., Wilhelmy, J., Winzeler, E. A., Yang, Y., Yen, G., Youngman, E., Yu, K., Bussey, H., Boeke, J. D., Snyder, M., Philippsen, P., Davis, R. W. and Johnston, M. 2002. Functional profiling of the *Saccharomyces cerevisiae* genome. *Nature* 418:387-391.

Jeon, J., Choi, J., Lee, G.-W., Dean, R. A. and Lee, Y.-H. 2013. Experimental evolution reveals genome-wide spectrum and dynamics of mutations in the rice blast fungus, *Magnaporthe oryzae*. *PLoS ONE* 8:e65416.

Jeon, J., Park, S.-Y., Chi, M.-H., Choi, J., Park, J., Rho, H.-S., Kim, S., Goh, J., Yoo, S., Choi, J., Park, J.-Y., Yi, M., Yang, S., Kwon, M.-J., Han, S.-S., Kim, B. R., Khang, C. H., Park, B., Lim, S.-E., Jung, K., Kong, S., Karunakaran, M., Oh, H.-S., Kim, H., Kim, S., Park, J., Kang, S., Choi, W.-B., Kang, S. and Lee, Y.-H. 2007. Genome-wide functional analysis of pathogenicity genes in the rice blast fungus. *Nat. Genet.* 39:561-565.

Kim, S., Park, S.-Y., Kim, K. S., Rho, H.-S., Chi, M.-H., Choi, J., Park, J., Kong, S., Park, J., Goh, J. and Lee, Y.-H. 2009. Homeobox transcription factors are required for conidiation and appressorium

development in the rice blast fungus *Magnaporthe oryzae*. *PLoS Genet.* 5:e1000757.

Manteau, S., Abouna, S., Lambert, B. and Legendre, L. 2003. Differential regulation by ambient pH of putative virulence factor secretion by the phytopathogenic fungus *Botrytis cinerea*. *FEMS Microbiol. Ecol.* 43:359-366.

Park, J., Kong, S., Kim, S., Kang, S. and Lee, Y.-H. 2014. Roles of forkhead-box transcription factors in controlling development, pathogenicity, and stress response in *Magnaporthe oryzae*. *Plant Pathol. J.* 30:1-15.

Prusky, D., McEvoy, J. L., Leverentz, B. and Conway, W. S. 2001. Local modulation of host pH by *Colletotrichum* species as a mechanism to increase virulence. *Mol. Plant Microbe Interact.* 14:1105-1113.

Prusky, D., McEvoy, J. L., Saftner, R., Conway, W. S. and Jones, R. 2004. Relationship between host acidification and virulence of *Penicillium* spp. on apple and citrus fruit. *Phytopathology* 94:44-51.

Prusky, D. and Yakoby, N. 2003. Pathogenic fungi: leading or led by ambient pH? *Mol. Plant Pathol.* 4:509-516.

Rando, O. J. and Verstrepen, K. J. 2007. Timescales of genetic and epigenetic inheritance. *Cell* 128:655-668.

Rollins, J. A. 2003. The *Sclerotinia sclerotiorum pac1* gene is required for

sclerotial development and virulence. *Mol. Plant Microbe Interact.* 16:785-795.

Solly, K., Wang, X., Xu, X., Strulovici, B. and Zheng, W. 2004. Application of real-time cell electronic sensing (RT-CES) technology to cell-based assays. *Assay Drug Dev. Technol.* 2:363-372.

Son, H., Seo, Y.-S., Min, K., Park, A. R., Lee, J., Jin, J.-M., Lin, Y., Cao, P., Hong, S.-Y., Kim, E.-K., Lee, S.-H., Cho, A., Lee, S., Kim, M.-G., Kim, Y., Kim, J.-E., Kim, J.-C., Choi, G. J., Yun, S.-H., Lim, J. Y., Kim, M., Lee, Y.-H., Choi, Y.-D. and Lee, Y.-W. 2011. A phenome-based functional analysis of transcription factors in the cereal head blight fungus, *Fusarium graminearum*. *PLoS Pathog.* 7:e1002310.

St Leger, R. J., Nelson, J. O. and Screen, S. E. 1999. The entomopathogenic fungus *Metarhizium anisopliae* alters ambient pH, allowing extracellular protease production and activity. *Microbiology* 145:2691-2699.

Sweigard, J. A., Carroll, A. M., Farrall, L., Chumley, F. G. and Valent, B. 1998. *Magnaporthe grisea* pathogenicity genes obtained through insertional mutagenesis. *Mol. Plant Microbe Interact.* 11:404-412.

Talbot, N. J., Ebbole, D. J. and Hamer, J. E. 1993. Identification and characterization of *MPG1*, a gene involved in pathogenicity from the

rice blast fungus *Magnaporthe grisea*. *Plant Cell* 5:1575-1590.

Warringer, J. and Blomberg, A. 2003. Automated screening in environmental arrays allows analysis of quantitative phenotypic profiles in *Saccharomyces cerevisiae*. *Yeast* 20:53-67.

Xu, X., Smith, S., Urban, J. and Cui, Z. 2006. An in line non-invasive optical system to monitor pH in cell and tissue culture. *Med. Eng. Phys.* 28:468-474.

CHAPTER 2

Roles of Forkhead-box Transcription Factors in Controlling Development, Pathogenicity, and Stress Response in *Magnaporthe oryzae*

ABSTRACT

Although multiple transcription factors (TFs) have been characterized via mutagenesis to understand their roles in controlling pathogenicity and infection-related development in *Magnaporthe oryzae*, the causal agent of rice blast, if and how forkhead-box (FOX) TFs contribute to these processes remain to be characterized. Four putative FOX TF genes were identified in the genome of *M. oryzae*, and phylogenetic analysis suggested that two of them (*MoFKH1* and *MoHCM1*) correspond to Ascomycota-specific members of the FOX TF family while the others (*MoFOX1* and *MoFOX2*) are Pezizomycotina-specific members. Deletion of *MoFKH1* (Δ*Mofkh1*) resulted in reduced mycelial growth and conidial germination, abnormal septation and stress response, and reduced virulence. Similarly, Δ*Mohcm1* exhibited reduced mycelial growth and conidial germination. Conidia of Δ*Mofkh1* and Δ*Mohcm1* were more sensitive to one or both of the cell cycle inhibitors hydroxyurea and benomyl, suggesting their role in cell cycle control. On the other hand, loss of *MoFOX1* (Δ*Mofox1*) did not show any noticeable changes in development, pathogenicity, and stress response. Deletion of *MoFOX2* was not successful even after repeated attempts. Taken together, these results suggested that *MoFKH1* and *MoHCM1* are important in fungal development and that

MoFKH1 is further implicated in pathogenicity and stress response in *M. oryzae*.

INTRODUCTION

The rice blast fungus *Magnaporthe oryzae* is a serious threat to rice production worldwide, causing losses enough to feed 60 million people every year (Dean et al., 2005). When typically three-celled conidia of *M. oryzae*, the primary inoculum, land on the surface of rice, they germinate and form specialized infection structures, such as the appressorium and invasive hyphae, in sequence to invade rice tissue. Following successful *in planta* proliferation, *M. oryzae* produces conidia to initiate next cycle (Ebbole, 2007; Talbot, 1995). Several genes required for appressorium formation (Soanes et al., 2012; Talbot, 2003; Wilson and Talbot, 2009) and those expressed *in planta* (Kim et al., 2010) have been identified. Systematic identification and characterization of candidate genes associated with infection-related traits have been greatly facilitated by the release of annotated genome sequences of *M. oryzae* (Dean et al., 2005).

Recently, a number of *M. oryzae* genes encoding transcription factors (TFs) have been characterized to determine their involvement in controlling pathogenicity and development. MoCRZ1, a calcineurin-responsive C2H2-type zinc finger TF, regulates growth and pathogenicity in response to Ca^{2+}-dependent signaling (Choi et al., 2009). The MIG1 protein, a MADS box TF,

functions downstream of the MAP kinase signaling pathway and is required for infectious growth (Mehrabi et al., 2008). Homeobox genes *MoHOX2*, *MoHOX7*, and *MST12* (=*MoHOX8*) encode developmental stage-specific TFs that control asexual reproduction, appressorium formation, and host penetration, respectively (Kim et al., 2009). The bZIP TF MoAP1 is critical for oxidative stress response, development, and pathogenicity (Guo et al., 2011). Gene expression analysis of most *M. oryzae* TF genes under diverse growth conditions and stresses and developmental stages provided comprehensive insights into the transcriptional regulatory network controlling and coordinating its growth, development, pathogenicity and stress responses (Park et al., 2013).

In the current study, we report the characterization of three members of the forkhead-box (FOX) TF gene family, which was named after the *Drosophila melanogaster* gene responsible for two spiked-head mutant (Jürgens et al., 1984; Weigel et al., 1989), in *M. oryzae*. FOX TFs contain a DNA binding domain of about 110 amino acids, which consists of three α-helices, three β-strands, and two 'wing' regions and forms a helix-turn-helix structure called 'winged helix'. Most FOX TFs bind to DNA as a monomer and are involved in controlling a wide range of biological processes such as cell cycle progression, growth and differentiation (Carlsson and Mahlapuu, 2002). The

genes for FOX TFs have been found in the genomes of animals and fungi, but not plants (Shimeld et al., 2010). In *Saccharomyces cerevisiae*, four FOX TFs, FKH1, FKH2, HCM1, and FHL1, have been characterized. FKH1 and FKH2 are regulators of genes involved in the G2 and M phases of cell cycle, and disruption of *FKH1* and *FKH2* caused impaired cell division and abnormal morphology (Koranda et al., 2000; Kumar et al., 2000; Zhu et al., 2000). HCM1 takes part in controlling the S phase and chromosome segregation (Pramila et al., 2006), while FHL1 seems to control rRNA processing (Hermann-Le Denmat et al., 1994). The four FOX TF genes in *Schizosaccharomyces pombe*, including *fkh2*$^{+}$, *sep1*$^{+}$, *mei4*$^{+}$ and *fhl1*$^{+}$, also are important for cell cycle control and morphogenesis. Fkh2, a homolog of *S. cerevisiae* FKH1 and FKH2, regulates the periodic expression of M- and G1-phase genes and is required for normal cell division (Bulmer et al., 2004). The *sep1*$^{+}$ gene controls cell separation and is transcribed in cell cycle dependent manner (Ribár et al., 1999). The *mei4*$^{+}$ gene encodes a meiosis-specific TF that is transcribed after premeiotic DNA replication (Horie et al., 1998) and *fhl1*$^{+}$, a homolog of *S. cerevisiae FHL1*, shows a non-periodical expression pattern and participates in cell morphogenesis (Szilagyi et al., 2005). *CaFKH*2 in *Candida albicans* controls yeast and true-hyphal morphogenesis. Mutant lacking *CaFKH2* formed pseudohyphae and lost its virulence (Bensen et al.,

2002). In *Aspergillus nidulans*, the *fkhF* and *fkhE* genes encode FOX TFs and are important for asexual development (Park et al., 2010). Lee et al. reported that *A. nidulans fhpA* gene is a possible regulator of sexual development (Lee et al., 2005).

To reveal the roles of FOX TFs in *M. oryzae*, we conducted phylogenetic analysis and functionally characterized FOX TF genes in *M. oryzae*. *MoFKH1* deletion (Δ*Mofkh1*) affected mycelial growth, conidial germination, septation, stress response, and pathogenicity. Loss of *MoHCM1* (Δ*Mohcm1*) caused defects in mycelial growth and conidial germination. Δ*Mofkh1* and Δ*Mohcm1* also showed higher sensitivity to cell cycle inhibitors. However, Δ*Mofox1* was indistinguishable from the wild-type and *MoFOX2* deletion was not successful even after repeated attempts. Overall, our results revealed roles of *MoFKH1* and *MoHCM1* in fungal development, pathogenicity, and stress response, which will contribute to elucidating the regulatory mechanism of *M. oryzae* infection.

MATERIALS AND METHODS

I. Fungal strains and culture conditions

M. oryzae wild-type strain KJ201 was obtained from the Center for Fungal Genetic Resources (CFGR, http://knrrb.knrrc.or.kr/index.jsp?rrb=cfgr). For conidial production, wild-type and mutant strains were grown at 25℃ on oatmeal agar (OMA, 50 g of oatmeal and 25 g of agar per liter) or V8 juice agar (V8A, 80 ml of V8 juice, 310 μl of 10N NaOH, and 15 g of agar per liter) under continuous fluorescent light. Conidia were harvested by rubbing the culture surface with sterilized distilled water followed by filtration through Miracloth (Calbiochem, USA). DNA was isolated from mycelia grown in liquid complete medium (CM, 6 g of yeast extract, 6 g of Casamino acids, and 10 g of sucrose per liter). To evaluate mycelial growth, modified complete agar (MCA, 10 g of glucose, 2 g of peptone, 1 g of yeast extract, 1 g of Casamino acids, 6 g of $NaNO_3$, 0.5 g of KCl, 0.5 g of $MgSO_4$, 1.5 g of KH_2PO_4, and 15 g of agar per liter supplemented with trace elements and vitamins) and modified minimal agar (MMA, MCA without peptone, yeast extract, and Casamino acids) (Talbot et al., 1993) were used.

II. Identification and phylogenetic analysis of putative fungal FOX TFs

Via InterProScan using the term IPR001766, which corresponds to the DNA binding domain of FOX TFs, putative FOX TFs were identified. Sequences of FOX TFs in various fungi were obtained from the Fungal Transcription Factor Database (FTFD, http://ftfd.snu.ac.kr) (Park et al., 2008) and Comparative Fungal Genomics Platform (CFGP, http://cfgp.snu.ac.kr/) (Choi et al., 2013) (Table 1). Protein sequences were aligned by ClustalW, and phylogenetic tree was constructed using the neighbor-joining method in MEGA program (Tamura et al., 2013). Phylogenetic relationships were tested with a bootstrap method using 2,000 repetitions.

Table 1. Number of FOX TFs in the fungal species shown in Fig. 1

Phylum	Subphylum	Species (strain)	Number of FOX TFs
Ascomycota	Pezizomycotina	*Aspergillus nidulans* (FGSC A4)	6
		Botrytis cinerea	4
		Coccidioides immitis	3
		Fusarium graminearum	4
		Histoplasma capsulatum (H88)	4
		Magnaporthe oryzae (70-15)	4
		Neurospora crassa	3
		Podospora anserina	4
	Saccharomycotina	*Ashbya gossypii* (ATCC 10895)	3
		Candida albicans (SC5314)	3
		Debaryomyces hansenii	3
		Kluyveromyces lactis	3
		Pichia stipitis	3
		Saccharomyces cerevisiae (S288C)	4
	Taphrinomycotina	*Schizosaccharomyces pombe*	4
Basidiomycota	Agaricomycotina	*Cryptococcus neoformans* (serotype A)	6
		Heterobasidion annosum	4
		Laccaria bicolor	4
		Serpula lacrymans (S7.3)	4
		Phanerochaete chrysosporium	5

III. Nucleic acid manipulation and fungal transformation

Genomic DNA was isolated using two different methods depending on experimental purpose. Genomic DNA for double-joint PCR and Southern blot was isolated according to a standard protocol (Sambrook and Russell, 2001). Genomic DNA used for gene deletion mutant screening by PCR was prepared using a quick extraction method (Chi et al., 2009b). Gene knockout constructs were produced using double-joint PCR (Yu et al., 2004), which fuses three different DNA fragments (two 1 to 1.5 kb fragments corresponding to the 5'- and 3'-flank regions of each target gene and a 2.1 kb fragment containing the Hygromycin B phosphotransferase gene) (Table 2). Resulting constructs were introduced into protoplasts of KJ201 as previously described (Sweigard et al., 1992). Hygromycin B-resistant transformants were screened first using PCR and confirmed by Southern analysis (Sambrook and Russell, 2001) (Fig. 2). Hybridization probes were prepared using the Rediprime^{TM} II DNA Labeling System (GE Healthcare, USA) according to the manufacturer's instructions, and signals on the membranes were detected using Phosphorimager (BAS-2040, Fuji Photo Film, Japan). For genetic complementation, an intact copy of the mutated gene was amplified by PCR and introduced into protoplasts of individual mutants using a geneticin-resistance gene as a selection marker.

Table 2. Primers used for producing gene knockout constructs

Name	Sequence (5' to 3')
MoFKH1_UF	AAGGCTCGGGCCTATCTATC
MoFKH1_UR	gcacaggtacacttgtttagagaAAGGTGAAGGGTGTGACAGG
MoFKH1_DF	ccttcaatatcatcttctgtcgaCTGCAAAGCCAGACACTCAG
MoFKH1_DR	TTCCCTACCATCAGCTGGAC
MoFKH1_UF_nested	GATGTGCCACGGATTGACC
MoFKH1_DR_nested	ACCCAGTCTCACCCATTCTC
MoHCM1_UF	CCCACGAACAAGGAAGGTAA
MoHCM1_UR	gcacaggtacacttgtttagagaGGGTCGCGACTCTGTACTGT
MoHCM1_DF	ccttcaatatcatcttctgtcgaCTTGTGATTCGCAAAAACGA
MoHCM1_DR	CCTCTGCCTTTTCCACCATA
MoHCM1_UF_nested	AAAACCTGGGTGTCAAAGC
MoHCM1_DR_nested	CTCCACCCGAATATCAAGG
MoFOX1_UF	CAGGAAATGAGCGGTCTATC
MoFOX1_UR	gcacaggtacacttgtttagagaGGCTGAGCGAGTAGGAATG
MoFOX1_DF	ccttcaatatcatcttctgtcgaTGAACCCTGCCCTATATCTGAC
MoFOX1_DR	GACGCAAATGGGACAAACTC
MoFOX1_UF_nested	CTTCCCTTGTGTACTTGTTGC
MoFOX1_DR_nested	CGTATCGTCTCCCTTCCTTC
Hyg B_f	CGACAGAAGATGATATTGAAGG
Hyg B_r	CTCTAAACAAGTGTACCTGTGC

* Linker sequences were denoted by lower case letters.

IV. Morphological and growth characteristics of mutant strains

To evaluate mycelial growth, the diameter of colonies grown on MCA and MMA was measured at 9 days post inoculation (dpi) with three replicates. The ability of asexual reproduction was assessed by counting the number of conidia harvested with 5 ml of sterilized distilled water from 6-day-old V8A cultures using a hemacytometer. The size of individual conidia was measured using a light microscope, and conidial germination and appressorium formation were evaluated on a hydrophobic coverslip. Three drops (40 μl per drop) of conidial suspension (approximately 2 to 5 × 10^4 conidia/ml) on a coverslip were placed in a container with wet paper towel and incubated at 25℃ for 4 and 24 hours. The proportions of germinating conidia and those forming the appressorium were microscopically counted (at least 100 conidia per replicate with three replicates). To visualize dead conidia, phloxine B was added to conidial suspensions harvested from two-week-old V8A cultures at the final concentration of 20 μg/ml and stained for 1 hour. To determine the number of cells in conidia, conidia harvested from 30-day-old OMA cultures were examined using a microscope (at least 500 conidia per replicate with three replicates). To visualize conidial cell wall and nuclei, calcofluor white and Hoechst 33342, respectively were used. To observe the septum formation in hyphae, conidia were inoculated on 50 to 100 μl drop of diluted complete

agar (0.6 g of yeast extract, 0.6 g of Casamino acids, 1 g of sucrose, and 15 g of agar per liter) on a slide glass or petri dish. After 36 to 48 hours of incubation at 25℃ under humid condition, agar drops were dried in a clean bench and observed using a light microscope. Hyphal morphology was observed using a light microscope after culturing conidia in liquid diluted CM (0.6 g of yeast extract, 0.6 g of Casamino acids, 1 g of sucrose per liter) for 2 days.

V. Assessment of sensitivity to cell cycle inhibitors and physiological response to various types of stresses

To assess the sensitivity to cell cycle inhibitors, conidial suspension (approximately 2 to 5 × 10^4 conidia/ml) was dropped on hydrophobic coverslip with 0.5 mM hydroxyurea and 2 μg/ml benomyl. Benomyl was dissolved in 95% EtOH to make a 1 mg/ml stock solution. Conidial germination and appressorium formation were microscopically evaluated at 24 hours post inoculation (hpi). For high or low temperature stresses, conidial suspension (approximately 2 to 5 × 10^4 conidia/ml) was dropped on hydrophobic coverslip, followed by incubation at 37℃ and 4℃. After 24 hpi, the samples were moved to 25℃ for further growth. Conidial germination and appressorium formation were evaluated at 48 hpi. Physiological response to

various chemicals that cause stress was evaluated using a novel colorimetric measurement method using a pH indicator (J. Park et al. manuscript in preparation). Conidial suspension (approximately 1×10^6 conidia/ml) was inoculated in wells of 384-well microtiter plate containing the following chemical solutions in water and incubated at 25℃ for 1 day: 100 mM NaCl, 150 mM KCl, 150 mM $MgCl_2$, 100 mM LiCl, 100 mM $CaCl_2$, 0.2 mM EDTA, 5 mM Caffeine, 0.2 mM $MnCl_2$, 0.08 mM $ZnSO_4$, 25 mM hydroxyurea, 5 μg/ml benomyl, 0.2 μM cycloheximide, 1.3 mM 3-Amino-1,2,4-triazole, 133 ppm calcofluor white, 0.002% SDS, 0.5 mM DTT, 0.0001% methyl viologen, 1 mM H_2O_2, 40 ppm p-coumaric acid, 13 mM $KClO_3$, and 0.4 mM $NaNO_2$. After the incubation, an alkalinization-inducing medium (L-aspartic acid solution at the final concentration of 2.5 mM with 0.008% bromocresol purple) was added to individual wells to monitor the ambient alkalinization process. Initial pH of the alkalinization-inducing medium was adjusted to be 4.6 by adding NaOH solution. Color change of bromocresol purple (from yellow to purple) was continuously measured for 24 hours at every 20 minutes using a microplate reader (Epoch, BioTek, USA) at 589 nm and 432 nm. The relative activity of alkalinization was used as an indirect indicator for physiological response of each strain to individual chemicals.

VI. Rice infection assays

Conidia were harvested from 7 to 14-day-old V8A cultures, and 10 ml of conidial suspension (approximately 5×10^4 conidia/ml) containing 250 ppm Tween 20 was sprayed onto susceptible rice seedlings (*Oryza sativa* cv. Nakdongbyeo) at the 4 to 5 leaf stage. The inoculated plants were kept in a dew chamber at 25℃ for 24 hours under darkness and then moved to a growth chamber with 16-h-light/8-h-dark cycle. Diseased leaves were evaluated at 6 to 7 dpi. Penetration assays were performed using rice sheaths. Conidial suspension (approximately 2×10^4 conidia/ml) was injected in rice sheath and incubated at 25℃ under high humidity. Invasive growth of *M. oryzae* strains was observed at 48 hpi using a light microscope.

RESULTS

I. The genome of *M. oryzae* encodes four FOX TFs

Species in the phyla Ascomycota and Basidiomycota carry 3 to 6 putative FOX TF genes with *M. oryzae* containing four (Table 1), according to data archived in the Fungal Transcription Factor Database (Park et al., 2008). To study how the *M. oryzae* FOX TFs have evolved and are related to previously characterized fungal FOX TFs, a phylogenetic analysis was conducted using FOX TFs in *M. oryzae* and 19 other species (Fig. 1). MGG_06258.7, a *M. oryzae* FOX TF belonging to Ascomycota clade 1, was closely related to *S. cerevisiae* FKH1 and FKH2, *S. pombe* Fkh2, and *C. albicans* CaFKH2, while MGG_06422.7 is orthologous to *S. cerevisiae* HCM1 and *S. pombe* Mei4 and Sep1 (Ascomycota clade 2). Accordingly, these proteins were named as MoFKH1 and MoHCM1, respectively. The remaining two FOX TFs in *M. oryzae* (MGG_01853.7 and MGG_14496.7) belong to Pezizomycotina-specific clades and were named MoFOX1 and MoFOX2, respectively. MoFOX1 is an ortholog of *A. nidulans* FhpA, which seems to be a regulator of sexual reproduction (Lee et al., 2005).

These *M. oryzae* FOX TF genes were mutagenized via transformation-mediated gene replacement to study their roles. Screening of 48, 48, 287, and

1,378 Hygromycin B-resistant transformants with mutant alleles of *MoFKH1*, *MoHCM1*, *MoFOX1*, and *MoFOX2*, respectively, resulted in 2, 4, 2, and 0 desired mutants. We used one mutant for each gene, including Δ*Mofkh1-1*, Δ*Mohcm1-4*, and Δ*Mofox1-1*, for phenotypic characterizations (Fig. 2 and Table 3). *MoFOX2* may be an essential gene given the failure of obtaining a mutant even after screening 1,378 transformants from three independent experiments.

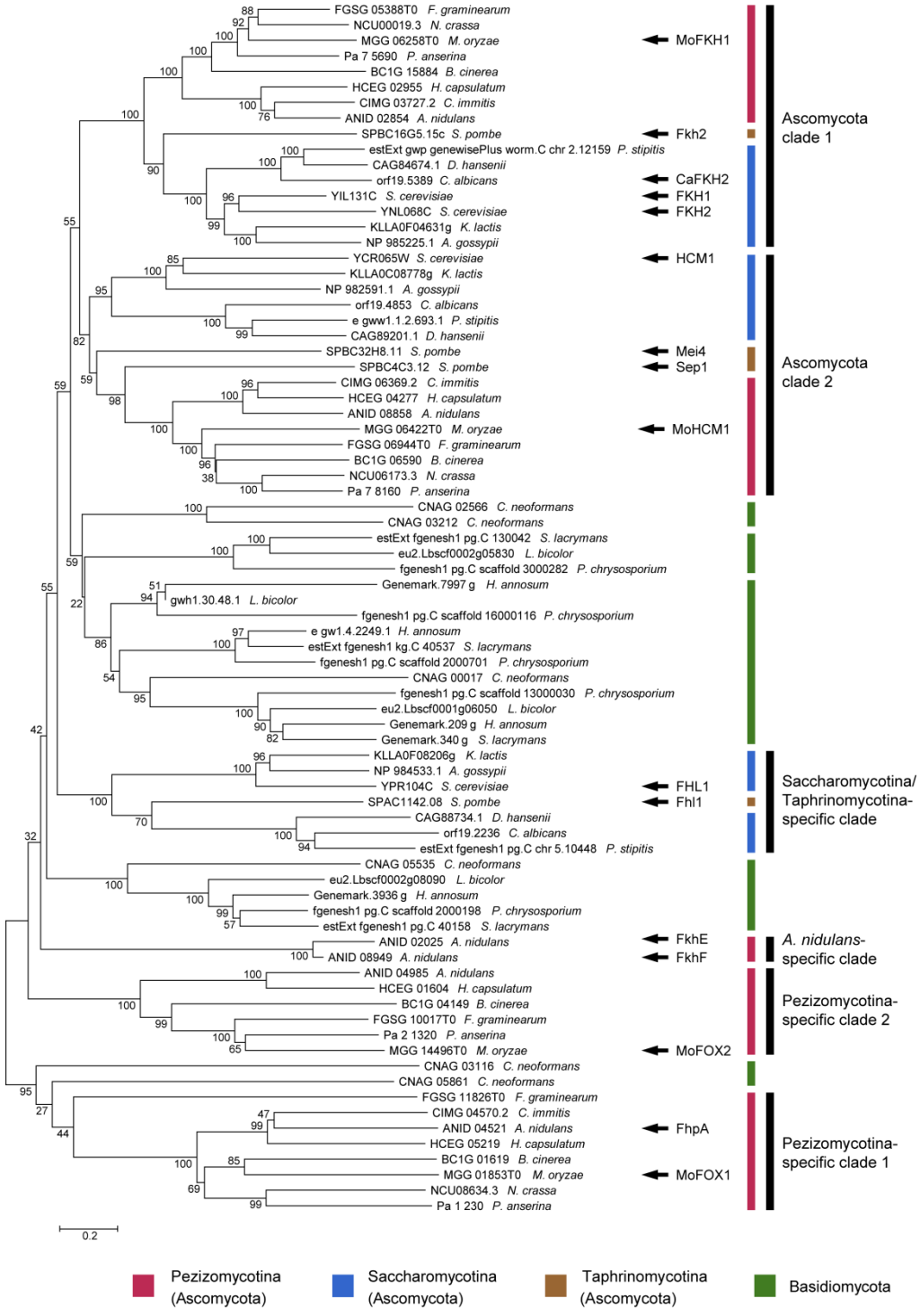
FGSG 05388T0 F. graminearum
NCU00019.3 N. crassa
MGG 06258T0 M. oryzae
Pa 7 5690 P. anserina
BC1G 15884 B. cinerea
HCEG 02955 H. capsulatum
CIMG 03727.2 C. immitis
ANID 02854 A. nidulans
SPBC16G5.15c S. pombe
estExt gwp genewisePlus worm.C chr 2.12159 P. stipitis
CAG84674.1 D. hansenii
orf19.5389 C. albicans
YIL131C S. cerevisiae
YNL068C S. cerevisiae
KLLA0F04631g K. lactis
NP 985225.1 A. gossypii
YCR065W S. cerevisiae
KLLA0C08778g K. lactis
NP 982591.1 A. gossypii
orf19.4853 C. albicans
e gww1.1.2.693.1 P. stipitis
CAG89201.1 D. hansenii
SPBC32H8.11 S. pombe
SPBC4C3.12 S. pombe
CIMG 06369.2 C. immitis
HCEG 04277 H. capsulatum
ANID 08858 A. nidulans
MGG 06422T0 M. oryzae
FGSG 06944T0 F. graminearum
BC1G 06590 B. cinerea
NCU06173.3 N. crassa
Pa 7 8160 P. anserina
CNAG 02566 C. neoformans
CNAG 03212 C. neoformans
estExt fgenesh1 pg.C 130042 S. lacrymans
eu2.Lbscf0002g05830 L. bicolor
fgenesh1 pg.C scaffold 3000282 P. chrysosporium
Genemark.7997 g H. annosum
gwh1.30.48.1 L. bicolor
fgenesh1 pg.C scaffold 16000116 P. chrysosporium
e gw1.4.2249.1 H. annosum
estExt fgenesh1 kg.C 40537 S. lacrymans
fgenesh1 pg.C scaffold 2000701 P. chrysosporium
CNAG 00017 C. neoformans
fgenesh1 pg.C scaffold 13000030 P. chrysosporium
eu2.Lbscf0001g06050 L. bicolor
Genemark.209 g H. annosum
Genemark.340 g S. lacrymans
KLLA0F08206g K. lactis
NP 984533.1 A. gossypii
YPR104C S. cerevisiae
SPAC1142.08 S. pombe
CAG88734.1 D. hansenii
orf19.2236 C. albicans
estExt fgenesh1 pg.C chr 5.10448 P. stipitis
CNAG 05535 C. neoformans
eu2.Lbscf0002g08090 L. bicolor
Genemark.3936 g H. annosum
fgenesh1 pg.C scaffold 2000198 P. chrysosporium
estExt fgenesh1 pg.C 40158 S. lacrymans
ANID 02025 A. nidulans
ANID 08949 A. nidulans
ANID 04985 A. nidulans
HCEG 01604 H. capsulatum
BC1G 04149 B. cinerea
FGSG 10017T0 F. graminearum
Pa 2 1320 P. anserina
MGG 14496T0 M. oryzae
CNAG 03116 C. neoformans
CNAG 05861 C. neoformans
FGSG 11826T0 F. graminearum
CIMG 04570.2 C. immitis
ANID 04521 A. nidulans
HCEG 05219 H. capsulatum
BC1G 01619 B. cinerea
MGG 01853T0 M. oryzae
NCU08634.3 N. crassa
Pa 1 230 P. anserina
0.2
MoFKH1
Fkh2
CaFKH2
FKH1
FKH2
HCM1
Mei4
Sep1
MoHCM1
FHL1
Fhl1
FkhE
FkhF
MoFOX2
FhpA
MoFOX1
Ascomycota clade 1
Ascomycota clade 2
Saccharomycotina/ Taphrinomycotina-specific clade
A. nidulans-specific clade
Pezizomycotina-specific clade 2
Pezizomycotina-specific clade 1
Pezizomycotina (Ascomycota)
Saccharomycotina (Ascomycota)
Taphrinomycotina (Ascomycota)
Basidiomycota

Fig. 1. Phylogenetic analysis of putative FOX TFs encoded by selected species in Ascomycota and Basidiomycota.

A phylogenetic tree based on their protein sequences was constructed using the neighbor-joining method with bootstrap analysis (2,000 replicates). Each number next to branches denotes the bootstrap value. Functionally characterized proteins and four putative FOX TFs in *M. oryzae* (MoFKH1, MoHCM1, MoFOX1, and MoFOX2) were noted with black arrows. Phylum and subphylum-specific clades in Ascomycota were marked by black lines.

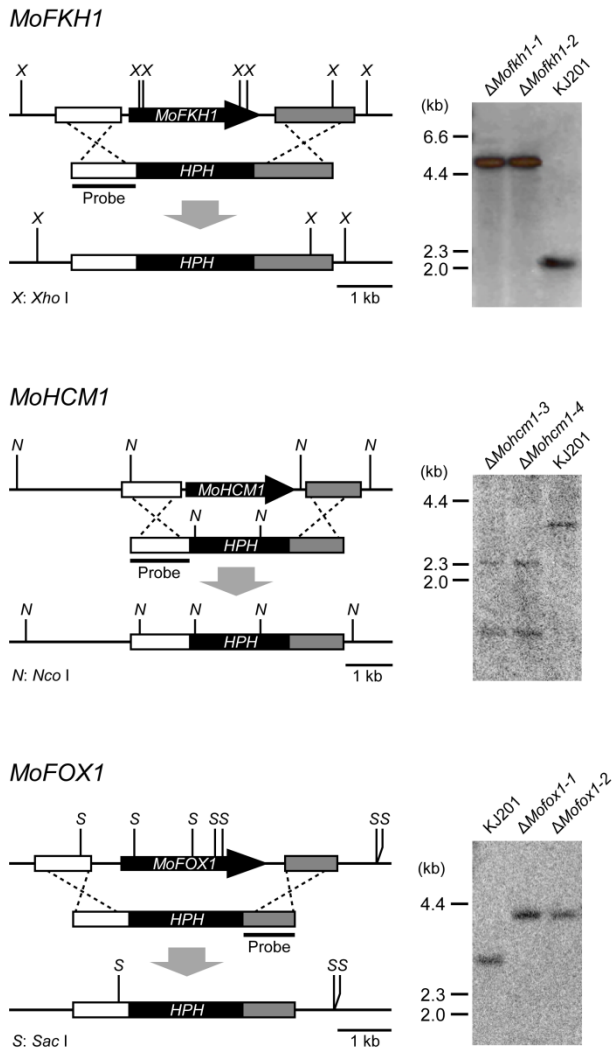

Fig. 2. Gene deletion strategy.

M. oryzae MoFKH1, *MoHCM1*, and *MoFOX1* were deleted via transformation-mediated targeted gene replacement. Southern results confirmed gene deletion.

Table 3. *M. oryzae* strains used in this study

Strains	Genotype
KJ201	Wild-type
Δ*Mofkh1*	Mutant of KJ201 with its *MoFKH1* deleted
Mofkh1c	Δ*Mofkh1* complemented with a wild-type copy of *MoFKH1*
Δ*Mohcm1*	Mutant of KJ201 with its *MoHCM1* deleted
Mohcm1c	Δ*Mohcm1* complemented with a wild-type copy of *MoHCM1*
Δ*Mofox1*	Mutant of KJ201 with its *MoFOX1* deleted

II. Δ*Mofkh1* and Δ*Mohcm1* showed defects in growth and conidial germination

Δ*Mofkh1* and Δ*Mohcm1* showed slightly reduced growth on MCA and MMA (Fig. 3A) as well as V8A and OMA (data not shown). The amount of conidia produced by Δ*Mofkh1* and Δ*Mohcm1* was similar to that of wild-type strain KJ201 (Fig. 3B), whereas conidial germination was decreased in these mutants (Fig. 3C). Approximately 70% and less than 90% of Δ*Mofkh1* and Δ*Mohcm1* conidia, respectively, germinated after 24 hours of incubation. Their reduced conidial germination was not complemented by additional nutrients or longer incubation (data not shown). To test if the reduced germination was due to lower conidial viability, we stained conidia with phloxine B, which accumulates in dead conidia. 10.8% of Δ*Mofkh1* conidia appeared dead, while Δ*Mohcm1* and KJ201 produced 0.5 to 1.9 % of stillbirth conidia (Fig. 3D), suggesting that the reduced conidial germination in Δ*Mofkh1* and Δ*Mohcm1* is not simply due to increased production of nonviable conidia. Growth retardation and germination defect in Δ*Mofkh1* and Δ*Mohcm1* were fully restored when an intact copy of the mutated gene was re-introduced. Δ*Mofox1* was indistinguishable from wild-type in growth and conidial production and germination.

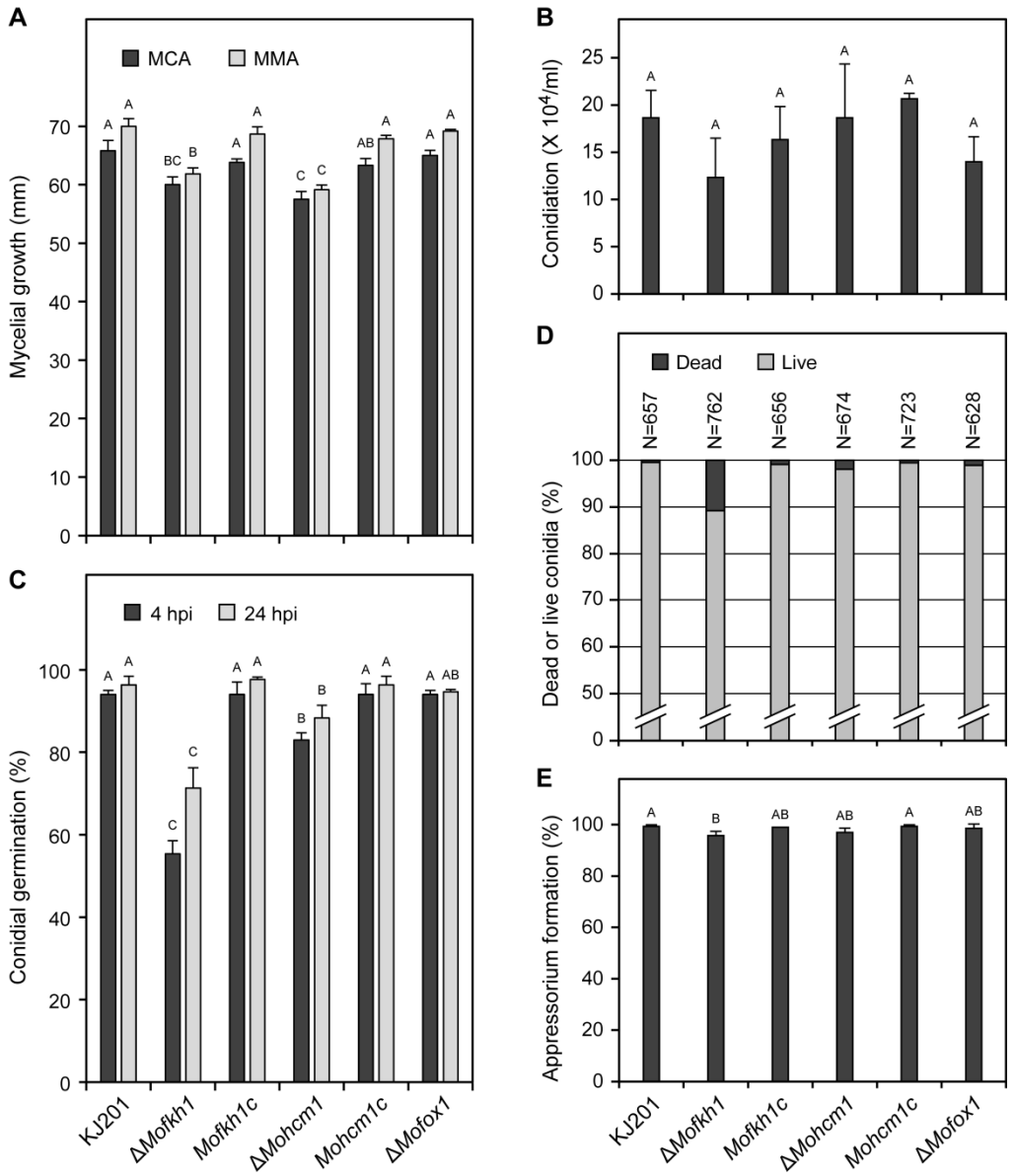

Fig. 3. Colonial growth, spore production and germination, and appressorium formation.

Fig. 3. (continued)

(A) Colony diameter of wild-type (KJ201), mutants (Δ*Mofkh1*, Δ*Mohcm1*, and Δ*Mofox1*) and complemented mutant strains (*Mofkh1c* and *Mohcm1c*) on MCA and MMA was measured at 9 dpi. (B) The numbers of conidia produced by the same strains are graphically presented. (C) Conidial germination at 4 hpi and 24 hpi is shown. (D) Percentages of dead conidia are shown. (E) Percentages of germinated conidia that formed the appressorium at 24 hpi are shown.

III. Appressorium formation of Δ*Mohcm1* was more severely affected by cell cycle inhibitors

Based on previous studies suggesting the involvement of the orthologs of MoFKH1 and MoHCM1 in cell cycle regulation in model yeasts (Pramila et al., 2006; Zhu et al., 2000), sensitivity of all three mutants to hydroxyurea and benomyl, cell cycle inhibitors, was measured. Hydroxyurea is a reversible inhibitor of ribonucleotide reductase and arrests the initiation and elongation of DNA replication. Benomyl causes spindle depolymerization, thus inhibiting chromosome segregation. While over 90% of germinated-conidia formed the appressorium at 24 hpi in all strains (Fig. 3E), in the presence of hydroxyurea, many more germinated-conidia failed to form appressoria in Δ*Mohcm1* compared to other strains (Fig. 4A). In the presence of benomyl, the percentage of appressorium formation was reduced to 52.2% in Δ*Mohcm1*, while ≥70% of them still formed the appressorium in other strains (Fig. 4B). Sensitivity of a complemented strain of Δ*Mohcm1* to these compounds was comparable to that of KJ201.

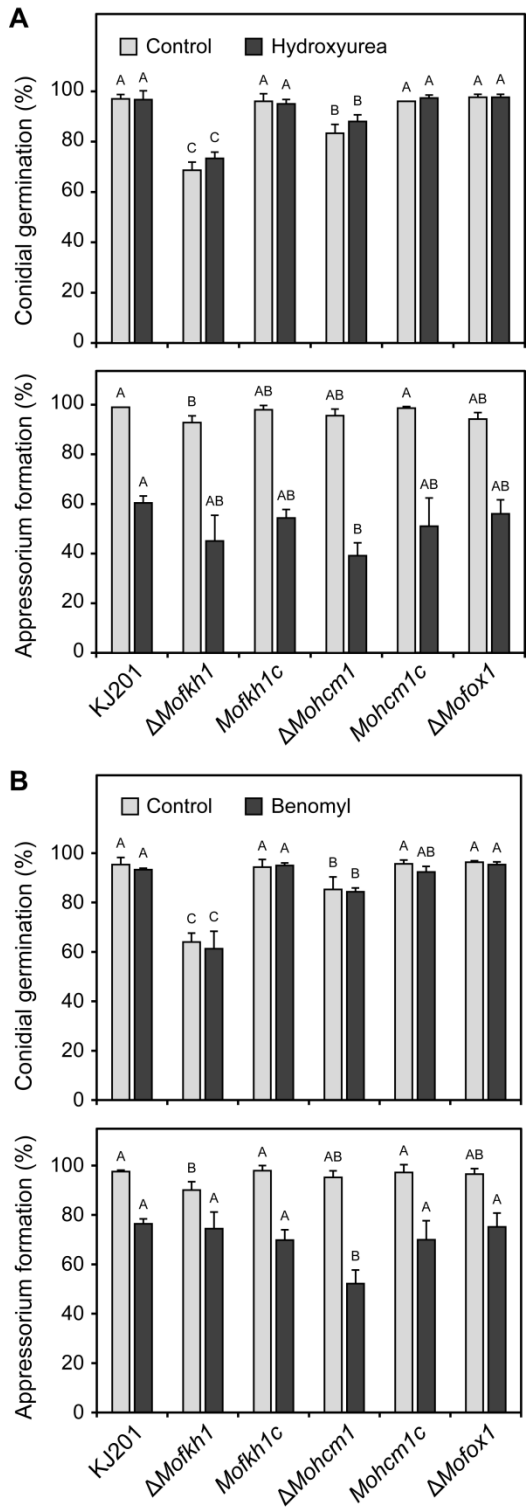
A
Control
Hydroxyurea
Conidial germination (%)
Appressorium formation (%)
KJ201
ΔMofkh1
Mofkh1c
ΔMohcm1
Mohcm1c
ΔMofox1
B
Control
Benomyl
Conidial germination (%)
Appressorium formation (%)
KJ201
ΔMofkh1
Mofkh1c
ΔMohcm1
Mohcm1c
ΔMofox1

Fig. 4. Effect of cell cycle inhibitors on conidial germination and appressorium formation.

Conidial germination and appressorium formation in the presence of (A) hydroxyurea (0.5 mM) and (B) benomyl (2 μg/ml with 0.19% EtOH) are shown. The control for benomyl treatment was 0.19% EtOH.

IV. Deletion of *MoFKH1* affected septum formation and cell division

Δ*Mofkh1* produced relatively smaller conidia than those produced by KJ201 (Fig. 5A and 5B). However, while KJ201 mainly produced typical three-celled conidia, >10% of Δ*Mofkh1* conidia contain ≥4 cells (Fig. 6A). The number of abnormal conidia increased as the culture aged with 15.9%, 2.3%, and 0.3% of the conidia containing four, five, and six cells, respectively after 30 days of incubation on OMA (Fig. 6B). Staining with Hoechst 33342 showed that the abnormal conidia of Δ*Mofkh1* also exhibited an increased number of nuclei (Fig. 6C), suggesting improper control of cell division in this mutant. In addition, Δ*Mofkh1* mycelia exhibited increased septation (Fig. 7A). When conidia in diluted CM were incubated at 25℃ for 2 days, uneven shaped hyphae formed by Δ*Mofkh1* (Fig. 7B). Imaging by scanning electron microscope revealed highly increased septum formation in this uneven shaped hyphae (Fig. 7C). The complemented strain *Mofkh1c* and other mutant strains (Δ*Mohcm1* and Δ*Mofox1*) displayed wild-type hyphal morphology and septation.

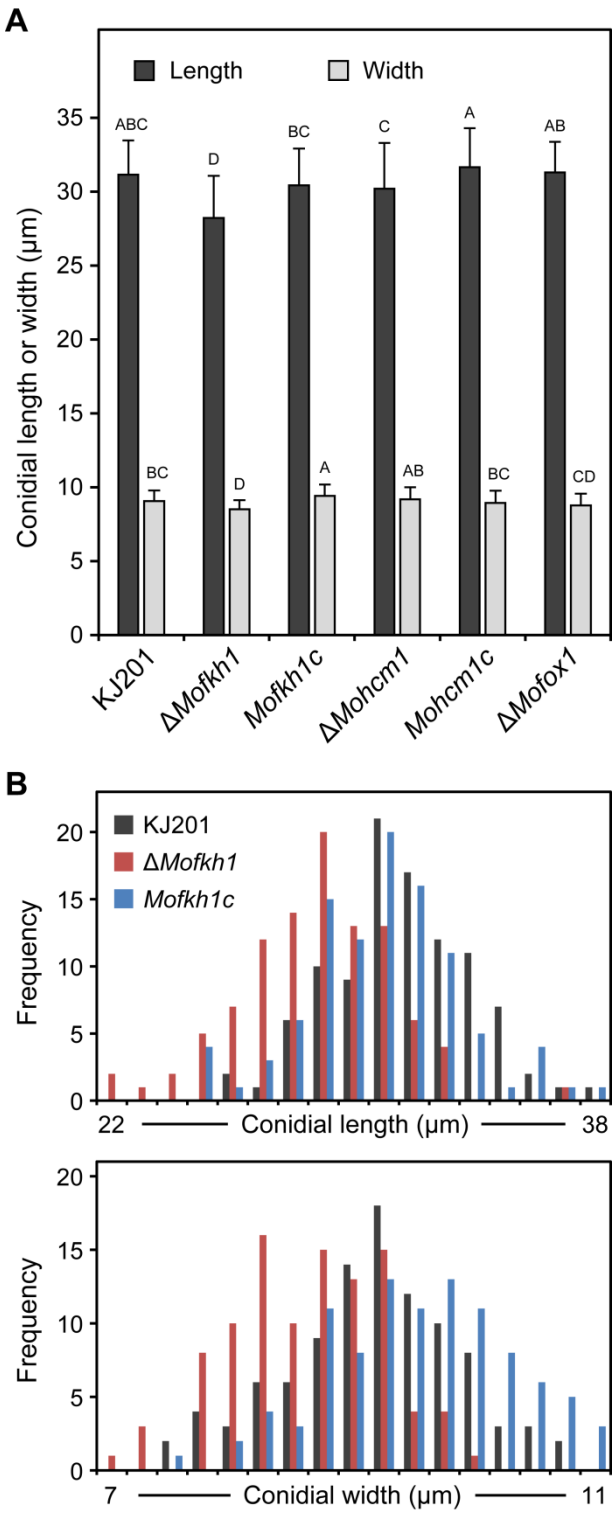
A
Length
Width
Conidial length or width (μm)
0
5
10
15
20
25
30
35
ABC
D
BC
C
A
AB
BC
D
A
AB
BC
CD
KJ201
ΔMofkh1
Mofkh1c
ΔMohcm1
Mohcm1c
ΔMofox1
B
KJ201
ΔMofkh1
Mofkh1c
Frequency
0
5
10
15
20
22
Conidial length (μm)
38
Frequency
0
5
10
15
20
7
Conidial width (μm)
11

Fig. 5. Effect of *MoFKH1* deletion on conidial size.

(A) The average length and width of conidia produced by KJ201, mutants (Δ*Mofkh1*, Δ*Mohcm1*, and Δ*Mofox1*) and complemented mutant strains (*Mofkh1c* and *Mohcm1c*) are shown. (B) Distribution patterns of conidial length and width among 100 conidia each from KJ201, Δ*Mofkh1* and *Mofkh1c* are shown.

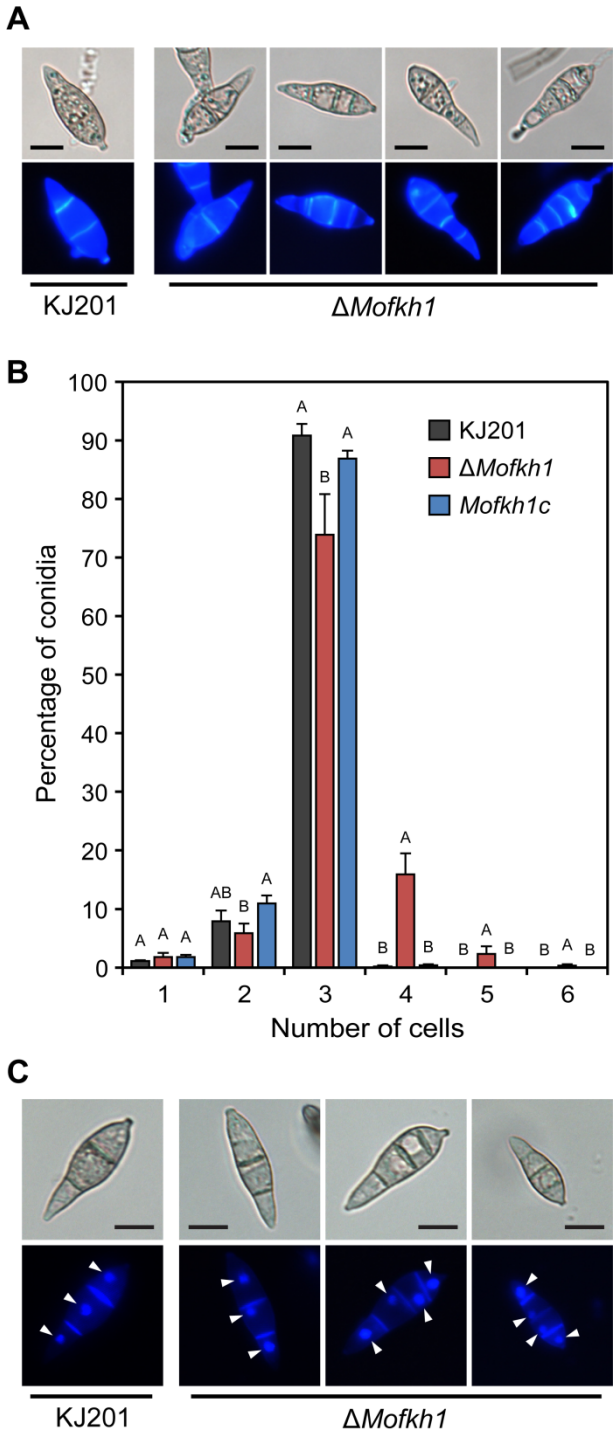
A
KJ201
ΔMofkh1
B
Percentage of conidia
Number of cells
KJ201
ΔMofkh1
Mofkh1c
C
KJ201
ΔMofkh1

Fig. 6. Changes in septation and cell number by Δ*Mofkh1*.

(A) Septation in KJ201 and Δ*Mofkh1* conidia was visualized by calcofluor white staining. Bars = 10 μm. (B) Increased cell numbers in Δ*Mofkh1* conidia. (C) Nuclei in KJ201 and Δ*Mofkh1* conidia were stained using Hoechst 33342. White arrows indicate nuclei. Bars = 10 μm.

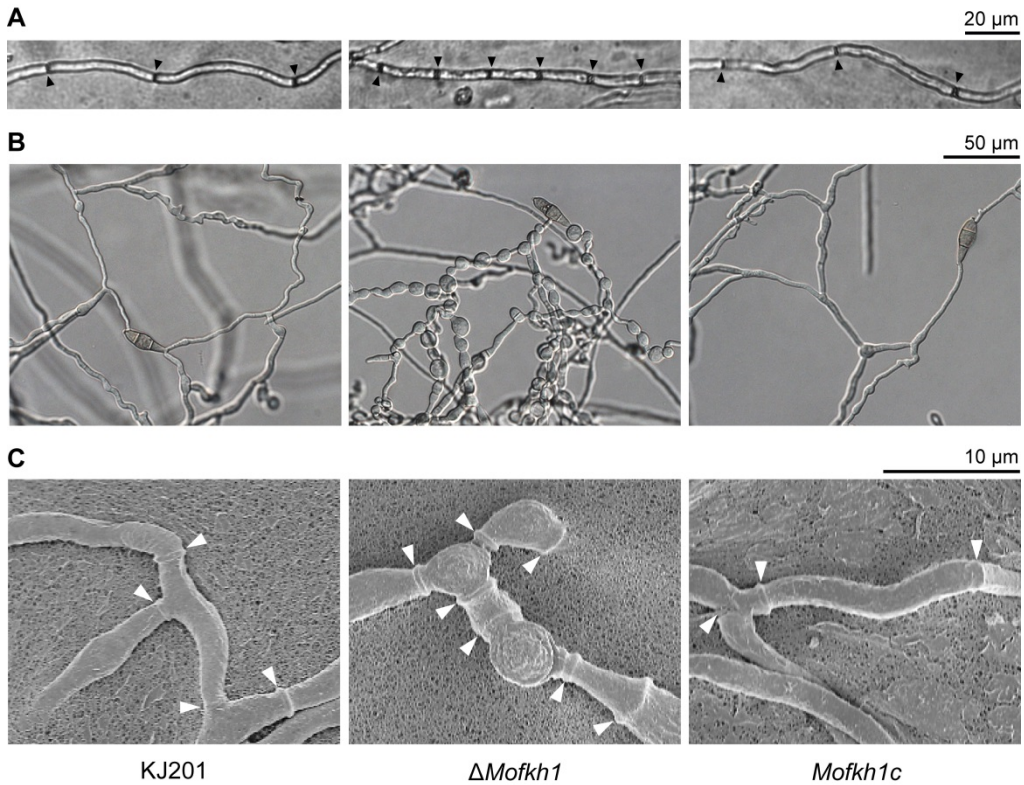

Fig. 7. Abnormal septation and morphology in Δ*Mofkh1* mycelia.

(A) Δ*Mofkh1* mycelia showed increased septation, which was denoted by black arrows. (B) Abnormal mycelial shapes of Δ*Mofkh1* observed using a light microscopy and (C) scanning electron microscopy are shown. Septa are marked using white arrows.

V. Differential physiological responses of FOX TF mutants to multiple chemical agents and temperature stresses

To study if and how individual mutations affect physiological response to various agents that cause stress, external pH change, as an indirect indicator of the physiological status of cells, was monitored via the use of a colorimetric measurement method (J. Park et al., manuscript in preparation) and compared with change in KJ201 (Table 4). Δ*Mofkh1* showed alkalinization activity significantly different from KJ201 in the presence of salts (NaCl, KCl, and LiCl), heavy metal ($ZnSO_4$), cell cycle inhibitor (benomyl), a plant phenolic compound (p-coumaric acid), and DTT that causes endoplasmic reticulum (ER) stress. The alkalinization activity of Δ*Mohcm1* and Δ*Mofox1* was comparable to that of KJ201 under all conditions.

To evaluate their sensitivity to high and low temperatures, we treated conidia of KJ201 and its mutants at 37℃ and 4℃ for 24 hours. Germination and appressorium formation rates of Δ*Mofkh1* conidia were reduced from 72.7% to 43% and 94.5% to 34.5%, respectively after heat treatment, while other strains showed slight or no reduction (Fig. 8A). Although the number of dead conidia in Δ*Mofkh1* slightly increased after the heat treatment, >80% of them were still viable. Other strains including KJ201 showed less than 3% of stillbirth

conidia after the heat treatment (Fig. 8B). All the mutant strains were not sensitive to the cold shock.

Table 4. Relative alkalinization activity of FOX TF mutants under various conditions

Treatments	Relative alkalinization activity of each strain[a]					
	KJ201	Δ*Mofkh1*	*Mofkh1c*	Δ*Mohcm1*	*Mohcm1c*	Δ*Mofox1*
NaCl	1.00^{A}	**0.73 ± 0.04^{B}**	1.06 ± 0.09^{A}	1.03 ± 0.03^{A}	1.12 ± 0.08^{A}	0.98 ± 0.11^{A}
KCl	1.00^{A}	**0.81 ± 0.11^{B}**	1.02 ± 0.05^{A}	1.03 ± 0.04^{A}	1.10 ± 0.03^{A}	0.94 ± 0.11^{AB}
$MgCl_2$	1.00^{A}	1.04 ± 0.19^{A}	1.00 ± 0.02^{A}	1.04 ± 0.05^{A}	1.10 ± 0.13^{A}	0.90 ± 0.12^{A}
LiCl	1.00^{A}	**0.69 ± 0.09^{B}**	1.01 ± 0.07^{A}	1.10 ± 0.09^{A}	1.12 ± 0.08^{A}	0.98 ± 0.14^{A}
$CaCl_2$	1.00^{A}	1.04 ± 0.21^{A}	1.00 ± 0.05^{A}	1.04 ± 0.07^{A}	1.12 ± 0.12^{A}	0.93 ± 0.08^{A}
EDTA	1.00^{AB}	0.85 ± 0.15^{B}	0.98 ± 0.19^{AB}	1.09 ± 0.06^{AB}	1.10 ± 0.09^{AB}	1.22 ± 0.08^{A}
Caffeine	1.00^{AB}	0.95 ± 0.03^{B}	0.99 ± 0.12^{B}	1.21 ± 0.05^{A}	1.10 ± 0.08^{AB}	1.05 ± 0.10^{AB}
$MnCl_2$	1.00^{A}	0.78 ± 0.08^{A}	1.05 ± 0.17^{A}	1.03 ± 0.11^{A}	1.16 ± 0.11^{A}	0.87 ± 0.30^{A}
$ZnSO_4$	1.00^{A}	**0.58 ± 0.14^{B}**	0.98 ± 0.09^{A}	0.96 ± 0.06^{A}	1.13 ± 0.15^{A}	0.92 ± 0.20^{A}
Hydroxyurea	1.00^{AB}	0.78 ± 0.10^{B}	1.07 ± 0.06^{A}	1.14 ± 0.06^{A}	1.14 ± 0.09^{A}	1.00 ± 0.20^{AB}
Benomyl	1.00^{A}	**0.59 ± 0.13^{B}**	1.01 ± 0.09^{A}	1.02 ± 0.05^{A}	1.14 ± 0.08^{A}	0.92 ± 0.10^{A}
Cycloheximide	1.00^{AB}	1.18 ± 0.11^{A}	0.94 ± 0.03^{B}	1.00 ± 0.06^{AB}	1.06 ± 0.06^{AB}	0.85 ± 0.14^{B}
3-Amino-1,2,4-triazole	1.00^{A}	0.96 ± 0.08^{A}	1.03 ± 0.16^{A}	1.07 ± 0.05^{A}	1.02 ± 0.01^{A}	0.97 ± 0.14^{A}
Calcofluor white	1.00^{A}	1.14 ± 0.09^{A}	0.98 ± 0.13^{A}	1.07 ± 0.07^{A}	0.96 ± 0.06^{A}	1.04 ± 0.12^{A}
SDS	1.00^{A}	0.76 ± 0.11^{A}	1.06 ± 0.26^{A}	1.24 ± 0.25^{A}	1.22 ± 0.16^{A}	1.22 ± 0.30^{A}
DTT	1.00^{A}	**0.32 ± 0.05^{B}**	1.25 ± 0.30^{A}	1.27 ± 0.10^{A}	1.19 ± 0.16^{A}	1.06 ± 0.25^{A}

Methyl viologen	1.00^{AB}	0.81 ± 0.13^{B}	1.10 ± 0.08^{A}	1.18 ± 0.08^{A}	1.09 ± 0.12^{A}	0.81 ± 0.09^{B}
H_2O_2	1.00^{A}	1.03 ± 0.22^{A}	1.02 ± 0.12^{A}	1.19 ± 0.20^{A}	1.04 ± 0.14^{A}	0.89 ± 0.17^{A}
p-Coumaric acid	1.00^{A}	**0.74 ± 0.05^{B}**	1.06 ± 0.08^{A}	1.00 ± 0.05^{A}	1.06 ± 0.10^{A}	0.92 ± 0.05^{A}
$KClO_3$	1.00^{A}	0.98 ± 0.11^{A}	1.07 ± 0.07^{A}	1.10 ± 0.04^{A}	1.05 ± 0.04^{A}	0.92 ± 0.16^{A}
$NaNO_2$	1.00^{A}	0.98 ± 0.12^{A}	1.07 ± 0.03^{A}	1.10 ± 0.10^{A}	1.03 ± 0.03^{A}	0.96 ± 0.10^{A}

[a] Relative alkalinization activity = (alkalinization activity of mutant in stress condition / alkalinization activity of mutant in NT) / (alkalinization activity of KJ201 in stress condition / alkalinization activity of KJ201 in NT)

* Alkalinization activity = area under the curve of a $\Delta\log_{10}$[OD at 589 nm / OD at 432 nm] versus time graph in the presence of pH indicator

* NT means non-treatment.

* Significant changes were bolded.

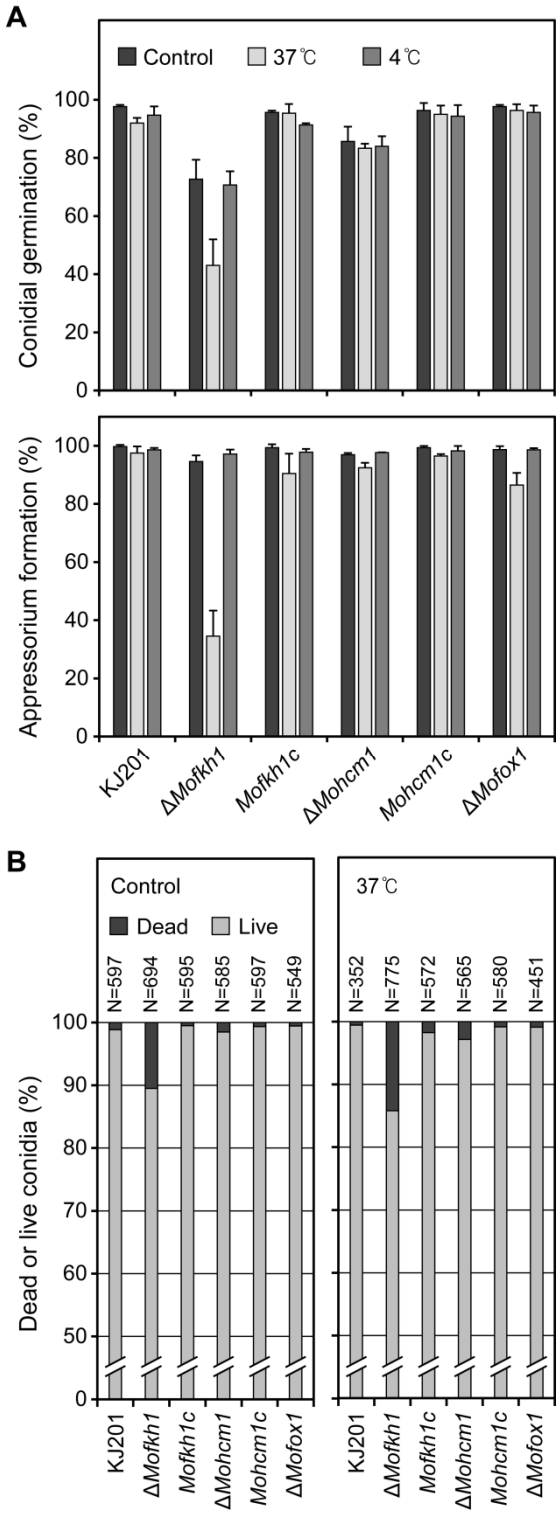
A
Control
37℃
4℃
Conidial germination (%)
Appressorium formation (%)
0
20
40
60
80
100
KJ201
ΔMofkh1
Mofkh1c
ΔMohcm1
Mohcm1c
ΔMofox1
B
Control
37℃
Dead
Live
Dead or live conidia (%)
N=597
N=694
N=595
N=585
N=597
N=549
N=352
N=775
N=572
N=565
N=580
N=451
0
50
60
70
80
90
100
KJ201
ΔMofkh1
Mofkh1c
ΔMohcm1
Mohcm1c
ΔMofox1

Fig. 8. Responses of conidia of FOX TF mutants to temperature stresses

(A) Conidial germination and appressorium formation after high (37℃) and low (4℃) temperature treatments are shown. (B) Percentages of dead conidia after harvest (left panel) and following an incubation at 37℃ for 24 hours (right panel) are shown.

VI. Loss of *MoFKH1* reduced virulence

To evaluate virulence, two methods were employed. Upon spray inoculation of susceptible rice seedlings with conidia, all three mutants and KJ201 caused lesions on rice leaves. However, Δ*Mofkh1* formed relatively smaller lesions than the others. Most lesions formed by Δ*Mofkh1* remained dark-brown spot and expanded more slowly compared to those caused by KJ201 (Fig. 9A). Invasive growth of Δ*Mofkh1* in rice sheath cells also was slightly reduced compared to that of KJ201 (Fig. 9B). Genetic complementation confirmed that loss of *MoFKH1* was responsible for reduced virulence.

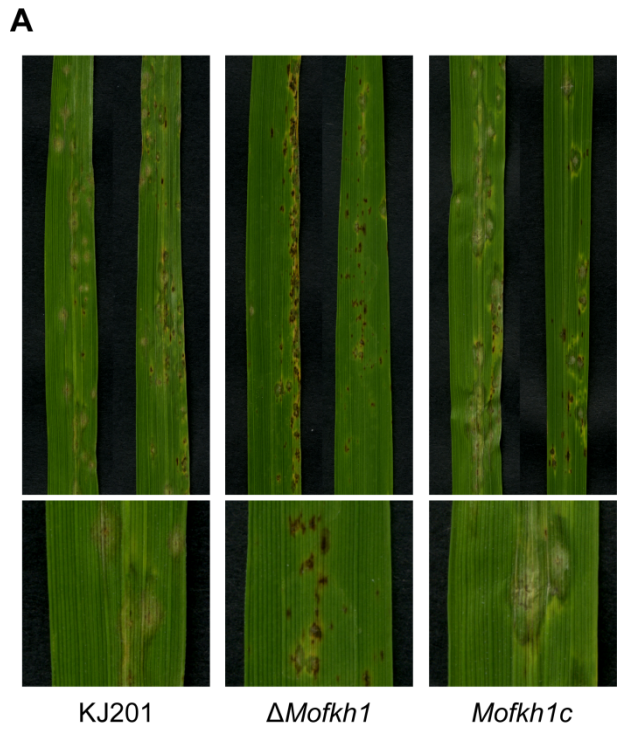
A
KJ201
ΔMofkh1
Mofkh1c
B
KJ201
ΔMofkh1
Mofkh1c

Fig. 9. Reduced symptoms on rice leaves and infectious growth in rice sheath cells by Δ*Mofkh1*.

(A) Lesions formed by KJ201, Δ*Mofkh1*, and *Mofkh1c* on rice leaves after spray inoculation are shown. (B) Invasive growth of KJ201, Δ*Mofkh1*, and *Mofkh1c* in rice sheath at 48 hpi. Bars = 50 μm.

DISCUSSION

TFs are pivotal components in controlling and coordinating diverse biological processes by orchestrating gene expression in response to various stimuli and developmental cues. Although well-annotated genome sequences have accelerated functional analyses of TFs in *M. oryzae* (Choi et al., 2009; Guo et al., 2011; Kim et al., 2009; Mehrabi et al., 2008; Park et al., 2008; Park et al., 2013), most predicted TFs still remain to be characterized. The focus of this study was on determining the roles of the FOX TF gene family, which consists of four genes, in controlling development, pathogenicity, and stress response.

Species in Ascomycota and Basidiomycota contain 3-6 FOX TF genes, whereas species in the phylum Zygomycota carry 10 or more (e.g., 10, 11, and 12 genes in *Mucor circinelloides*, *Phycomyces blakesleeanus*, and *Rhizopus oryzae*, respectively) (Park et al., 2008). Phylogenetic analysis using characterized and predicted fungal FOX TFs revealed multiple seemingly phylum- or subphylum-specific clades. The number variation and taxon-specific distribution of members of this gene family suggest its dynamic evolution probably driven by unique regulatory needs in individual taxa.

MoFKH1 is a homolog of *S. cerevisiae* FKH1 and FKH2 (Zhu et al., 2000), *S. pombe* Fkh2 (Bulmer et al., 2004), and *C. albicans* CaFKH2 (Bensen et al.,

2002). These proteins participate in controlling cell cycle, cell separation, and/or morphogenesis. Since septation is linked to cell cycle progression, abnormal septation observed in Δ*Mofkh1* in conidia and mycelia (Fig. 6 and 7) suggest the involvement of MoFKH1 in cell cycle control. Increased number of nuclei in Δ*Mofkh1* conidia and its susceptibility to benomyl also support this supposition. Although conidial germination and appressorium formation was not hindered by benomyl, the alkalinization activity in Δ*Mofkh1* was significantly reduced compared to that of KJ201, suggesting that loss of *MoFKH1* affects the regulation of certain physiological processes. Results from this and previous studies (Bulmer et al., 2004; Zhu et al., 2000) suggest that the function of MoFKH1 and its orthologs is conserved within Ascomycota. Reduced germination rate of Δ*Mofkh1* conidia may be due to a combination of increased production of stillbirth conidia and unknown defects in controlling germ tube emergence. Park et al. (2013) reported that expression of *MoFKH1* increased in conidia, supporting its role in controlling the production of conidia.

As demonstrated in this study (Table 4), the use of ambient pH change as an indicator for monitoring physiological change in response to various agents that cause cellular stress offers a novel means for studying gene function. Given that many physiological processes affect ambient pH, this assay alone is

not sufficient for revealing the nature of physiological change(s) caused by individual mutations, but provides useful clues to recognizing potential defects. In addition, because it employs microtiter plates and a plate reader, mutant responses to multiple stimuli can be quickly assayed. Reduced ambient alkalinization in the presence of ionic stresses (NaCl, KCl, LiCl, and $ZnSO_4$) suggests a role of MoFKH1 in controlling cellular processes affected by these stresses. Higher sensitivity of Δ*Mofkh1* to DTT and heat shock also indicated that the function of MoFKH1 might be related to the unfolded protein response. Compared to Δ*des1* (Chi et al., 2009a), which drastically affected alkalinization activity in response to H_2O_2 (data not shown), Δ*Mofkh1* was indistinguishable from KJ201 under that condition. This suggests that reduced virulence of Δ*Mofkh1* may be caused by defects other than its reduced ability to manage oxidative stress. One possible defect is unstable cell cycle progression. Several studies indicated the connection of orderly cell cycle control to proper development and pathogenicity in *M. oryzae*. SEP1, a putative homolog of Cdc7 in *S. pombe*, is essential for positioning of cell division sites, and its temperature-sensitive mutant showed reduced virulence (Saunders et al., 2010). MoCDC15, a homolog of Cdc15 in *S. pombe*, is important for growth, septation, asexual development and pathogenicity (Goh et al., 2011). Expression of *MoCDC15* was elevated in Δ*Mofkh1* (Goh et al.,

2011), suggesting that MoFKH1 controls cell cycle control by modulating the expression of MoCDC15. When the phenotypes of Δ*Mofkh1* and Δ*MoCDC15*$^{T\text{-}DNA}$ are compared, they displayed similar reduction in mycelial growth, abnormal septation, reduced conidial germination, increased number of dead conidia, and reduced pathogenicity. The reduced alkalinization activity of Δ*Mofkh1* in response to a plant phenolic compound (p-coumaric acid) suggests that reduced virulence in Δ*Mofkh1* is in part caused by defect in responding to plant chemical defense.

MoHCM1 is homologous to *S. cerevisiae* HCM1 (Pramila et al., 2006), *S. pombe* Sep1 (Ribár et al., 1999) and Mei4 (Horie et al., 1998). Benomyl sensitivity of Δ*Mohcm1* was similar to that of the *S. cerevisiae HCM1* mutant, suggesting their involvement in regulating conserved cell cycle-related processes. Given that Δ*Mohcm1* normally formed septa, its role in cell cycle control may be distinct from that of MoFKH1. *MoHCM1* was required for normal germination and growth but dispensable for virulence and several stress responses. The failure in disrupting *MoFOX2* may be due to low frequency of homologous recombination at this locus or lethality of resulting mutants. MoFOX1 is an ortholog of *A. nidulans* FhpA, a predicted regulator of sexual reproduction. However, we could not test its role in sexual reproduction because *M. oryzae* KJ201 is infertile. Loss of *MoFOX1* did not cause

noticeable defects in development, pathogenicity, and all of tested stress conditions. Taken together, results from this study contribute to uncovering the transcriptional regulatory network controlling development, pathogenicity, and stress response in *M. oryzae*.

LITERATURE CITED

Bensen, E. S., Filler, S. G. and Berman, J. 2002. A forkhead transcription factor is important for true hyphal as well as yeast morphogenesis in *Candida albicans*. *Eukaryot. Cell* 1:787-798.

Bulmer, R., Pic-Taylor, A., Whitehall, S. K., Martin, K. A., Millar, J. B. A., Quinn, J. and Morgan, B. A. 2004. The forkhead transcription factor Fkh2 regulates the cell division cycle of *Schizosaccharomyces pombe*. *Eukaryot. Cell* 3:944-954.

Carlsson, P. and Mahlapuu, M. 2002. Forkhead transcription factors: key players in development and metabolism. *Dev. Biol.* 250:1-23.

Chi, M.-H., Park, S.-Y., Kim, S. and Lee, Y.-H. 2009a. A novel pathogenicity gene is required in the rice blast fungus to suppress the basal defenses of the host. *PLoS Pathog.* 5:e1000401.

Chi, M.-H., Park, S.-Y. and Lee, Y.-H. 2009b. A quick and safe method for fungal DNA extraction. *Plant Pathol. J.* 25:108-111.

Choi, J., Cheong, K., Jung, K., Jeon, J., Lee, G.-W., Kang, S., Kim, S., Lee, Y.-W. and Lee, Y.-H. 2013. CFGP 2.0: a versatile web-based platform for supporting comparative and evolutionary genomics of fungi and Oomycetes. *Nucleic Acids Res.* 41:D714-D719.

Choi, J., Kim, Y., Kim, S., Park, J. and Lee, Y.-H. 2009. *MoCRZ1*, a gene encoding a calcineurin-responsive transcription factor, regulates fungal growth and pathogenicity of *Magnaporthe oryzae*. *Fungal Genet. Biol.* 46:243-254.

Dean, R. A., Talbot, N. J., Ebbole, D. J., Farman, M. L., Mitchell, T. K., Orbach, M. J., Thon, M., Kulkarni, R., Xu, J.-R., Pan, H., Read, N. D., Lee, Y.-H., Carbone, I., Brown, D., Oh, Y. Y., Donofrio, N., Jeong, J. S., Soanes, D. M., Djonovic, S., Kolomiets, E., Rehmeyer, C., Li, W., Harding, M., Kim, S., Lebrun, M.-H., Bohnert, H., Coughlan, S., Butler, J., Calvo, S., Ma, L.-J., Nicol, R., Purcell, S., Nusbaum, C., Galagan, J. E. and Birren, B. W. 2005. The genome sequence of the rice blast fungus *Magnaporthe grisea*. *Nature* 434:980-986.

Ebbole, D. J. 2007. Magnaporthe as a model for understanding host-pathogen interactions. *Annu. Rev. Phytopathol.* 45:437-456.

Goh, J., Kim, K. S., Park, J., Jeon, J., Park, S.-Y. and Lee, Y.-H. 2011. The cell cycle gene *MoCDC15* regulates hyphal growth, asexual development and plant infection in the rice blast pathogen *Magnaporthe oryzae*. *Fungal Genet. Biol.* 48:784-792.

Guo, M., Chen, Y., Du, Y., Dong, Y., Guo, W., Zhai, S., Zhang, H., Dong, S., Zhang, Z., Wang, Y., Wang, P. and Zheng, X. 2011. The bZIP

transcription factor MoAP1 mediates the oxidative stress response and is critical for pathogenicity of the rice blast fungus *Magnaporthe oryzae*. *PLoS Pathog.* 7:e1001302.

Hermann-Le Denmat, S., Werner, M., Sentenac, A. and Thuriaux, P. 1994. Suppression of yeast RNA polymerase III mutations by *FHL1*, a gene coding for a *fork head* protein involved in rRNA processing. *Mol. Cell. Biol.* 14:2905-2913.

Horie, S., Watanabe, Y., Tanaka, K., Nishiwaki, S., Fujioka, H., Abe, H., Yamamoto, M. and Shimoda, C. 1998. The *Schizosaccharomyces pombe mei4*+ gene encodes a meiosis-specific transcription factor containing a forkhead DNA-binding domain. *Mol. Cell. Biol.* 18:2118-2129.

Jürgens, G., Wieschaus, E., Nüsslein-Volhard, C. and Kluding, H. 1984. Mutations affecting the pattern of the larval cuticle in *Drosophila melanogaster*. II. Zygotic loci on the third chromosome. *Roux's Arch. Dev. Biol.* 193:283-295.

Kim, S., Park, J., Park, S.-Y., Mitchell, T. K. and Lee, Y.-H. 2010. Identification and analysis of *in planta* expressed genes of *Magnaporthe oryzae*. *BMC Genomics* 11:104.

Kim, S., Park, S.-Y., Kim, K. S., Rho, H.-S., Chi, M.-H., Choi, J., Park, J.,

Kong, S., Park, J., Goh, J. and Lee, Y.-H. 2009. Homeobox transcription factors are required for conidiation and appressorium development in the rice blast fungus *Magnaporthe oryzae*. *PLoS Genet.* 5:e1000757.

Koranda, M., Schleiffer, A., Endler, L. and Ammerer, G. 2000. Forkhead-like transcription factors recruit Ndd1 to the chromatin of G2/M-specific promoters. *Nature* 406:94-98.

Kumar, R., Reynolds, D. M., Shevchenko, A., Shevchenko, A., Goldstone, S. D. and Dalton, S. 2000. Forkhead transcription factors, Fkh1p and Fkh2p, collaborate with Mcm1p to control transcription required for M-phase. *Curr. Biol.* 10:896-906.

Lee, B.-Y., Han, S.-Y., Choi, H. G., Kim, J. H., Han, K.-H. and Han, D.-M. 2005. Screening of growth- or development-related genes by using genomic library with inducible promoter in *Aspergillus nidulans*. *J. Microbiol.* 43:523-528.

Mehrabi, R., Ding, S. and Xu, J.-R. 2008. MADS-box transcription factor Mig1 is required for infectious growth in *Magnaporthe grisea*. *Eukaryot. Cell* 7:791-799.

Park, J., Park, J., Jang, S., Kim, S., Kong, S., Choi, J., Ahn, K., Kim, J., Lee, S., Kim, S., Park, B., Jung, K., Kim, S., Kang, S. and Lee, Y.-H. 2008.

FTFD: an informatics pipeline supporting phylogenomic analysis of fungal transcription factors. *Bioinformatics* 24:1024-1025.

Park, M.-H., Kim, H.-Y., Kim, J. H. and Han, K.-H. 2010. Gene structure and function of *fkhE* a forkhead gene in a filamentous fungus *Aspergillus nidulans*. *Kor. J. Mycol.* 38:160-166.

Park, S.-Y., Choi, J., Lim, S.-E., Lee, G.-W., Park, J., Kim, Y., Kong, S., Kim, S., Rho, H.-S., Jeon, J., Chi, M.-H., Kim, S., Khang, C. H., Kang, S. and Lee, Y.-H. 2013. Global expression profiling of transcription factor genes provides new insights into pathogenicity and stress responses in the rice blast fungus. *PLoS Pathog.* 9:e1003350.

Pramila, T., Wu, W., Miles, S., Noble, W. S. and Breeden, L. L. 2006. The Forkhead transcription factor Hcm1 regulates chromosome segregation genes and fills the S-phase gap in the transcriptional circuitry of the cell cycle. *Genes Dev.* 20:2266-2278.

Ribár, B., Grallert, A., Oláh, É. and Szállási, Z. 1999. Deletion of the *sep1*+ forkhead transcription factor homologue is not lethal but causes hyphal growth in *Schizosaccharomyces pombe*. *Biochem. Biophys. Res. Commun.* 263:465-474.

Sambrook, J. and Russell, D. W. 2001. Molecular cloning: a laboratory manual. Cold Spring Harbor Laboratory Press, Cold Spring Harbor, NY.

Saunders, D. G. O., Dagdas, Y. F. and Talbot, N. J. 2010. Spatial uncoupling of mitosis and cytokinesis during appressorium-mediated plant infection by the rice blast fungus *Magnaporthe oryzae*. *Plant Cell* 22:2417-2428.

Shimeld, S. M., Degnan, B. and Luke, G. N. 2010. Evolutionary genomics of the Fox genes: origin of gene families and the ancestry of gene clusters. *Genomics* 95:256-260.

Soanes, D. M., Chakrabarti, A., Paszkiewicz, K. H., Dawe, A. L. and Talbot, N. J. 2012. Genome-wide transcriptional profiling of appressorium development by the rice blast fungus *Magnaporthe oryzae*. *PLoS Pathog.* 8:e1002514.

Sweigard, J. A., Chumley, F. G. and Valent, B. 1992. Disruption of a *Magnaporthe grisea* cutinase gene. *Mol. Gen. Genet.* 232:183-190.

Szilagyi, Z., Batta, G., Enczi, K. and Sipiczki, M. 2005. Characterisation of two novel fork-head gene homologues of *Schizosaccharomyces pombe*: their involvement in cell cycle and sexual differentiation. *Gene* 348:101-109.

Talbot, N. J. 1995. Having a blast: exploring the pathogenicity of *Magnaporthe grisea*. *Trends Microbiol.* 3:9-16.

Talbot, N. J. 2003. On the trail of a cereal killer: exploring the biology of *Magnaporthe grisea*. *Annu. Rev. Microbiol.* 57:177-202.

Talbot, N. J., Ebbole, D. J. and Hamer, J. E. 1993. Identification and characterization of *MPG1*, a gene involved in pathogenicity from the rice blast fungus *Magnaporthe grisea*. *Plant Cell* 5:1575-1590.

Tamura, K., Stecher, G., Peterson, D., Filipski, A. and Kumar, S. 2013. MEGA6: molecular evolutionary genetics analysis version 6.0. *Mol. Biol. Evol.* 30:2725-2729.

Weigel, D., Jürgens, G., Küttner, F., Seifert, E. and Jäckle, H. 1989. The homeotic gene *fork head* encodes a nuclear protein and is expressed in the terminal regions of the Drosophila embryo. *Cell* 57:645-658.

Wilson, R. A. and Talbot, N. J. 2009. Under pressure: investigating the biology of plant infection by *Magnaporthe oryzae*. *Nat. Rev. Microbiol.* 7:185-195.

Yu, J.-H., Hamari, Z., Han, K.-H., Seo, J.-A., Reyes-Domínguez, Y. and Scazzocchio, C. 2004. Double-joint PCR: a PCR-based molecular tool for gene manipulations in filamentous fungi. *Fungal Genet. Biol.* 41:973-981.

Zhu, G., Spellman, P. T., Volpe, T., Brown, P. O., Botstein, D., Davis, T. N. and Futcher, B. 2000. Two yeast forkhead genes regulate the cell cycle and pseudohyphal growth. *Nature* 406:90-94.

CHAPTER 3

Bidirectional Genetics Platform: a Dual Purpose Mutagenesis Strategy for Filamentous Fungi

ABSTRACT

Rapidly increasing fungal genome sequences call for efficient ways of generating mutants to translate quickly gene sequences into their functions. A reverse genetic strategy via targeted gene replacement (TGR) has been inefficient in many filamentous fungi due to dominant production of undesirable ectopic transformants. Although a large-scale random insertional mutagenesis via transformation (i.e., forward genetics) facilitates high-throughput uncovering of novel genes of interest, generating a huge number of transformants, which is necessary to ensure the likelihood of mutagenizing most genes, is time-consuming. We propose a new strategy, entitled the Bidirectional Genetics (BiG) platform, which combines both forward- and reverse genetic strategies by recycling ectopic transformants from TGR as a source for random insertional mutants. The BiG platform was evaluated using the rice blast fungus *Magnaporthe oryzae* as a model. Over 10% of >1,000 *M. oryzae* ectopic transformants, generated while disrupting specific genes, displayed abnormality in vegetative growth, pigmentation, and/or asexual reproduction. In this pool of putative mutants, we isolated insertional mutants in three genes involved in histidine biosynthesis (*MoHIS5*), vegetative growth

(*MoVPS74*), or conidiophore formation (*MoFRQ*) supporting the utility of this platform for systematic gene functional studies.

INTRODUCTION

Rapid advances in DNA sequencing technology have accelerated the generation of genome sequences. More than 300 fully sequenced fungal genomes have been publicly released (Choi et al., 2013), and there exist bioinformatic schemes to annotate gene structures and functions (Haas et al., 2011; Yandell and Ence, 2012). However, many hypothetical genes remain to be experimentally characterized (Galperin and Koonin, 2010), and even for most genes with functions predicted from sequence conservation, their functions have yet to be corroborated experimentally. The widening gap between rapidly accumulating genome sequences and slow progress in experimental characterization/validation calls for more efficient tools and approaches for gene functional studies.

Currently, experimental approaches for investigating fungal gene function via genome alteration are divided into two. Targeted gene replacement (TGR) via the homologous recombination (HR) is a straightforward reverse genetics strategy, and its efficiency typically depends on the DNA repair system of individual target organisms (Capecchi, 1989). In *Saccharomyces cerevisiae* in which HR is predominant, it was reported that only 40 bp of homology was sufficient to facilitate successful TGR (Hua et al., 1997; Manivasakam et al.,

1995). Similarly, *Schizosaccharomyces pombe* showed over 50% efficiency of HR with 60-80 bp of homology (Bähler et al., 1998). However, most filamentous fungi another DNA repair system, the non-homologous end joining (NHEJ) (Critchlow and Jackson, 1998), preferentially operates during transformation, resulting in very low success rates of TGR even with the homology that is longer than 500 bp (Weld et al., 2006; Xu et al., 2006). Low and variable frequencies of gene targeting via HR have been reported in many actively researched species, such as *Acremonium chrysogenum* (Liu et al., 2001), *Alternaria alternata* (Wang et al., 2011), *Aspergillus* spp. (Bird and Bradshaw, 1997; da Silva Ferreira et al., 2006; Krappmann et al., 2006; Nayak et al., 2006; Takahashi et al., 2006), *Botrytis cinerea* (Choquer et al., 2008; Soulié et al., 2003), *Claviceps purpurea* (Scheffer et al., 2005a; Scheffer et al., 2005b), *Colletotrichum higginsianum* (Ushimaru et al., 2010), *Cryphonectria parasitica* (Gao et al., 1996; Park et al., 2004; Segers et al., 2004), *Hypocrea jecorina* (Guangtao et al., 2009), *Magnaporthe oryzae* (Kito et al., 2008; Villalba et al., 2008), *Neurospora crassa* (Ninomiya et al., 2004), *Penicillium chrysogenum* (Casqueiro et al., 1999), and *Podospora anserina* (El-Khoury et al., 2008). Although efforts to increase the HR frequency in fungi through the inactivation of NHEJ-associated components such as Ku70, Ku80, or DNA ligase IV have been successful (Kück and Hoff, 2010), its use is time-

consuming and hindered by a number of issues: i) loci-dependent TGR efficiency (Kito et al., 2008; Villalba et al., 2008; Wang et al., 2011), ii) undesirable effects such as the difficulty of genetic complementation by ectopic integration (Carvalho et al., 2010) and elevated susceptibility to DNA damaging conditions (Meyer et al., 2007), and iii) difficulties of removing the background mutation before phenotypic characterization for species in which sexual reproduction is rare or unknown (Xu et al., 2006).

Random insertional mutagenesis via transformation as a forward genetic strategy has been widely utilized for high-throughput gene characterization in filamentous fungi. Restriction enzyme-mediated integration (REMI) was applied to generate mutants through the random integration of transforming DNA, which is supposedly facilitated by cleavage of chromosomal DNA by a restriction enzyme introduced with transforming DNA (Bölker et al., 1995; Liu et al., 1998; Riggle and Kumamoto, 1998; Shi et al., 1995). One big advantage of REMI over chemical- or radiation-induced random mutagenesis is that the disrupted gene can be easily identified using the inserted DNA as a tag for recovering flanking genomic sequences. However, REMI often produces genomic rearrangements, large deletions, and high number of untagged mutants (Sweigard et al., 1998). Alternatively, *Agrobacterium tumefaciens*-mediated transformation (ATMT) has been employed (Bundock

and Hooykaas, 1996; de Groot et al., 1998; Michielse et al., 2005; Mullins et al., 2001; Rho et al., 2001). ATMT utilizes the ability of *A. tumefaciens* to directly introduce T-DNA to the target genome and can transform a broad range of fungal materials. Transformation-mediated random mutagenesis is time-consuming and labor intensive, because tens of thousands of transformants are typically needed to saturate the target genome with mutation. For example, to discover 202 pathogenicity-related loci in *M. oryzae*, a total of 21,070 transformants were generated by ATMT and screened (Jeon et al., 2007).

To improve the efficiency of gene characterization, especially for filamentous fungi with low frequencies of HR, we propose a strategy entitled the Bidirectional Genetics (BiG) platform. This strategy combines forward- and reverse genetic approaches by directing ectopic transformants from TGR to a pipeline for screening random insertional mutants.

We chose the rice blast fungus *M. oryzae* to evaluate the feasibility and efficiency of this platform. This fungus is regarded as a model phytopathogenic fungus due to its economic impact, suitable feature for handle in laboratory, and available genomic data (Dean et al., 2005; Talbot, 2003; Valent and Chumley, 1991). Although several gene manipulation tools such as TGR, REMI, and ATMT, are available for *M. oryzae*, most predicted genes

still remain uncharacterized experimentally. We validated the BiG platform using *M. oryzae* by successfully characterizing the function of three genes.

MATERIALS AND METHODS

I. Fungal strains and culture conditions

M. oryzae wild-type strain KJ201, obtained from Center for Fungal Genetic Resources (CFGR; http://genebank.snu.ac.kr), and its transformants were grown on V8 juice agar (V8A) (80 ml of V8 juice, 310 μl of 10N NaOH, and 15 g of agar per liter) under 25℃ and constant fluorescent light to promote conidiation. For genomic DNA extraction, wild-type and transformants were cultured in liquid complete medium (10 g of sucrose, 6 g of yeast extract, and 6 g of casamino acids per liter) for 5-7 days under 25℃ in darkness.

II. Generation of gene knockout constructs and fungal transformation for TGR

Constructs for deleting target genes were created by double-joint PCR (Yu et al., 2004) with 1-1.5 kb-long 5'- and 3'-flank regions of each of the targets, and a 2.1 kb region of pBCATPH (Yun, 1998) that contains the hygromycin B phosphotransferase (*HPH*) gene. The 5'- and 3'-flank regions of each target gene were amplified and fused to the HPH cassette using primers with a 23 bp tail in the reverse primer of the 5'-flanking region and the forward primer of

the 3'-flanking region. Amplified knockout construct was introduced into protoplasts of KJ201. Protocols for protoplast preparation and transformation were adopted from a previous study (Sweigard et al., 1992). Selection of hygromycin B-resistant transformants was conducted on TB3 agar (3 g of yeast extract, 3 g of casamino acids, 10 g of glucose, 200 g of sucrose, and 8 g of agar per liter) amended with 200 μg ml^{-1} hygromycin B.

III. Fungal DNA isolation

Genomic DNA isolation was conducted via two methods. Genomic DNA for Southern blot analysis and inverse-PCR was isolated by a standard protocol (Sambrook and Russell, 2001). Genomic DNA of transformants for PCR-based screening was prepared using a quick extraction method (Chi et al., 2009).

IV. PCR-based mutant screening

Individual hygromycin B-resistant transformants were screened by PCR to determine whether they correspond to a gene deletion mutant or ectopic transformant. A primer pairs, including HPH_Sf (5'-CAAGCCTACAGGACACACATTC -3') / SF (specific primer at the upstream of the 5'-flanking region) and HPH_Sr (5'-GGCTGATCTGACCAGTTGC-3')

/ SR (specific primer at the downstream of the 3'-flanking region), was used. Genomic DNA extracted via the use of a quick extraction method (Chi et al., 2009) and a small piece of mycelial tissue from 36-hour-old V8A culture of individual transformants were employed as template for routine PCR and direct-PCR, respectively.

V. Phenotype-based screening of ectopic transformants

For rapid phenotypic evaluation, individual transformants were grown on 24-well plate filed with V8A. To assess vegetative growth, the diameter of each colony was measured at 3 days post inoculation (dpi), and ectopic transformants showing less than 80% of the wild-type growth were selected. Pigmentation was observed after 5-10 days of incubation, and transformants displaying more- or less-pigmentation than KJ201 were selected. A microscope at 50× magnification was used to estimate asexual reproduction visually and qualitatively. The ectopic transformants showing abnormal aerial hyphae (fluffy or smooth), reduced conidiation, and/or abnormal morphology of conidiophore were identified. The putative mutants that were identified via the three methods were transferred to a 6-well plate containing V8A to confirm their phenotypes. At 3 and 5 dpi, vegetative growth was evaluated, and those exhibiting the original growth phenotype were subjected to further

characterization. Additionally, since varied sizes of inoculum could affect the colony diameter, some ectopic transformants showing reduced growth rate (vegetative growth/day) were also selected. Pigmentation was observed at 5-10 dpi, and asexual reproduction was examined at 10 dpi.

VI. Characterization of selected ectopic transformants

Genomic insertion sites in individual ectopic transformants were identified by inverse-PCR followed by sequencing. For inverse-PCR, genomic DNA of each ectopic transformant was digested with a restriction enzyme that does not cleave the HPH cassette, and resulting fragments were self-ligated using T4 DNA ligase (Takara Bio Inc., Japan). A pair of primers located in the HPH cassette, HPH_Sf and HPH_Sr, was used to amplifying the regions flanking the insertion site. Amplified DNA was directly sequenced via the Sanger sequencing method (3730 DNA Analyzer, Applied Biosystems, USA) using a specific primer designed to generate sequences of the flanking region.

VII. In-depth phenotype analysis for gene functional characterization

Vegetative growth was measured on modified complete agar (CMA) and minimal agar (MMA) (Talbot et al., 1993) at 9 dpi, with three replicates. To

test histidine auxotrophy, candidate mutants were grown on MMA and MMA supplemented with 0.5-10 mM L-histidine. Quantitative assessment of conidiation was conducted by counting the number of conidia from 10-day-old culture growing on V8A with or without supplemented 0.5-10 mM L-histidine. Conidia were collected using 5 ml of sterilized distilled water, and the concentration of conidial suspension was measured using a haemacytometer under a light microscope. Conidial germination and appressorium formation were measured on a hydrophobic coverslip. Conidia harvested from 10-day-old V8A culture were suspended in sterilized distilled water at the concentration of approximately 2×10^4 conidia/ml. Three drops of this conidial suspension (40 μl per drop) were placed onto a coverslip and placed in a moistened box at 25℃. After 24 h of incubation, the percentages of germinated conidia and germinated conidia that formed the appressorium were determined via microscopic examination (three replicates with 100 conidia per replicate). For evaluating pathogenicity, after harvesting conidia from 7-14 dpi cultures on V8A, 10 ml of conidial suspension (approximately 5×10^4 conidia/ml) containing 250 ppm Tween 20 were sprayed onto susceptible rice seedlings (*Oryza sativa* cv. Nakdongbyeo) at the four- to five-leaf stage. The infected plants were kept in a dew chamber at 25℃ for 24 h in darkness and subsequently moved to a growth chamber with a 16-h-light/8-h-dark cycle.

Disease severity was measured at 6-7 dpi. To assess mycelial morphology, 100-200 conidia were spread on hydrophilic slide glass with 200 μl of diluted liquid complete medium (1 g of sucrose, 0.6 g of yeast extract, and 0.6 g of casamino acids per liter). After 2 days of incubation at 25℃, grown mycelia were observed by light microscope. Neutral Red (final concentration at 0.2 mg/ml) was added and stained for 1 h to visualize vacuoles in mycelia.

RESULTS AND DISCUSSION

I. Design of the BiG platform for *M. oryzae*

In *M. oryzae*, about 100-500 transformants are typically generated in standard protoplast transformation (Sweigard et al., 1995) for TGR with most of them being ectopic transformants. Assuming that about 200 ectopic transformants are generated from each transformation, only 100 trials of transformation are sufficient for creating a pool of 20,000 insertional mutants. This number is similar to those generated through massive random insertional mutagenesis via REMI and ATMT (Balhadère et al., 1999; Jeon et al., 2007; Sweigard et al., 1998). To test if transformants from this platform are suitable for identifying mutants of interesting phenotypes, we screened collected ectopic transformants. In the first round of screening, the ectopic transformants were grown on 24-well plates containing V8 juice agar (V8A) for a few days to identify those showing defects in three phenotypes, including vegetative growth, pigmentation and asexual development, compared to the wild-type strain KJ201. After the initial screening, the phenotypes of candidate mutants were further evaluated by growing them on V8A in 6-well plates to reevaluate their phenotypes. Only the transformants showing reproducible phenotypes through both screenings were characterized via Southern blot analysis to

determine the copy number of inserted DNA construct. Finally, the insertion site was identified by inverse-PCR (Ochman et al., 1988) and sequencing (Fig. 1).

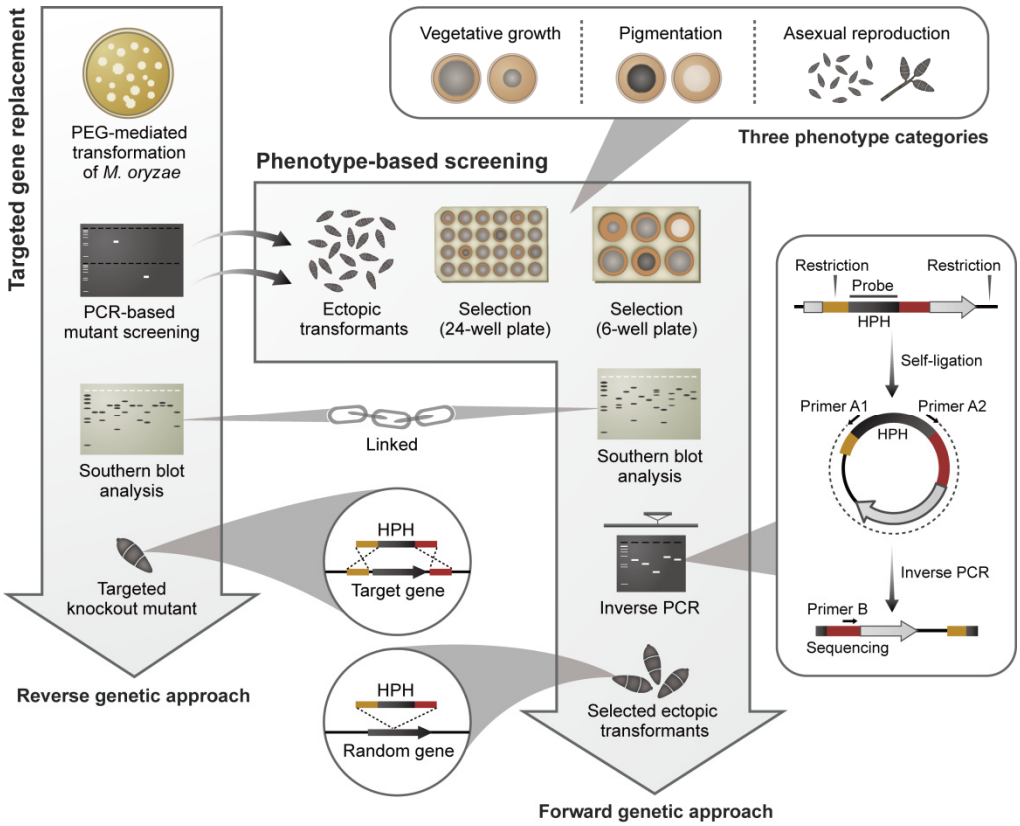

Fig. 1. Schematic diagram of the BiG platform

This platform combines forward- and reverse genetic approaches by recycling ectopic transformants generated from routine TGR experiments to identify interesting insertional mutants via phenotype-based screening. From a single experiment of transformation, one can obtain both of targeted knockout mutants and a large number of random insertional mutants. After PCR-based screening for target gene knockout mutants, ectopic transformants were collected and screened by their phenotypes in vegetative growth, pigmentation,

Fig. 1. (continued)

and asexual reproduction. A double screening of mutant phenotypes, first in the 24-well plate format followed by the 6 well plate format, decreases false positives. Southern blot analysis demonstrates the single integration of transforming DNA in selected ectopic transformants and inverse-PCR followed by sequencing identifies the location of insertion.

II. Over 10% of the ectopic transformants screened displayed one or more phenotypic abnormalities

To evaluate the effectiveness of the BiG platform, we screened 180 and 959 ectopic transformants resulted from TGR of two different genes, MGG_09225.7 and MGG_14496.7, respectively. A total of 20 ectopic transformants from MGG_09225.7 TGR (11.1% of the total) and 108 ectopic transformants from MGG_14496.7 TGR (11.3% of the total) showed reproducible abnormalities in one or more of the three phenotypes (Table 1). Most mutants were defective in vegetative growth, while defects in pigmentation were least common, which is consistent with the fact that more genes are involved in vegetative growth than pigmentation. Similar frequencies of recovering putative mutants in two independently generated pools of ectopic transformants support the utility of the BiG platform. Initial screening of transformants generated by a previous random mutagenesis of KJ201 via ATMT also yielded 11.3% (2,151/18,968) of putative mutants showing reductions in vegetative growth, abnormal pigmentation, and/or reductions in conidiation (Jeon et al., 2007).

We analyzed ectopic transformants showing abnormalities in three phenotype categories by Southern blot. Though over 50% of transformants showed single- or double-copy insertions of transforming DNA in both MGG_09225.7

and MGG_14496.7 TGR, proportions of single-copy insertions were different. Single- and double-copy insertion rates were 52.9% (9/17) and 5.9% (1/17) in MGG_09225.7 TGR and 17.8% (18/101) and 33.7% (34/101) in MGG_14496.7 TGR, respectively. It provides direction for further research to investigate the insertion event by NHEJ with different types of transforming DNA.

Table 1. Number of selected ectopic transformants by their abnormal phenotypes

Category	From TGR for		Total
	MGG_09225.7	MGG_14496.7	
Total ectopic transformants	180	959	1,139
Ectopic transformants with phenotype(s)	20 (11.1%)[a]	108 (11.3%)	128 (11.2%)
- Vegetative growth	17 (9.4%)	88 (9.2%)	105 (9.2%)
- Pigmentation	1 (0.6%)	17 (1.8%)	18 (1.6%)
- Asexual reproduction	8 (4.4%)	53 (5.5%)	61 (5.4%)
- Vegetative growth & Pigmentation	1 (0.6%)	14 (1.5%)	15 (1.3%)
- Vegetative growth & Asexual reproduction	5 (2.8%)	35 (3.6%)	40 (3.5%)
- Pigmentation & Asexual reproduction	0	13 (1.4%)	13 (1.1%)
- Vegetative growth & Pigmentation & Asexual reproduction	0	12 (1.3%)	12 (1.1%)

[a] (Number of selected ectopic transformants / Number of total ectopic transformants)×100%

III. Characterization of MoHIS5, MoVPS74, and MoFRQ

To demonstrate that the BiG platform can be used to identify genes of interesting phenotypes, we identified and characterized three genes in the selected ectopic transformants. One mutant, named as MoHIS5^{BiG}, was selected based on its defect in vegetative growth, pigmentation and asexual reproduction. Genomic characterization revealed that a single copy of introduced DNA construct disrupted the *MoHIS5* (MGG_14904.7) gene, which encodes a putative histidinol-phosphate aminotransferase (Fig. 2A). It is similar to *Saccharomyces cerevisiae* HIS5, which plays a role in the seventh step of histidine biosynthesis (Nishiwaki et al., 1987). MoHIS5^{BiG} was a histidine auxotroph and could not grow on minimal agar (MMA). Although MoHIS5^{BiG} could grow on modified complete agar (CMA), its growth was reduced compared with that of KJ201. An intact copy of the *MoHIS5* gene was re-introduced to MoHIS5^{BiG}, and resulting transformants grew normally on both MMA and CMA (Fig. 2B). Although the application of external L-histidine enabled its growth on MMA, the restoration of growth was still partial (Fig. 2C). It was possibly due to: i) insufficient and limited capacity of histidine uptake to fully supplement the growth requirement, ii) an adverse effect of biosynthetic intermediate that accumulates in the mutant, and/or iii) an additional function of MoHIS5 that required for vegetative growth.

Moreover, MoHIS5^{BiG} could not produce conidia on V8A, while its conidiation was partially recovered when histidine was added (Fig. 2D). Although conidia of MoHIS5^{BiG} normally germinated and formed the appressorium, pathogenic growth in rice leaves was impaired (Fig. 2E and 2F). Because the environment inside the plant cell was expected to resemble the minimal medium, MoHIS5^{BiG}, an auxotrophic mutant, probably could not grow well. Similarly, Sweigard et al. reported that one of the reduced virulence mutants generated via REMI showed partial histidine auxotrophy. In this mutant, insertion occurred in the gene encoding imidazole glycerol phosphate dehydratase, an enzyme required for sixth step of histidine biosynthesis (Sweigard et al., 1998).

The second mutant, termed MoVPS74^{BiG}, was selected based on its defect in vegetative growth and pigmentation. In this mutant, an insertion occurred in the putative promoter region of *MoVPS74* (MGG_00839.7) (Fig. 3A). MoVPS74 is a homolog of vacuolar protein sorting-associated protein 74 (VPS74) of *S. cerevisiae*, which was shown to be important for proper vacuole function (Bonangelino et al., 2002). MoVPS74^{BiG} showed abnormal mycelial shapes with swelled hyphal tips and strikingly reduced radial growth. To demonstrate that these phenotypic changes were caused by disruption of *MoVPS74*, genetic complementation was conducted, which generated

transformants that are indistinguishable to KJ201 (Fig. 3B and 3C). Vacuole staining also exhibited dramatic differences between KJ201 and MoVPS74^{BiG}. Vacuoles of MoVPS74^{BiG} were smaller than that of KJ201, and only the circular types were observed in the mutant (Fig. 3D). Additionally, MoVPS74^{BiG} could germinate and form the appressorium on hydrophobic surfaces but showed a reduced virulence, which probably was caused by its retarded mycelial growth (Fig. 3E and 3F). These observations suggest that vacuole functions under the control of MoVPS74 can affect vegetative growth, cell maintenance, and virulence, while conidiation, conidial germination, and appressorium formation were not affected by this gene product.

The last mutant MoFRQ^{BiG} showed abnormal morphology during conidiophore formation. Genomic characterization revealed that *MoFRQ* (MGG_17344.7) was disabled by insertion (Fig. 4A). MoFRQ is a homolog of the *N. crassa* Frequency protein, a key regulator of the circadian rhythm (McClung et al., 1989). MoFRQ^{BiG} was indistinguishable from KJ201 in vegetative growth (Fig. 4B) and pathogenicity (data not shown). MoFRQ^{BiG} produced relatively short conidiophores and hold conidia densely. Genetic complementation was performed to confirm that disruption of *MoFRQ* was responsible (Fig. 4C). Since MoFRQ is a homolog of a circadian clock-related protein, our data suggest a potential relationship between circadian clock and

conidiophore morphology.

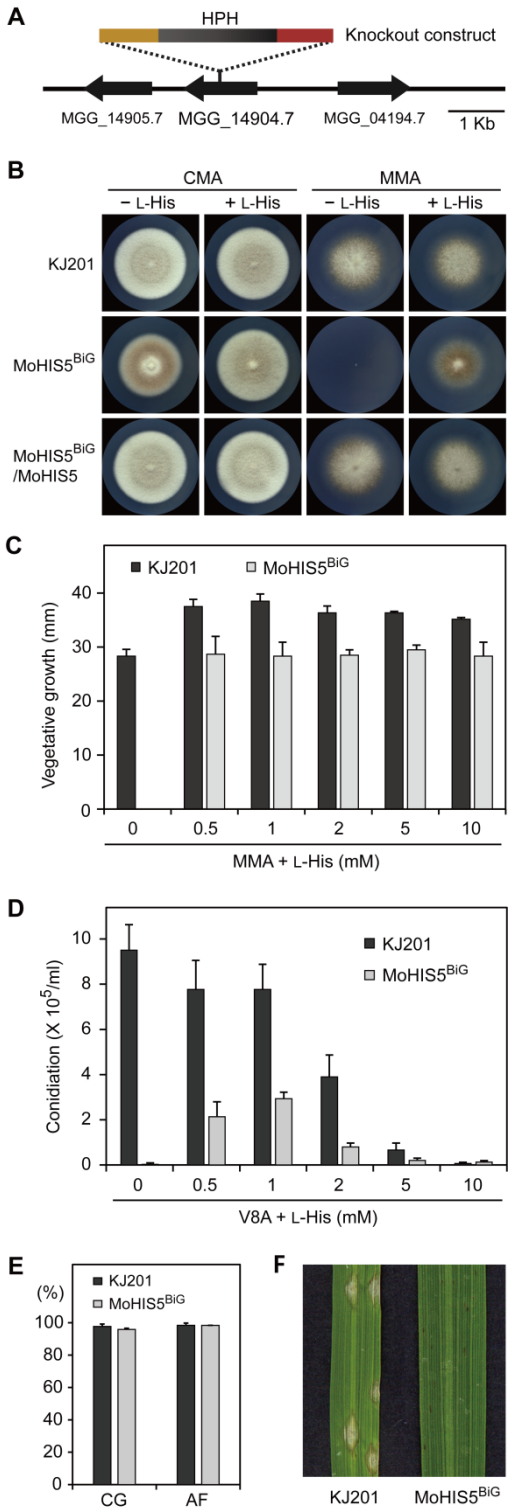
A
HPH
Knockout construct
MGG_14905.7
MGG_14904.7
MGG_04194.7
1 Kb
B
CMA
MMA
− L-His
+ L-His
− L-His
+ L-His
KJ201
MoHIS5BiG
MoHIS5BiG /MoHIS5
C
KJ201
MoHIS5BiG
Vegetative growth (mm)
0
10
20
30
40
0
0.5
1
2
5
10
MMA + L-His (mM)
D
KJ201
MoHIS5BiG
Conidiation (X 10^5/ml)
0
2
4
6
8
10
0
0.5
1
2
5
10
V8A + L-His (mM)
E
KJ201
MoHIS5BiG
(%)
0
20
40
60
80
100
CG
AF
F
KJ201
MoHIS5BiG

Fig. 2. Functional characterization of MoHIS5^{BiG}

(A) Ectopic integration disrupted the MGG_14904.7 locus, which encodes a putative histidinol-phosphate aminotransferase. (B) Vegetative growth of KJ201, MoHIS5^{BiG}, and complemented strain (MoHIS5^{BiG}/MoHIS5) on CMA and MMA with or without exogenous L-histidine. (C) Vegetative growth of KJ201 and MoHIS5^{BiG} on MMA supplemented with 0 to 10 mM L-histidine. (D) Quantitative analysis of conidiation on V8A supplemented with 0 to 10 mM L-histidine. (E) Assessment of conidial germination rate (CG) and appressorium formation (AF) of KJ201 and MoHIS5^{BiG}. (F) Lesions formed on rice leaves infected with conidia of KJ201 and MoHIS5^{BiG}.

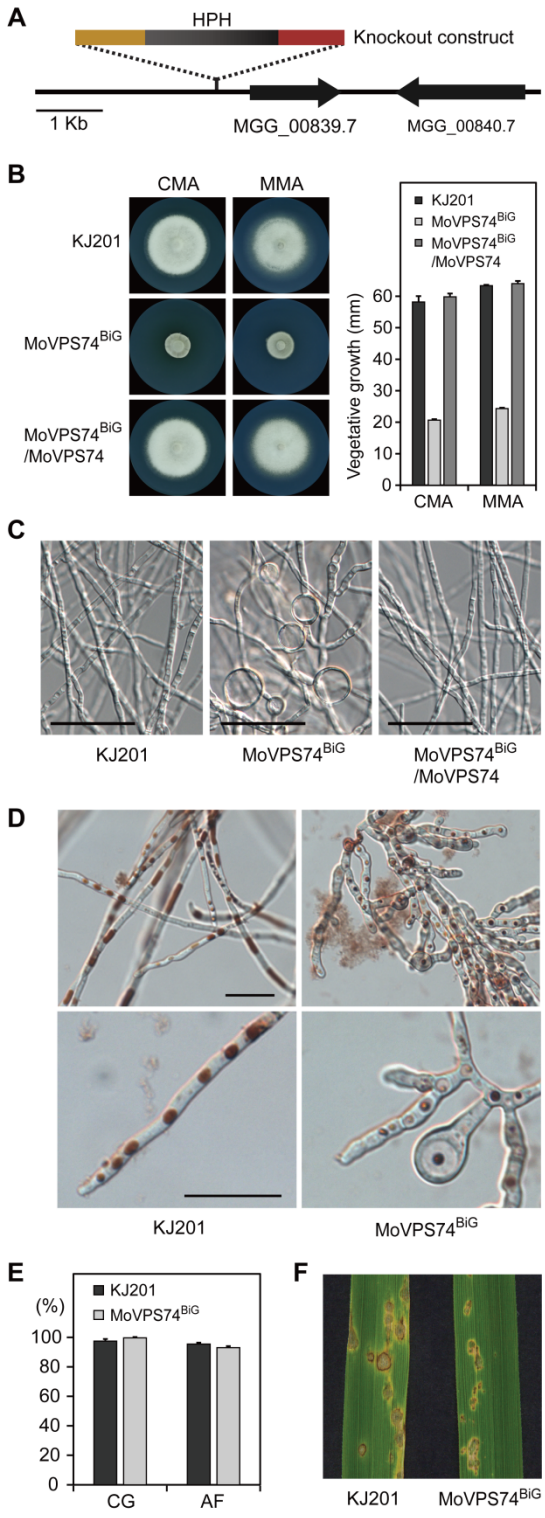
A
HPH
Knockout construct
1 Kb
MGG_00839.7
MGG_00840.7
B
CMA
MMA
KJ201
MoVPS74BiG
MoVPS74BiG /MoVPS74
KJ201
MoVPS74BiG
MoVPS74BiG /MoVPS74
Vegetative growth (mm)
0
10
20
30
40
50
60
CMA
MMA
C
KJ201
MoVPS74BiG
MoVPS74BiG /MoVPS74
D
KJ201
MoVPS74BiG
E
(%)
KJ201
MoVPS74BiG
100
80
60
40
20
0
CG
AF
F
KJ201
MoVPS74BiG

Fig. 3. Functional characterization of MoVPS74^{BiG}

(A) Ectopic integration disrupted the promoter region of the MGG_00839.7 locus, which encodes a homolog of the vacuolar protein sorting-associated protein 74 (VPS74) of *S. cerevisiae*. (B) Vegetative growth of KJ201, MoVPS74^{BiG}, and complement strain (MoVPS74^{BiG}/MoVPS74) on CMA and MMA. (C) MoVPS74^{BiG} formed swollen hyphal tips during vegetative growth. Bars = 50 μm. (D) Vacuole shapes in vegetative mycelia were observed by staining with neutral red. Bars = 20 μm. (E) Assessment of conidial germination rate (CG) and appressorium formation (AF) of KJ201 and MoVPS74^{BiG}. (F) Lesions formed on rice leaves inoculated with KJ201 and MoVPS74^{BiG}.

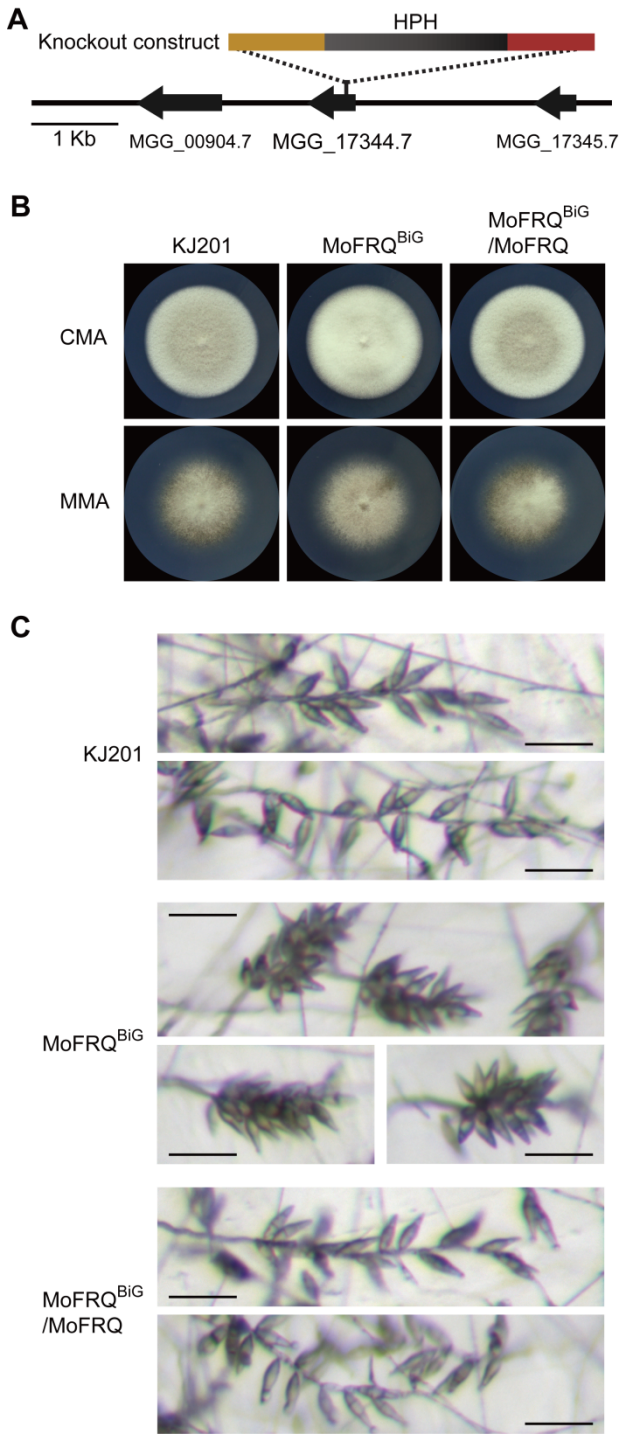
A
Knockout construct
HPH
1 Kb
MGG_00904.7
MGG_17344.7
MGG_17345.7
B
KJ201
MoFRQ^BiG
MoFRQ^BiG /MoFRQ
CMA
MMA
C
KJ201
MoFRQ^BiG
MoFRQ^BiG /MoFRQ

Fig. 4. Functional characterization of MoFRQ^{BiG}

(A) Ectopic integration disrupted the MGG_17344.7 locus encoding a homolog of the *N. crassa* Frequency protein. (B) Vegetative growth of KJ201, MoFRQ^{BiG}, and complemented strain (MoFRQ^{BiG}/MoFRQ) on CMA and MMA. (C) Disruption of MoFRQ caused irregular conidiophore morphology. MoFRQ^{BiG} had a defect in conidiophore elongation compared to KJ201, and genetic complementation (MoFRQ^{BiG}/MoFRQ) restored the wild-type phenotype.

IV. Conclusion

Application of the BiG platform to *M. oryzae* led to the discovery of three genes involved in vegetative growth, pigmentation, asexual development, and/or pathogenicity. Our data suggest that this novel approach compensates the low efficiency of gene disruption by TGR by reusing undesirable ectopic transformants as a source for identifying novel mutations. In this study, we found novel functions associated with *MoVPS74* and *MoFRQ* in the maintenance of cell shape and conidiophore elongation, respectively. This platform will help researchers generate useful forward and reverse genetics data simultaneously. Compared to ATMT in which random integration of T-DNA prefers promoter regions (Choi et al., 2007), the BiG platform can potentially increase the randomness of integration due to the generation of ectopic transformants using various types of transforming DNAs. Analysis of many more insertion sites will be necessary to test this idea. In conclusion, this platform offers a novel and efficient method for elucidating the molecular functions of both known and novel genes, thus facilitating rapid genetic research in filamentous fungi, even if their TGR efficiency is very low.

LITERATURE CITED

Bähler, J., Wu, J.-Q., Longtine, M. S., Shah, N. G., McKenzie, A., 3rd, Steever, A. B., Wach, A., Philippsen, P. and Pringle, J. R. 1998. Heterologous modules for efficient and versatile PCR-based gene targeting in *Schizosaccharomyces pombe*. *Yeast* 14:943-951.

Bölker, M., Böhnert, H. U., Braun, K. H., Görl, J. and Kahmann, R. 1995. Tagging pathogenicity genes in *Ustilago maydis* by restriction enzyme-mediated integration (REMI). *Mol. Gen. Genet.* 248:547-552.

Balhadère, P. V., Foster, A. J. and Talbot, N. J. 1999. Identification of pathogenicity mutants of the rice blast fungus *Magnaporthe grisea* by insertional mutagenesis. *Mol. Plant Microbe Interact.* 12:129-142.

Bird, D. and Bradshaw, R. 1997. Gene targeting is locus dependent in the filamentous fungus *Aspergillus nidulans*. *Mol. Gen. Genet.* 255:219-225.

Bonangelino, C. J., Chavez, E. M. and Bonifacino, J. S. 2002. Genomic screen for vacuolar protein sorting genes in *Saccharomyces cerevisiae*. *Mol. Biol. Cell* 13:2486-2501.

Bundock, P. and Hooykaas, P. J. J. 1996. Integration of *Agrobacterium tumefaciens* T-DNA in the *Saccharomyces cerevisiae* genome by

illegitimate recombination. *Proc. Natl. Acad. Sci. U.S.A.* 93:15272-15275.

Capecchi, M. R. 1989. Altering the genome by homologous recombination. *Science* 244:1288-1292.

Carvalho, N. D. S. P., Arentshorst, M., Kwon, M. J., Meyer, V. and Ram, A. F. J. 2010. Expanding the *ku70* toolbox for filamentous fungi: establishment of complementation vectors and recipient strains for advanced gene analyses. *Appl. Microbiol. Biotechnol.* 87:1463-1473.

Casqueiro, J., Gutiérrez, S., Bañuelos, O., Hijarrubia, M. J. and Martín, J. F. 1999. Gene targeting in *Penicillium chrysogenum*: disruption of the *lys2* gene leads to penicillin overproduction. *J. Bacteriol.* 181:1181-1188.

Chi, M.-H., Park, S.-Y. and Lee, Y.-H. 2009. A quick and safe method for fungal DNA extraction. *Plant Pathol. J.* 25:108-111.

Choi, J., Cheong, K., Jung, K., Jeon, J., Lee, G.-W., Kang, S., Kim, S., Lee, Y.-W. and Lee, Y.-H. 2013. CFGP 2.0: a versatile web-based platform for supporting comparative and evolutionary genomics of fungi and Oomycetes. Nucleic Acids Res. 41:D714-D719.

Choi, J., Park, J., Jeon, J., Chi, M.-H., Goh, J., Yoo, S.-Y., Park, J., Jung, K., Kim, H., Park, S.-Y., Rho, H.-S., Kim, S., Kim, B. R., Han, S.-S., Kang,

S. and Lee, Y.-H. 2007. Genome-wide analysis of T-DNA integration into the chromosomes of *Magnaporthe oryzae*. *Mol. Microbiol.* 66:371-382.

Choquer, M., Robin, G., Le Pêcheur, P., Giraud, C., Levis, C. and Viaud, M. 2008. *Ku70* or *Ku80* deficiencies in the fungus *Botrytis cinerea* facilitate targeting of genes that are hard to knock out in a wild-type context. *Fems Microbiol. Lett.* 289:225-232.

Critchlow, S. E. and Jackson, S. P. 1998. DNA end-joining: from yeast to man. *Trends Biochem. Sci.* 23:394-398.

da Silva Ferreira, M. E., Kress, M. R. V. Z., Savoldi, M., Goldman, M. H. S., Härtl, A., Heinekamp, T., Brakhage, A. A. and Goldman, G. H. 2006. The *akuB*(KU80) mutant deficient for nonhomologous end joining is a powerful tool for analyzing pathogenicity in *Aspergillus fumigatus*. *Eukaryot. Cell* 5:207-211.

de Groot, M. J. A., Bundock, P., Hooykaas, P. J. J. and Beijersbergen, A. G. M. 1998. *Agrobacterium tumefaciens*-mediated transformation of filamentous fungi. *Nat. Biotechnol.* 16:839-842.

Dean, R. A., Talbot, N. J., Ebbole, D. J., Farman, M. L., Mitchell, T. K., Orbach, M. J., Thon, M., Kulkarni, R., Xu, J.-R., Pan, H., Read, N. D., Lee, Y.-H., Carbone, I., Brown, D., Oh, Y. Y., Donofrio, N., Jeong, J. S.,

Soanes, D. M., Djonovic, S., Kolomiets, E., Rehmeyer, C., Li, W., Harding, M., Kim, S., Lebrun, M.-H., Bohnert, H., Coughlan, S., Butler, J., Calvo, S., Ma, L.-J., Nicol, R., Purcell, S., Nusbaum, C., Galagan, J. E. and Birren, B. W. 2005. The genome sequence of the rice blast fungus *Magnaporthe grisea*. *Nature* 434:980-986.

El-Khoury, R., Sellem, C. H., Coppin, E., Boivin, A., Maas, M. F. P. M., Debuchy, R. and Sainsard-Chanet, A. 2008. Gene deletion and allelic replacement in the filamentous fungus *Podospora anserina*. *Curr. Genet.* 53:249-258.

Galperin, M. Y. and Koonin, E. V. 2010. From complete genome sequence to 'complete' understanding? *Trends Biotechnol.* 28:398-406.

Gao, S., Choi, G. H., Shain, L. and Nuss, D. L. 1996. Cloning and targeted disruption of *enpg-1*, encoding the major in vitro extracellular endopolygalacturonase of the chestnut blight fungus, *Cryphonectria parasitica*. *Appl. Environ. Microbiol.* 62:1984-1990.

Guangtao, Z., Hartl, L., Schuster, A., Polak, S., Schmoll, M., Wang, T., Seidl, V. and Seiboth, B. 2009. Gene targeting in a nonhomologous end joining deficient *Hypocrea jecorina*. *J. Biotechnol.* 139:146-151.

Haas, B. J., Zeng, Q., Pearson, M. D., Cuomo, C. A. and Wortman, J. R. 2011. Approaches to fungal genome annotation. *Mycology* 2:118-141.

Hua, S.-b., Qiu, M., Chan, E., Zhu, L. and Luo, Y. 1997. Minimum length of sequence homology required for *in vivo* cloning by homologous recombination in yeast. *Plasmid* 38:91-96.

Jeon, J., Park, S.-Y., Chi, M.-H., Choi, J., Park, J., Rho, H.-S., Kim, S., Goh, J., Yoo, S., Choi, J., Park, J.-Y., Yi, M., Yang, S., Kwon, M.-J., Han, S.-S., Kim, B. R., Khang, C. H., Park, B., Lim, S.-E., Jung, K., Kong, S., Karunakaran, M., Oh, H.-S., Kim, H., Kim, S., Park, J., Kang, S., Choi, W.-B., Kang, S. and Lee, Y.-H. 2007. Genome-wide functional analysis of pathogenicity genes in the rice blast fungus. *Nat. Genet.* 39:561-565.

Kück, U. and Hoff, B. 2010. New tools for the genetic manipulation of filamentous fungi. *Appl. Microbiol. Biotechnol.* 86:51-62.

Kito, H., Fujikawa, T., Moriwaki, A., Tomono, A., Izawa, M., Kamakura, T., Ohashi, M., Sato, H., Abe, K. and Nishimura, M. 2008. MgLig4, a homolog of *Neurospora crassa* Mus-53 (DNA ligase IV), is involved in, but not essential for, non-homologous end-joining events in *Magnaporthe grisea*. *Fungal Genet. Biol.* 45:1543-1551.

Krappmann, S., Sasse, C. and Braus, G. H. 2006. Gene targeting in *Aspergillus fumigatus* by homologous recombination is facilitated in a nonhomologous end-joining-deficient genetic background. *Eukaryot. Cell* 5:212-215.

Liu, G., Casqueiro, J., Bañuelos, O., Cardoza, R. E., Gutiérrez, S. and Martín, J. F. 2001. Targeted inactivation of the *mecB* gene, encoding cystathionine-γ-lyase, shows that the reverse transsulfuration pathway is required for high-level cephalosporin biosynthesis in *Acremonium chrysogenum* C10 but not for methionine induction of the cephalosporin genes. *J. Bacteriol.* 183:1765-1772.

Liu, S., Wei, R., Arie, T. and Yamaguchi, I. 1998. REMI mutagenesis and identification of pathogenic mutants in blast fungus (*Magnaporthe grisea*). *Chin. J. Biotechnol.* 14:133-139.

Manivasakam, P., Weber, S. C., McElver, J. and Schiestl, R. H. 1995. Micro-homology mediated PCR targeting in *Saccharomyces cerevisiae*. *Nucleic Acids Res.* 23:2799-2800.

McClung, C. R., Fox, B. A. and Dunlap, J. C. 1989. The *Neurospora* clock gene *frequency* shares a sequence element with the *Drosophila* clock gene *period*. *Nature* 339:558-562.

Meyer, V., Arentshorst, M., El-Ghezal, A., Drews, A.-C., Kooistra, R., van den Hondel, C. A. M. J. J. and Ram, A. F. J. 2007. Highly efficient gene targeting in the *Aspergillus niger kusA* mutant. *J. Biotechnol.* 128:770-775.

Michielse, C. B., Hooykaas, P. J. J., van den Hondel, C. A. M. J. J. and Ram, A.

F. J. 2005. *Agrobacterium*-mediated transformation as a tool for functional genomics in fungi. *Curr. Genet.* 48:1-17.

Mullins, E. D., Chen, X., Romaine, P., Raina, R., Geiser, D. M. and Kang, S. 2001. *Agrobacterium*-mediated transformation of *Fusarium oxysporum*: an efficient tool for insertional mutagenesis and gene transfer. *Phytopathology* 91:173-180.

Nayak, T., Szewczyk, E., Oakley, C. E., Osmani, A., Ukil, L., Murray, S. L., Hynes, M. J., Osmani, S. A. and Oakley, B. R. 2006. A versatile and efficient gene-targeting system for *Aspergillus nidulans*. *Genetics* 172:1557-1566.

Ninomiya, Y., Suzuki, K., Ishii, C. and Inoue, H. 2004. Highly efficient gene replacements in *Neurospora* strains deficient for nonhomologous end-joining. *Proc. Natl. Acad. Sci. U.S.A.* 101:12248-12253.

Nishiwaki, K., Hayashi, N., Irie, S., Chung, D.-H., Harashima, S. and Oshima, Y. 1987. Structure of the yeast *HIS5* gene responsive to general control of amino acid biosynthesis. *Mol. Gen. Genet.* 208:159-167.

Ochman, H., Gerber, A. S. and Hartl, D. L. 1988. Genetic applications of an inverse polymerase chain reaction. *Genetics* 120:621-623.

Park, S.-M., Choi, E.-S., Kim, M.-J., Cha, B.-J., Yang, M.-S. and Kim, D.-H. 2004. Characterization of HOG1 homologue, CpMK1, from

Cryphonectria parasitica and evidence for hypovirus-mediated perturbation of its phosphorylation in response to hypertonic stress. Mol. Microbiol. 51:1267-1277.

Rho, H.-S., Kang, S. and Lee, Y.-H. 2001. *Agrobacterium tumefaciens*-mediated transformation of the plant pathogenic fungus, *Magnaporthe grisea*. *Mol. Cells.* 12:407-411.

Riggle, P. J. and Kumamoto, C. A. 1998. Genetic analysis in fungi using restriction-enzyme-mediated integration. *Curr. Opin. Microbiol.* 1:395-399.

Sambrook, J. and Russell, D. W. 2001. Molecular cloning: A laboratory manual. Cold Spring Harbor Laboratory Press, Cold Spring Harbor

Scheffer, J., Chen, C., Heidrich, P., Dickman, M. B. and Tudzynski, P. 2005a. A CDC42 homologue in *Claviceps purpurea* is involved in vegetative differentiation and is essential for pathogenicity. *Eukaryot. Cell* 4:1228-1238.

Scheffer, J., Ziv, C., Yarden, O. and Tudzynski, P. 2005b. The COT1 homologue CPCOT1 regulates polar growth and branching and is essential for pathogenicity in *Claviceps purpurea*. *Fungal Genet. Biol.* 42:107-118.

Segers, G. C., Regier, J. C. and Nuss, D. L. 2004. Evidence for a role of the

regulator of G-protein signaling protein CPRGS-1 in Gα subunit CPG-1-mediated regulation of fungal virulence, conidiation, and hydrophobin synthesis in the chestnut blight fungus *Cryphonectria parasitica*. *Eukaryot. Cell* 3:1454-1463.

Shi, Z., Christian, D. and Leung, H. 1995. Enhanced transformation in *Magnaporthe grisea* by restriction enzyme mediated integration of plasmid DNA. *Phytopathology* 85:329-333.

Soulié, M.-C., Piffeteau, A., Choquer, M., Boccara, M. and Vidal-Cros, A. 2003. Disruption of *Botrytis cinerea* class I chitin synthase gene *Bcchs1* results in cell wall weakening and reduced virulence. *Fungal Genet. Biol.* 40:38-46.

Sweigard, J. A., Carroll, A. M., Farrall, L., Chumley, F. G. and Valent, B. 1998. *Magnaporthe grisea* pathogenicity genes obtained through insertional mutagenesis. *Mol. Plant Microbe Interact.* 11:404-412.

Sweigard, J. A., Carroll, A. M., Kang, S., Farrall, L., Chumley, F. G. and Valent, B. 1995. Identification, cloning, and characterization of *PWL2*, a gene for host species specificity in the rice blast fungus. *Plant Cell* 7:1221-1233.

Sweigard, J. A., Chumley, F. G. and Valent, B. 1992. Disruption of a *Magnaporthe grisea* cutinase gene. *Mol. Gen. Genet.* 232:183-190.

Takahashi, T., Masuda, T. and Koyama, Y. 2006. Enhanced gene targeting frequency in *ku70* and *ku80* disruption mutants of *Aspergillus sojae* and *Aspergillus oryzae*. *Mol. Genet. Genomics* 275:460-470.

Talbot, N. J. 2003. On the trail of a cereal killer: exploring the biology of *Magnaporthe grisea*. *Annu. Rev. Microbiol.* 57:177-202.

Talbot, N. J., Ebbole, D. J. and Hamer, J. E. 1993. Identification and characterization of *MPG1*, a gene involved in pathogenicity from the rice blast fungus *Magnaporthe grisea*. *Plant Cell* 5:1575-1590.

Ushimaru, T., Terada, H., Tsuboi, K., Kogou, Y., Sakaguchi, A., Tsuji, G. and Kubo, Y. 2010. Development of an efficient gene targeting system in *Colletotrichum higginsianum* using a non-homologous end-joining mutant and *Agrobacterium tumefaciens*-mediated gene transfer. *Mol. Genet. Genomics* 284:357-371.

Valent, B. and Chumley, F. G. 1991. Molecular genetic analysis of the rice blast fungus, *Magnaporthe grisea*. *Annu. Rev. Phytopathol.* 29:443-467.

Villalba, F., Collemare, J., Landraud, P., Lambou, K., Brozek, V., Cirer, B., Morin, D., Bruel, C., Beffa, R. and Lebrun, M.-H. 2008. Improved gene targeting in *Magnaporthe grisea* by inactivation of *MgKU80* required for non-homologous end joining. *Fungal Genet. Biol.* 45:68-75.

Wang, N.-Y., Yang, S. L., Lin, C.-H. and Chung, K.-R. 2011. Gene inactivation in the citrus pathogenic fungus *Alternaria alternata* defect at the *Ku70* locus associated with non-homologous end joining. *World J. Microbiol. Biotechnol.* 27:1817-1826.

Weld, R. J., Plummer, K. M., Carpenter, M. A. and Ridgway, H. J. 2006. Approaches to functional genomics in filamentous fungi. *Cell Res.* 16:31-44.

Xu, J.-R., Peng, Y.-L., Dickman, M. B. and Sharon, A. 2006. The dawn of fungal pathogen genomics. *Annu. Rev. Phytopathol.* 44:337-366.

Yandell, M. and Ence, D. 2012. A beginner's guide to eukaryotic genome annotation. *Nat. Rev. Genet.* 13:329-342.

Yu, J.-H., Hamari, Z., Han, K.-H., Seo, J.-A., Reyes-Domínguez, Y. and Scazzocchio, C. 2004. Double-joint PCR: a PCR-based molecular tool for gene manipulations in filamentous fungi. *Fungal Genet. Biol.* 41:973-981.

Yun, S. H. 1998. Molecular genetics and manipulation of pathogenicity and mating determinants in *Mycoshpaerella zeae-maydis* and *Cochliobolus heterostrophus*. PhD dissertation (Ithaca, NY: Cornell University)

CHAPTER 4

A Quick and Accurate Screening Method for Fungal Gene-deletion Mutants by Direct, Priority-based, and Inverse PCRs

ABSTRACT

Using two-step-PCR screening which consists of 1) direct and priority-based PCR and 2) inverse PCR, fungal gene-deletion mutants were selected quickly and accurately. It omits genomic DNA extraction and Southern blotting steps and prevents misinterpretations caused by PCR failure. It is anticipated to facilitate large-scale reverse genetic studies in fungi.

INTRODUCTION

Discovery of novel genes and experimental validation of their functions constitute the foundation of functional genomics. Targeted gene replacement (TGR) is a method commonly employed in fungal reverse genetics, whereby a target gene is deleted via homologous recombination. However, the TGR process entails laborious steps to select desired mutants from the pool of transformants and is a bottleneck in rapid, large-scale analyses. Since many filamentous fungi show a low frequency of homologous recombination during TGR (Park and Lee, 2013, Weld et al., 2006), it is common that hundreds of transformants should be screened to identify the desired mutant via PCR-based screening, followed by Southern blotting. Although several methods including double-joint PCR (Yu et al., 2004) and quick genomic DNA extraction (Chi et al., 2009) were developed to enhance the productivity of TGR, there is still room to improve cost-effectiveness.

As a solution, we propose an enhanced method of mutant screening in TGR with several improvements: 1) minimal use of target gene-specific primers, 2) optimized protocol for direct PCR that eliminates the need to extract genomic DNA, 3) priority-based PCR to detect false-negatives, and 4) inverse PCR to bypass Southern blotting (Fig. 1). The validity of this redesigned process was

confirmed using the rice blast fungus, *Magnaporthe oryzae*, as a model. *M. oryzae* is the causal agent of the most devastating disease in cultivated rice and has also served as a model system for studying plant-pathogen interactions since the public release of its annotated genome information (Dean et al., 2005).

METHODS, RESULTS, AND DISCUSSION

I. Step 1. Mutant screening via direct and priority-based PCR

The gene knockout constructs containing the hygromycin B resistance marker (Yun, 1998) were generated by double-joint PCR and fungal transformation was conducted by the protoplast-based method as previously described (Sweigard et al., 1992). After transferring the transformants to V8 juice agar (V8A, 80 ml of V8 juice, 310 μl of 10N NaOH, and 15 g of agar per liter), we firstly screened them by direct and priority-based PCR (Fig. 1). In direct PCR, a small piece of mycelia (≤1 mm^3) taken from the border region of a young colony (24 to 48 hpi) was directly placed into a PCR tube (leave the tube caps closed to prevent desiccation), followed by adding ≥40 μl of reaction mixture. Amplification with Phire® Hot Start II DNA polymerase (Thermo Fisher scientific Inc., USA) following the manufacturer's instructions (including longer initial denaturation, 5 minutes at 98℃, and 40 PCR cycles) resulted in almost 100% success rate for a ≤3 kb product. We used two pairs of primers together in each reaction to amplify the correctly deleted target locus (UP1 and SP, located on the hygromycin B resistance marker and a specific site nearby the deleted region, respectively) and/or a control locus (UP2 and UP3, located on MGG_09898.7) (Table 1). Melting temperatures of UP1 and SP (>60℃)

are higher than that of UP2 and UP3 (<60℃) so that the gene-deleted locus is preferentially amplified if the knockout construct has successfully replaced the target locus. On the other hand, ectopic transformants showed a single amplicon for the control locus, which confirmed successful PCR and helped to avoid false-negatives. The amplicons were distinguished by size (Fig. 2).

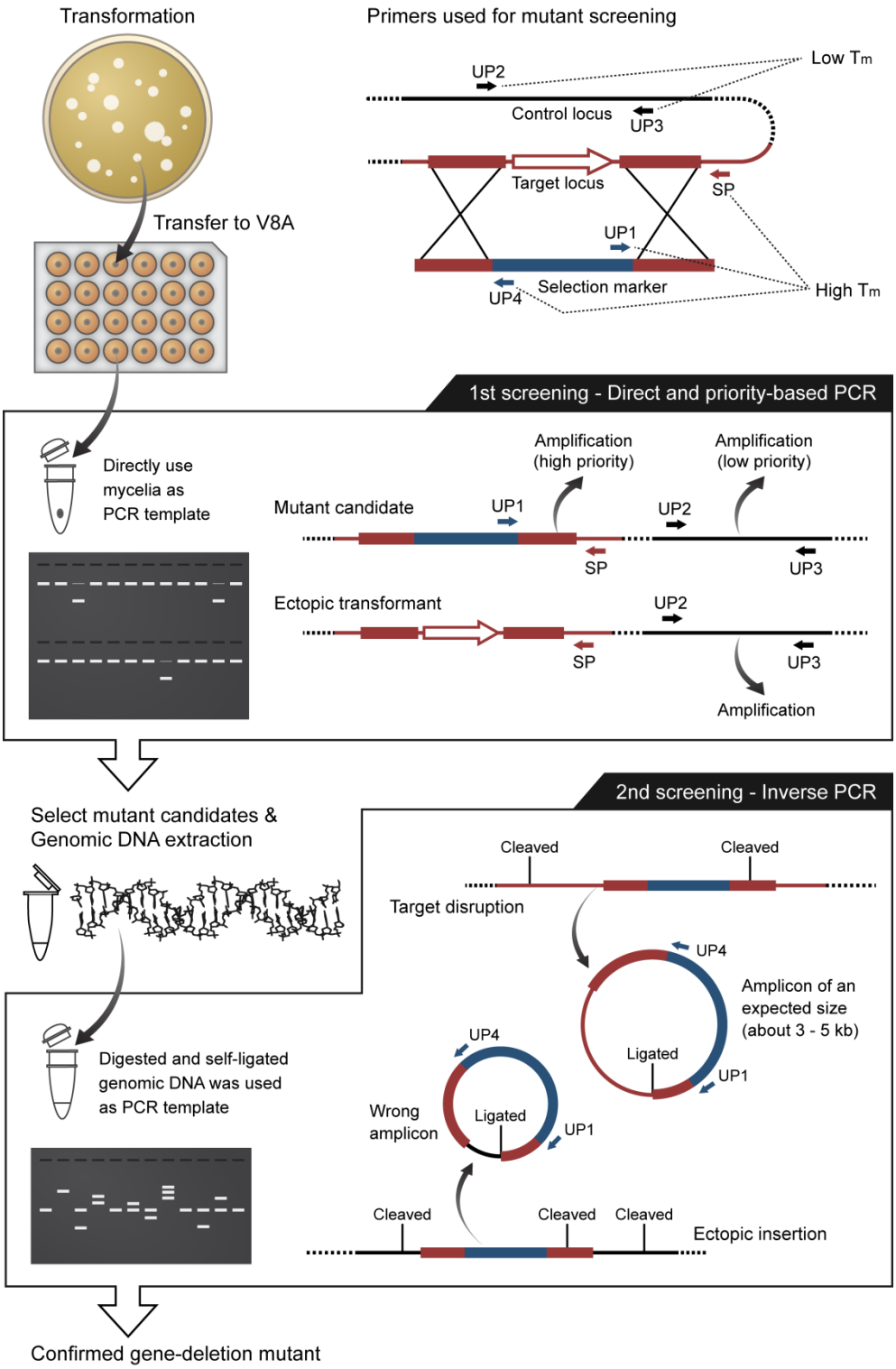
Transformation
Transfer to V8A
Primers used for mutant screening
UP2
Low Tm
Control locus
UP3
Target locus
SP
UP1
Selection marker
UP4
High Tm
1st screening - Direct and priority-based PCR
Directly use mycelia as PCR template
Amplification (high priority)
Amplification (low priority)
Mutant candidate
UP1
UP2
SP
UP3
Ectopic transformant
UP2
SP
UP3
Amplification
Select mutant candidates & Genomic DNA extraction
2nd screening - Inverse PCR
Cleaved
Cleaved
Target disruption
UP4
Amplicon of an expected size (about 3 - 5 kb)
Ligated
UP1
Digested and self-ligated genomic DNA was used as PCR template
UP4
Wrong amplicon
Ligated
UP1
Cleaved
Cleaved
Cleaved
Ectopic insertion
Confirmed gene-deletion mutant

Fig. 1. Schematic diagram of mutant screening in TGR via direct and priority-based PCR and inverse PCR

Hygromycin B-resistant transformants are screened by direct and priority-based PCR. Simultaneous amplification using two primer pairs UP1/SP and UP2/UP3 with different efficiencies allows distinction between candidates of gene-deletion mutant and ectopic transformants. Selected mutant candidates are further screened by inverse PCR. Expected size of a single amplicon produced by the UP1/UP4 primer pair indicates correct deletion of the target locus.

Table 1. Primers used for mutant screening

Name	Sequence (5’ to 3’)
UP1	GGCTGATCTGACCAGTTGC
UP2	GACCCTCAATGTGTCTTCT
UP3	GTGGAGACTCAAGTTGTGA
UP4	CAAGCCTACAGGACACACATTC

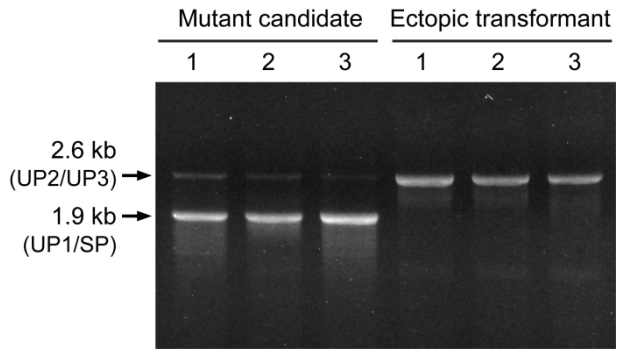

Fig. 2. Representative result of *M. oryzae* mutant screening via direct and priority-based PCR.

Amplicons from the direct and priority-based PCR using three individual mutant candidates and ectopic transformants in MGG_04615.7 deletion.

II. Step 2. Mutant screening via inverse PCR

Secondly, mutant candidates were further screened via inverse PCR to confirm the disruption of the target gene and to detect additional ectopic insertions (Fig. 1). Genomic DNA of each candidate was treated with a 6-cutter restriction enzyme that did not cleave the marker in the knockout construct and was then self-ligated by T4 DNA ligase, and amplified in a PCR using the UP1/UP4 primer pair. Correct deletion mutants showed a single amplicon of an expected size while the ectopic transformants or candidates containing additional insertions showed an amplicon of the wrong size or multiple amplicons (Fig. 3). To elevate accuracy, we conducted two independent PCRs using different restriction enzymes and the candidates showing positive results were defined as desired mutants. When we compared the inverse PCR with Southern blot results, where 52 out of 54 tests showed correct results and only one false-positive was found (Table 2).

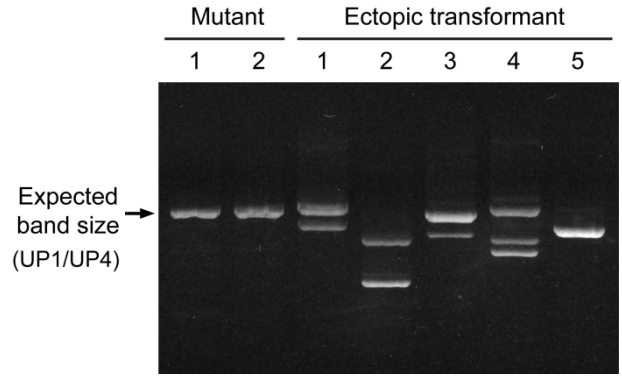

Fig. 3. Representative result of *M. oryzae* mutant screening via inverse PCR.

Amplicons from the inverse PCR to confirm deletion of MGG_06258.7 using *Eco*R V.

Table 2. Accuracy of mutant screening by inverse PCR

Target loci	Mutant candidates	Restriction enzyme	Correct results[a]		Incorrect results		Ambiguous (PCR fail)
			True-positive	True-negative	False-positive	False-negative	
MGG_01812.7	6	*Hin*d III	2	4	0	0	0
MGG_06258.7	7	*Eco*R V	2	5	0	0	0
	7	*Xho* I	2	4	1	0	0
MGG_09225.7	9	*Sac* I	7	2	0	0	0
	9	*Sma* I	6	2	0	0	1
MGG_17453.7	8	*Kpn* I	7	1	0	0	0
	8	*Xho* I	7	1	0	0	0

[a] Inverse PCR showed the same result as Southern blotting

III. Conclusion

This PCR-only method of mutant screening retains high accuracy and dramatically reduces the time, labor, and expenditure. It requires only one specific primer for each target gene and avoids large-scale genomic DNA extractions. Furthermore, it does not demand the materials and facilities for Southern blot. Although we found a single false-positive in the inverse PCR, it could be solved by double checking using different restriction enzymes once the candidates have been narrowed down. Overall, we anticipate that our method will accelerate high-throughput TGR for functional genomics in fungi.

LITERATURE CITED

Chi, M.-H., Park, S.-Y. and Lee, Y.-H. 2009. A quick and safe method for fungal DNA extraction. Plant Pathol. J. 25:108-111.

Dean, R. A., Talbot, N. J., Ebbole, D. J., Farman, M. L., Mitchell, T. K., Orbach, M. J., Thon, M., Kulkarni, R., Xu, J.-R., Pan, H., Read, N. D., Lee, Y.-H., Carbone, I., Brown, D., Oh, Y. Y., Donofrio, N., Jeong, J. S., Soanes, D. M., Djonovic, S., Kolomiets, E., Rehmeyer, C., Li, W., Harding, M., Kim, S., Lebrun, M.-H., Bohnert, H., Coughlan, S., Butler, J., Calvo, S., Ma, L.-J., Nicol, R., Purcell, S., Nusbaum, C., Galagan, J. E. and Birren, B. W. 2005. The genome sequence of the rice blast fungus *Magnaporthe grisea*. Nature 434:980-986.

Park, J. and Lee, Y.-H. 2013. Bidirectional-genetics platform, a dual-purpose mutagenesis strategy for filamentous fungi. Eukaryot. Cell 12:1547-1553.

Sweigard, J. A., Chumley, F. G. and Valent, B. 1992. Disruption of a *Magnaporthe grisea* cutinase gene. Mol. Gen. Genet. 232:183-190.

Weld, R. J., Plummer, K. M., Carpenter, M. A. and Ridgway, H. J. 2006. Approaches to functional genomics in filamentous fungi. Cell Res. 16:31-44.

Yu, J.-H., Hamari, Z., Han, K.-H., Seo, J.-A., Reyes-Domínguez, Y. and Scazzocchio, C. 2004. Double-joint PCR: a PCR-based molecular tool for gene manipulations in filamentous fungi. Fungal Genet. Biol. 41:973-981.

Yun, S. H. 1998. Molecular genetics and manipulation of pathogenicity and mating determinants in *Mycoshpaerella zeae-maydis* and *Cochliobolus heterostrophus*. Ph.D. dissertation. Cornell University, Ithaca, NY.

벼 도열병균 Forkhead 유전자군 특성 규명 및 새로운 유전체 기능 분석법 개발

박 재 진

초 록

축적된 유전체 데이터와 대량 형질전환 기술은 유전자 기능 규명 연구의 속도를 가속시켰다. 하지만 형질전환체들의 표현형을 관찰, 분석하는 단계는 여전히 병목구간으로 존재하며, 많은 시간과 노력을 소요케 하고 있다. 따라서 이러한 문제를 해결할 대량 표현형 스크리닝(high-throughput phenotyping)방법의 중요성이 날로 증대되고 있는데, 현재의 스크리닝 방법으로는 사상성 곰팡이와 같은 다세포 생물을 분석하기에는 한계가 있었다. 그 이유는 사상성 곰팡이가 배양액 내에서 불균등하게 분포하며 자라기 때문인데, 따라서 사상성 곰팡이에 최적화된 새로운 대량 표현형 스크리닝 시스템을 목표

로 삼아, 본 연구에서는 pHenome 플랫폼을 개발하였다. 이 방법은 곰팡이가 생장 과정 중 배양액 내 pH를 지속적으로 변화시킨다는 사실에 근거하여, pH 변화 측정을 통해 특정 환경에 대한 세포 반응을 관찰하였다. 이 방법의 효용성을 입증하기 위해 사상성 곰팡이 중 식물병원균인 벼 도열병균 (*Magnaporthe oryzae*)를 모델로 삼았고, 특화된 알칼리화 촉진배지와 pH 지시약(bromocresol purple, phenol red)을 사용했다. 이는 384-well microplate와 microplate reader를 사용하여 24시간 이내에 결과를 볼 수 있게 해주며, 따라서 위에서 제기한 병목현상 문제를 상당부분 해결할 수 있을 것으로 기대했다. 한편, pHenome의 적용을 포함하여 실제 벼 도열병균의 유전자 기능 규명을 수행했다. 목표 유전자는 Forkhead-box(FOX) 군의 전사인자를 암호화 할 것으로 예측된 4개의 유전자로써, 이 중 2개(*MoFKH1*과 *MoHCM1*)는 자낭균문 내에 ortholog가 고루 분포하였고, 이들이 결손된 변이체는 생장감소, 포자 발아 감소 및 세포분열 저해제(hydroxyurea와 benomyl)에 감수성을 보여, 세포분열에 두 유전자가 관여되어 있음이 예상되었다. 더불어 *MoFKH1* 유전자의 결손은 격벽 형성과 스트레스 반응에 이상을 불러왔고 병원성의 감소도 일으켰다. 한편, 남은 2개의 FOX 유전자는 주발버섯아

문에만 ortholog가 분포했으며 해당 유전자의 결손이 수 차례의 시도에도 불구하고 이루어지지 않거나(*MoFOX2*), 또는 발달, 병원성, 스트레스 반응에 아무런 영향을 주지 않았다(*MoFOX1*). 이 같은 결과들로 *MoFKH1*과 *MoHCM1* 유전자는 벼 도열병균의 발달과정에서 기능하며, 더 나아가 MoFKH1은 병원성 및 스트레스 반응에도 관여되어있음을 규명하였다. 또한 FOX 전사인자 유전자들의 결손변이체를 만드는 과정에서 다량의 원치 않는 ectopic 형질전환체들이 생겨났는데, 이 역시 유전자 연구의 효율을 저하시키기에, 저하된 효율을 보상하는 방안으로써 Bidirectional-Genetics (BiG) 플랫폼을 만들었다. 이는 ectopic 형질전환체를 무작위 삽입 변이체로 여겨 재사용하게끔 했는데, 이를 통해 벼 도열병균의 히스티딘 생합성, 영양생장, 분생자꼭지 형성에 각각 관련된 *MoHIS5*, *MoVPS74*, 및 *MoFRQ* 유전자를 발굴하였고, 전체적으로 형질전환 과정의 효율성을 향상시켰다. 그리고 마지막으로, BiG 플랫폼의 사용을 촉진하기 위하여, 형질전환체가 원하는 변이체인지 아니면 ectopic 형질전환체인지를 빠르게 분류해주는 스크리닝 방법을 제안하였다. 대량의 DNA 추출 및 Southern blot과정을 생략하고, 오직 두 단계의 PCR만을 통해 형질전환체를 스크리닝 하는 이 방법은, 높은 정확도를

유지하면서도 시간과 노력은 크게 줄여주었다. 종합하자면, 본 연구는 벼 도열병균을 모델로 삼아 그 유전자를 연구함과 동시에 도열병균을 포함한 여러 곰팡이 종에서 사용할 수 있는 보다 효과적인 유전자 연구체계를 마련하였다.

주요어: 벼 도열병균 (*Magnaporthe oryzae*), Forkhead-box 전사조절 인자, Bidirectional genetics platform, 두 단계 PCR 기반 형질전환체 스크리닝법, pHenome platform, High-throughput 표현형 스크리닝 시스템.

학 번: 2007-21371